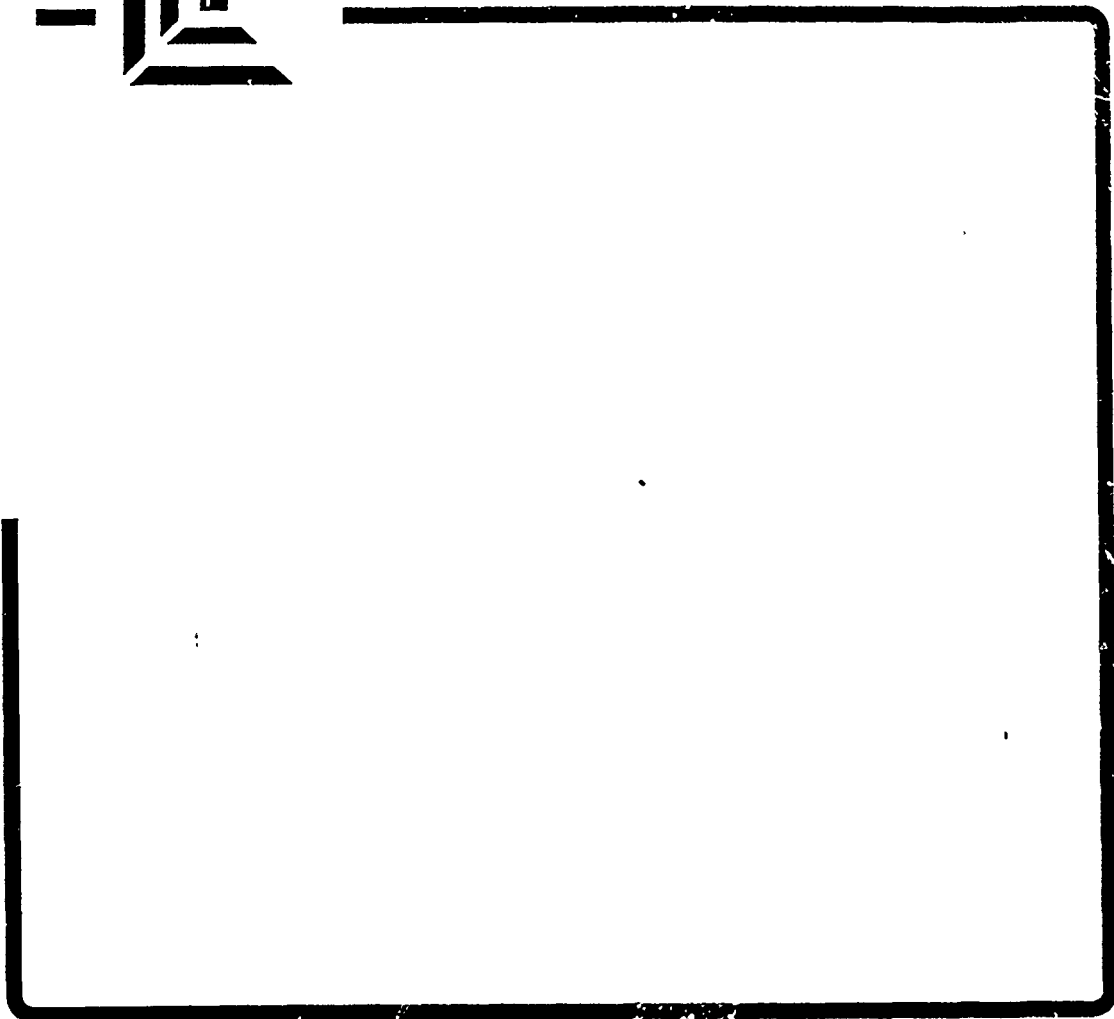
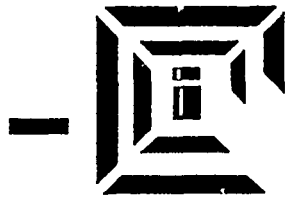




AD-A219 421



**S** DTIC  
ELECTE  
MAR 15 1990  
**E D**

**CONSULTANT'S CHOICE, INC.**

8800 Roswell Road, Atlanta, Georgia 30350

\*Original contains color plates: All DTIC reproductions will be in black and white\*

DISTRIBUTION STATEMENT A  
Approved for public release;  
Distribution Unlimited

90 03 13 155

①

# PHASE II FINAL REPORT ADVANCED MESOSCALE WEATHER FORECASTING TO SUPPORT TACTICAL OPERATIONS ON THE AIRLAND BATTLEFIELD

Accession For	
NTIS GRA&I	<input checked="" type="checkbox"/>
DTIC TAB	<input type="checkbox"/>
Unannounced	<input type="checkbox"/>
Justification	
By _____	
Distribution/	
Availability Codes	
Dist	Avail and/or Special
A-1	



**DTIC**  
**ELECTE**  
MAR 15 1990  
**S E D**

\*Original contains color plates; All DTIC reproductions will be in black and white\*

The views, opinions, and findings contained in this report are those of the authors and should not be construed as official ASL position, policy or decision, unless so designated by other documentation.

Copyright (c) 1990 by Consultant's Choice, Inc.

**DISTRIBUTION STATEMENT A**  
Approved for public release;  
Distribution Unlimited

**REPORT DOCUMENTATION PAGE**

1a. REPORT SECURITY CLASSIFICATION Unclassified		1b. RESTRICTIVE MARKINGS N/A	
2a. SECURITY CLASSIFICATION AUTHORITY N/A		3. DISTRIBUTION/AVAILABILITY OF REPORT  UNCLASSIFIED/UNLIMITED	
2b. DECLASSIFICATION/DOWNGRADING SCHEDULE N/A			
4. PERFORMING ORGANIZATION REPORT NUMBER(S)  CCI-G88-042-01		5. MONITORING ORGANIZATION REPORT NUMBER(S)	
6a. NAME OF PERFORMING ORGANIZATION  Consultant's Choice, Inc.	6b. OFFICE SYMBOL (if applicable)	7a. NAME OF MONITORING ORGANIZATION  Atmospheric Sciences Laboratory	
6c. ADDRESS (City, State, and ZIP Code)  8800 Roswell Road Atlanta, GA 30350		7b. ADDRESS (City, State, and ZIP Code)  Commander/Director, ASL ATTN: SLCAS-AE-A White Sands Missile Range, New Mexico 88002	
8a. NAME OF FUNDING/SPONSORING ORGANIZATION	8b. OFFICE SYMBOL (if applicable)	9. PROCUREMENT INSTRUMENT IDENTIFICATION NUMBER  DAAD07-88-C-0045	
8c. ADDRESS (City, State, and ZIP Code)		10. SOURCE OF FUNDING NUMBERS	
		PROGRAM ELEMENT NO.	PROJECT NO.
		TASK NO.	WORK UNIT ACCESSION NO.
11. TITLE (Include Security Classification)  Advanced Mesoscale Weather Forecasting to Support Tactical Operations on the Airland Battlefield			
12. PERSONAL AUTHOR(S) Lampru, Paul D. Jr.; Atkinson, Lee A.; Perrone, Marc, (Consultant's Choice) and Young, Kenneth C., (ThinkNet, Inc.)			
13a. TYPE OF REPORT J - FINAL	13b. TIME COVERED FROM 88-07-01 TO 89-12-31	14. DATE OF REPORT (Year, Month, Day) 90-02-28	15. PAGE COUNT 120
16. SUPPLEMENTARY NOTATION			
17. CODES		18. SUBJECT TERMS (Continue on reverse if necessary and identify by block number) Pattern Detection, Neural Networks, Weather Prediction, WX Forecasting, Tactical Weather.	
FIELD	GROUP		
19. ABSTRACT (Continue on reverse if necessary and identify by block number)  This work resulted in the test and evaluation of a hybrid statistical neural net program called Goal-Oriented Pattern Detection (GOPAD) and the development of a cloud tracking program that uses weather satellite imagery as input. Both technologies show great promise to provide better weather products to the tactical military user.			
20. DISTRIBUTION/AVAILABILITY OF ABSTRACT <input checked="" type="checkbox"/> UNCLASSIFIED/UNLIMITED <input type="checkbox"/> SAME AS RPT. <input type="checkbox"/> DTIC USERS		21. ABSTRACT SECURITY CLASSIFICATION UNCLASSIFIED	
22a. NAME OF RESPONSIBLE INDIVIDUAL H. Bennett Teates		22b. TELEPHONE (Include Area Code) (404) 992-8430	22c. OFFICE SYMBOL

**PHASE II FINAL REPORT  
ADVANCED MESOSCALE WEATHER FORECASTING  
TO SUPPORT TACTICAL OPERATIONS  
ON THE AIRLAND / BATTLEFIELD**

Contract No. DAAD07-88-C-0045

01 JUL 88 - 31 DEC 89

Prepared by

Paul D. Lampru, Jr.  
Lee A. Atkinson  
Marc Perrone

of

Consultant's Choice, Inc.  
8800 Roswell Road, Suite 130  
Atlanta, Georgia 30350

and

Dr. Kenneth C. Young

of

ThinkNet, Inc.  
4145 E. 6th Street  
Tucson, Arizona 85711

for

U.S. Army White Sands Missile Range  
White Sands Missile Range, New Mexico 88002

February 1990

Availability Codes	
Distribution	
Availability Codes	
Special	
Dist	Special
A-T	

## Executive Summary

### ADVANCED MESOSCALE WEATHER FORECASTING TO SUPPORT TACTICAL OPERATIONS ON THE AIRLAND BATTLEFIELD

The wide dispersion of combat forces on the modern battlefield and the complexity of electro-optical weapon systems have increased the need for forecasted weather parameters that could be used as input to Tactical Decisions Aids (TDA). The Integrated Meteorological System (IMETS) will enable the Air Force Staff Weather Officer, who is assigned to Army Divisions and Corps, to provide weather forecasts and weather effects information. This innovative research, designed to support IMETS, used three advanced software technologies (i.e., a traditional neural net, a hybrid neural net, and image understanding) to provide rapid and accurate tactical weather forecasting models. CCI believes they are foundation technologies for advanced weather forecasting and satellite image processing.

A traditional neural net learning algorithm, back-propagation, was used to create an optimal weather forecasting model (BP-Atlanta) whose performance could be directly compared to the GOPAD-Atlanta-RIR model developed during Phase I, the LFM/MOS, and the National Weather Service Forecast Office (NWSFO). This investigation also sought to observe how different back-propagation parameters affected the performance of the model, and whether the weighting values on the interconnections between the nodes might be useful for identifying important variables.

The hybrid neural net approach is based upon an algorithm called **Goal Oriented Pattern Detection (GOPAD)**, which is technically described as a statistical, optimizing, machine-learning, analogue, forecast model creation, software tool. The output from GOPAD is a tactical or mesoscale, real-time weather forecasting software program that executes in seconds on any computer and in any language. During the summer of 1989, a GOPAD forecast model was independently tested by NOAA during a real-time severe and significant weather forecasting exercise called SHOOTOUT-89 that took place around Boulder, Colorado.

An innovative, non-digital, symbolic image representation scheme, technically described as a width-encoded medial axis (WEMA), was used to perform image understanding by perceptual grouping. A software program called **Cloud Image Representation, Recognition, and Understanding Software (CIRRUS-I)** was developed to demonstrate a capability to intelligently track clouds in multi-temporal satellite imagery. The symbolic representation of segmented, or sliced, cloud regions makes it possible to manipulate individual cloud regions, to attach knowledge to cloud objects, to use shape information, to use the relative proximity of one object to another, to infer cloud behavior, to compute the orientation and magnitude of cloud displacements, and to intelligently deduce the direction of movement of tracked clouds. CIRRUS-I produces cloud/temperature displacement vectors that could be passed into a vorticity model to compute synoptic wind patterns across the continent. These wind patterns could then be used as input into mesoscale weather forecast models.

## TABLE OF CONTENTS

<u>Section</u>	<u>Page</u>
1.0 RESEARCH OVERVIEW-----	1
1.1 Phase I Background-----	1
1.2 Phase II Background-----	2
2.0 PHASE II RESEARCH OBJECTIVES-----	3
3.0 ARTIFICIAL NEURAL NETS-----	4
3.1 Research Overview-----	4
3.2 Training and Testing Data Base-----	4
3.3 Ground Truth Data Base-----	5
3.4 LFM/MOS and NWSFO Forecasts-----	5
3.5 Optimal Forecast Model Research-----	6
3.5.1 Objective-----	6
3.5.2 Research Results-----	6
3.5.2.1 Learning Rate Experiment-----	7
3.5.2.2 Hidden Nodes Experiment-----	8
3.5.2.3 Passes Experiment-----	10
3.5.2.4 Momentum Experiment-----	11
3.5.2.5 Iterations Experiment-----	11
3.5.2.6 Sigmoid Table Experiment-----	12
3.5.2.7 Input-Output Layer Connection Experiment-----	12
3.6 Evaluation and Comparisons Research-----	12
3.6.1 Overall Goals-----	12
3.6.2 General Approach-----	13
3.6.3 Spreadsheet Calculation of Skill Score-----	14
3.6.4 Comparative Performance Evaluations-----	15
3.6.4.1 Objectives and Approaches-----	15
3.6.4.2 Research Results-----	15
3.6.5 Identification of Important Predictor Variables-----	18
3.6.5.1 Objective-----	18
3.6.5.2 Research Results-----	18
4.0 GOAL ORIENTED PATTERN DETECTION-----	20
4.1 Background-----	20
4.2 GOPAD Description-----	21
4.3 Conclusions-----	22
5.0 MESOSCALE WEATHER FORECASTING EXERCISE-SHOOTOUT-89-----	22
5.1 Background-----	22
5.2 SHOOTOUT-89 Evaluations-----	23
5.2.1 NOAA/FSL Comparative Evaluation-----	23
5.2.2 Performance Evaluation-----	23
5.3 Conclusions-----	23

(continued)

**TABLE OF CONTENTS**  
(concluded)

<u>Section</u>	<u>Page</u>
6.0 CLOUD IMAGE REPRESENTATION, RECOGNITION, AND UNDERSTANDING SOFTWARE -----	24
6.1 Background -----	24
6.2 CIRRUS-I Data Flow -----	25
6.3 CIRRUS-I Performance -----	25
6.4 Conclusions -----	25
7.0 PHASE II RECOMMENDATIONS -----	26
 APPENDIX A Brier-Based Skill Scores for BP-Atlanta-241 Using Optimal Parameters	
 APPENDIX B Goal-Oriented Pattern Detection (GOPAD) For Tactical Mesoscale Weather Forecasting	
 APPENDIX C A Quantitative Comparison of Forecast Models That Participated in NOAA/FSL SHOOTOUT-89 Exercise	
 APPENDIX D Cloud Tracked Winds Derived From Satellite Imagery Using an Image Understanding Approach	
 APPENDIX E CIRRUS-I Processing Steps and Performance	

## LIST OF TABLES

<u>Table</u>		<u>Page</u>
1	Architecture and Parameters for BP-ATLANTA-241-----	7
2	Five-Month Skill Scores for Various Learning Rates-----	7
3	Weekly Skill Scores for Various Learning Rates-----	8
4	Hidden Nodes Experiment-----	9
5	Weekly Skill Scores for Various Numbers of Hidden Nodes-----	9
6	Passes Experiment-----	10
7	Weekly Skill Scores for Various Numbers of Passes-----	10
8	Momentum Experiment-----	11
9	Iterations Experiment-----	11
10	Sigmoid Table Experiment-----	12
11	Learning Rate Experiment-----	12
12	Three-Month Skill Scores Using BP-ATLANTA-241 Parameter Settings-----	16
13	Monthly Skill Scores Using BP-ATLANTA-241 Parameter Settings-----	17
14	Weekly Skill Scores Using BP-ATLANTA-241 Parameter Settings-----	17
15	Weekly Skill Scores Using BP-ATLANTA-241 Parameter Settings-----	18
16	Summary of Weights Along the Interconnections from Each Input Node to the Output Node for the GOPAD Selected Variables-----	20
17	Skill Scores for Severe Weather in Regions II, III, and IV-----	24
18	Skill Scores for Severe Weather in Region IV-----	24

## PHASE II FINAL REPORT

### 1.0 RESEARCH OVERVIEW

The wide dispersion of combat forces on the modern battlefield and the complexity of electro-optical weapon systems have increased the need for forecasted weather parameters that could be used as input to Tactical Decisions Aids (TDA). The Integrated Meteorological System (IMETS) will enable the Air Force Staff Weather Officer, who is assigned to Army Divisions and Corps, to provide weather forecasts and weather effects information. CCI's research was designed to support IMETS using two advanced software technologies (i.e., neural nets and symbolic image processing) to provide rapid and accurate tactical weather forecasts. CCI believes these are foundation technologies for weather forecasting and satellite image processing.

#### 1.1 Phase I Background

In the fall of 1987, the Atmospheric Effects Division, U.S. Army Atmospheric Sciences Laboratory (ASL), supported as Small Business Innovative Research (SBIR) a Phase I project by Consultant's Choice, Inc. (CCI) to develop analysis and graphics techniques to display current weather-related information over a limited tactical area, and to experiment with an innovative proprietary software program, called Goal Oriented Pattern Detection (GOPAD), for creating weather forecasting models. Two prototype software demonstrations were developed and delivered to the Government: (1) an MS-DOS-based, attributed vector map representation that could support an object-oriented programming paradigm, and (2) a Probability of Precipitation (PoP) forecasting model for Hartsfield International Airport in Atlanta, Georgia.

The attributed vector map representation was designed to demonstrate a capability to support an advanced programming paradigm that would be created in Phase II called Frame-Based Reasoning for an MS-DOS computer. However, after the Phase II was awarded, it was determined that the research should focus on symbolic image processing research that would be more beneficial to the Government.

The GOPAD-Atlanta-RIR probability of precipitation (PoP) model was compared to the forecasts issued by the National Weather Service Forecasters and LFM/MOS model for June, July, and August of 1987. It is important to note that the GOPAD model used

data from only three rawinsondes from the 12Z sounding to produce a forecast at 1230Z for the 12-24Z period, whereas the LFM/MOS used the 0Z sounding in order to issue a forecast at approximately the same time as the GOPAD model. The performance or skill of all forecasts models was evaluated based upon the Brier scores. The skill scores for the summer, 1987, were computed as follows: (a) LFM/MOS 16.3%; (b) NWSFO 20.9%; and (c) GOPAD 27.6%. These preliminary performance results and the potential to further improve GOPAD forecast models by adding new sources of predictor variables were sufficient to justify further experimentation in Phase II with the GOPAD approach, and a more traditional neural net approach, based on the back-propagation learning algorithm.<sup>1</sup>

## 1.2 Phase II Background

In the fall of 1988, the Atmospheric Effects Division, U.S. Army Atmospheric Sciences Laboratory (ASL), supported a Small Business Innovative Research (SBIR) Phase II project by Consultant's Choice, Inc. (CCI) to investigate Goal Oriented Pattern Detection (GOPAD), Artificial Neural Nets (ANS), and a symbolic satellite image processing technique to support tactical weather forecasting on the AirLand Battlefield. The overall goals of the research were to develop technologies that could be used to automate the production of weather forecasting models, to evaluate the performance of prototype forecasting models, and to demonstrate how an innovative symbolic image representation scheme could be used to automatically track clouds in multi-temporal GOES imagery.

CCI's neural net approach was based upon an algorithm called **Goal Oriented Pattern Detection (GOPAD)** and the back-propagation learning algorithm. GOPAD is technically described as a statistical, optimizing, machine-learning, analogue, forecast model creation, software tool. The output from GOPAD is a tactical or mesoscale, real-time weather forecasting software program data that executes in seconds on any computer and in any language. During the summer of 1989, a GOPAD forecast model was independently tested by NOAA during a real-time severe and significant weather forecasting exercise called SHOOTOUT-89 that took place in the Boulder and Denver, Colorado, area. CCI believes that the GOPAD technology will represent a significant improvement in the ability to forecast a wide variety of mesoscale weather phenomena.

---

<sup>1</sup>Lippmann, Richard P., An Introduction to Computing with Neural Nets, IEEE ASSP Magazine, April, 1987, pages 4-22.

CCI's symbolic image processing approach was based upon the Digital [image] to Symbolic Image Transformation Algorithm (DSTA). This transformation algorithm operates on a segmented digital image to produce a discrete width-encoded medial axis (WEMA) in a LISP list format. This type of symbolic representation facilitates image understanding by perceptual grouping.<sup>2</sup> A software program called **Cloud Image Representation, Recognition, and Understanding Software (CIRRUS-I)** was developed to exploit the WEMA by demonstrating a capability to intelligently track clouds in multi-temporal satellite imagery. CIRRUS-I produces cloud/temperature displacement vectors that could be passed into a vorticity model to compute synoptic wind patterns across the continent.

## 2.0 PHASE II RESEARCH OBJECTIVES

There were five broad research objectives in Phase II.

- a. To develop a Probability of Precipitation (PoP) forecast model, called BP-Atlanta, for Hartsfield International Airport using the back-propagation learning algorithm (BP) and the same rawinsonde data bases used to train and test the GOPAD-Atlanta model.
- b. To compare the performance of the BP-Atlanta forecasts to the performance of GOPAD-Atlanta, LFM/MOS, and the NWSFO forecasts.
- c. To develop a severe and significant mesoscale weather forecasting model, called GOPAD-RT89, for an NOAA/FSL sponsored forecasting exercise called SHOOTOUT-89.
- d. To compare and evaluate the performance of the GOPAD-RT89 model to the other forecast models that participated in SHOOTOUT-89.
- e. To demonstrate the capability of a width-encoded medial axis (WEMA) to track homogenous temperature regions (i.e., clouds) in GOES IR imagery.

---

<sup>2</sup>Biederman, Irving. Human Image Understanding: Recent Research and a Theory. Computer Vision, Graphics, and Image Processing 32, 1985, pages 329-73.

### 3.0 ARTIFICIAL NEURAL NETS

#### 3.1 Research Overview

This research was structured to develop, modify, test, evaluate, and compare the usefulness of **Artificial Neural Nets (ANS)** as an approach to developing tactical weather forecasting models. In Phase I, **Goal Oriented Pattern Detection (GOPAD1)** was used to develop a Probability of Precipitation (PoP) forecast model for Hartsfield International Airport in Atlanta, Georgia. The high skill scores achieved by this hybrid neural net approach suggested that perhaps a more traditional neural net approach using the **back-propagation (BP)** learning algorithm might be able to outperform a GOPAD1 model. In addition, GOPAD1 (i.e., the BASIC language version) appeared to have several problems that might limit its usefulness as a tool for creating tactical weather forecasting models. Although many of these limitations were eventually mitigated by the evolution of GOPAD1 into GOPAD2, we believed that it would be prudent to investigate the potential of a traditional neural net approach, since the data bases were readily available for direct comparisons.

#### 3.2 Training and Testing Data Base

The **training data base** consisted of rawinsonde data from three sites: Athens, Georgia; Waycross, Georgia; and Centerville, Alabama, for a 7-month period (i.e., April to October) and for a 10-year period (i.e., 1975 to 1984).

The **testing data base** consisted of rawinsonde data for a 5-month period (i.e., May to September) during 1987. The testing data base consisted of the same variables that were in the training data base.

Both data bases were composed of the twice daily (i.e., 0Z and 12Z) rawinsonde soundings. Each sounding was composed of four variables (i.e., temperature, relative humidity, and wind direction and speed) for ten levels in the atmosphere (i.e., 900, 800, 700, 600, 500, 400, 300, 200, 150, and 100 mb). The wind direction and speed were converted to u (east-west) and v (north-south) components. All variables were normalized to have a mean of zero and a standard deviation of one. Thus, the historical training data base consisted of 2,130 records or data points (i.e., 213 days/year x 10 years), whereas the testing data base consisted of 153 records. Each record in the

training and testing data bases had 241 predictor variables (i.e., 4 variables/level x 10 levels/rawinsonde x 3 sites x 2 rawinsondes/sites) plus the day-number).

### 3.3 Ground Truth Data Base

The ground truth data, obtained from the National Climatic Data Center (NCDC), consisted of hourly precipitation data for the National Weather Service Forecast Office at Hartsfield International Airport in Atlanta, Georgia. The time variable was shifted to Greenwich (Z) time and summarized in six-hour totals ending at 6Z, 12Z, 18Z, and 24Z. All variables were normalized to have a mean of zero and a standard deviation of one.

### 3.4 LFM/MOS and NWSFO Forecasts

The forecasts issued by the National Weather Service Forecast Office (NWSFO) at Hartsfield International Airport in Atlanta and the Limited Fine Mesh/Model Output Statistics (LFM/MOS) data were obtained from the hand-written reports maintained by the NWSFO. This information was obtained for the 3-month period June to August, 1987. This data was used as a benchmark during Phase I and Phase II to compare the performance of GOPAD and BP forecast models.

It is important to note that the LFM/MOS forecasts used the 0Z sounding for the 12-24Z forecast period, whereas GOPAD-ATLANTA and BP-ATLANTA models used the 12Z sounding to produce the 12-24Z forecasts. These times were used because, in an operational setting, the LFM/MOS 12-24Z forecast based upon the 12Z sounding is not available until about 15-17Z, whereas the GOPAD-ATLANTA and the BP-ATLANTA models are available seconds after the 12Z sounding data arrives (i.e., about 1230Z). Thus, in order for LFM/MOS to provide timely information to a forecaster, it must use the 0Z sounding, whereas a GOPAD or BP model can be based upon the 12Z sounding. While this difference may appear to disadvantage LFM/MOS vis-a-vis GOPAD and BP, it is also important to note the great advantage that LFM/MOS has had in research and development time compared to the limited experimentation with GOPAD and BP models. The point is that perfectly matched, objective comparisons are not yet possible. However, future research and development will eventually make direct quantitative and qualitative comparisons possible.

### 3.5 Optimal Forecast Model Research

#### 3.5.1 Objective

The objective of this research was to identify the optimal combination of BP parameters that would produce a PoP forecast model with the highest possible Brier-based skill score.<sup>3</sup> The optimal ANS model that was produced is referred to as **BP-ATLANTA-241**.

#### 3.5.2 Research Results

This research was performed during December, 1988, and January, 1989. The approach used to find the optimal parameters was trial and error. The measurement used to identify the optimal model was the single (Brier) skill score obtained for the combined months of May, June, July, August, and September, 1987. The training and testing data bases were the data bases that were prepared for GOPAD during Phase I. The climatology used to compute skill score for each of the five months was 22%. In later experiments, the climatology was computed for each month in the training data base. Consequently, slight differences in skill scores occur between the following tables in this section and the tables in other paragraphs.

The BP architecture and parameter settings for BP-Atlanta-241 which produced the highest Brier-based skill score are listed in Table 1. The skill score obtained for these settings was 20.19%.

---

<sup>3</sup>Murphy, A.H., and Daan, H., "Forecast Evaluation", Probability, Statistics, and Decision Making in the Atmospheric Sciences, Westview Press, 1985, pp. 379-437.

TABLE 1  
ARCHITECTURE AND PARAMETERS FOR BP-ATLANTA-241

3	Number of input, hidden, and output layers
241	Number of nodes on input layer
30	Number of nodes on the hidden layer
1	Number of nodes on the output layer
10	Number of passes
1	Number of iterations
0.01	Learning rate
0.90	Momentum
Table	Source for Sigmoid function
n/a	Random seed
no	Input and output slabs connected

### 3.5.2.1 Learning Rate Experiment

The purpose of this experiment was to observe the effects of changing the learning rate parameter while keeping all other network parameters constant. Table 2 shows initial research using the preprocessed data with five-month skill scores, while Table 3 shows the weekly skill scores after the training and testing data bases were reconstructed.

TABLE 2  
FIVE-MONTH SKILL SCORES FOR VARIOUS LEARNING RATES

<u>Learning Rate</u>	<u>Brier-based Skill Score</u>	<u>Time (hr:min:sec)</u>
.005	+ 17.79%	7.11
.010	+ 20.19%	7.11
.020	+ 18.45%	7.11
.025	+ 14.07%	7.11
.030	+ 13.24%	7.11
.040	+ 5.20%	7.11
.050	+ 4.06%	7.11
.075	+ 2.47%	7.11
.100	- 3.56%	7.11

TABLE 3  
WEEKLY SKILL SCORES FOR VARIOUS LEARNING RATES

Summer 1987	LEARNING RATES								
	.005	.010	.020	.025	.030	.040	.050	.750	.100
June 7	22.1	18.1	22.5	18.6	15.5	41.2	66.2	74.1	7.6
14	38.7	32.4	21.5	19.3	22.0	77.6	67.1	66.0	8.3
21	58.9	62.1	60.9	25.6	38.0	14.4	71.5	74.0	73.3
28	32.8	40.2	22.1	17.4	34.2	-22.4	6.0	8.7	53.7
July 5	23.4	30.6	19.2	-6.3	-3.8	-22.1	-16.0	-0.5	-7.8
12	-5.7	8.9	13.7	15.3	20.3	-86.7	-131.0	-107.5	-20.9
19	27.7	28.4	10.6	4.9	4.9	-6.3	-3.8	-3.0	30.0
26	-10.2	-10.2	-5.5	-8.0	-17.1	15.9	18.3	9.3	-3.6
August 2	2.4	-4.3	-11.2	-12.9	-27.2	-66.8	-84.5	-65.3	-11.3
9	12.0	17.3	-2.0	-3.2	-5.5	-21.6	15.3	6.1	1.2
16	15.4	-10.8	-30.5	-10.8	-19.2	78.5	49.5	35.1	-304.4
23	41.0	50.1	51.3	65.4	75.8	83.0	-0.3	-39.0	3.1
30	-14.0	-7.5	2.3	62.3	71.2	91.2	-99.5	-217.2	-102.0
Averages:	18.8	19.6	13.4	14.4	16.1	13.5	-3.6	-12.6	-21.4
Combined Skill Scores:									
J-J-A	23.9	26.1	18.6	9.9	12.3	-0.2	9.5	8.5	11.8
M-J-J-A-S	19.0	21.4	19.6	15.3	14.5	6.6	5.5	3.9	-2.0

### 3.5.2.2 Hidden Nodes Experiment

The purpose of this experiment was to observe the effects of changing the number of hidden nodes while keeping all other network parameters constant. Table 4 shows initial research using the preprocessed data with five-month skill scores, while Table 5 shows the weekly skill scores after the training and testing data bases were reconstructed.

TABLE 4  
HIDDEN NODES EXPERIMENT

<u>Hidden Nodes</u>	<u>Brier-based Skill Score</u>	<u>Time (hr:min.sec)</u>
10	+12.76%	2.46
20	+12.71%	4.54
30	+ 20.19%	7.11
40	+18.64%	9.29
50	+14.50%	11.47
60	+18.44%	14.04
70	+16.52%	16.22
80	+8.87%	18.41
90	+10.37%	20.58
100	+4.84%	23.16

TABLE 5  
WEEKLY SKILL SCORES FOR VARIOUS NUMBERS OF HIDDEN NODES

Summer- 1987	NUMBER OF HIDDEN NODES								
	10	20	30	40	50	60	70	80	90
June 7	-1.7	18.2	18.1	28.5	14.4	15.7	6.7	17.3	37.4
14	15.7	29.7	32.4	18.5	34.2	27.3	26.9	39.2	33.1
21	65.8	64.2	62.1	56.6	43.9	54.4	54.6	56.1	57.6
28	51.3	54.5	40.2	44.7	28.8	36.9	39.0	42.4	32.9
July 5	29.1	15.6	30.6	22.7	24.2	22.0	47.2	0.2	18.4
12	-19.3	-19.6	8.9	-10.7	-22.6	26.1	6.6	5.7	-33.3
19	49.5	33.3	28.4	11.6	7.5	5.5	13.4	15.0	18.8
26	-5.9	27.7	-10.2	18.6	-3.5	19.0	-0.4	5.1	0.5
2	-3.1	-12.7	-4.3	-11.9	-31.3	-34.8	-53.7	-35.5	-37.6
August 9	19.4	5.7	17.3	25.6	26.8	22.8	9.7	5.1	12.2
16	-66.7	-72.5	-10.8	12.9	1.6	-63.7	-83.3	-127.9	-28.2
23	-25.7	30.9	50.1	19.9	-40.0	40.6	64.3	-19.8	-35.6
30	-131.2	23.0	-7.5	19.4	55.5	-0.2	34.5	-70.4	-86.4
Averages:	-1.8	15.3	19.6	19.7	10.7	13.2	12.7	-5.233	-0.8
Combined Skill Scores:									
J-J-A	20.3	23.8	26.1	25.5	17.5	23.2	20.3	13.8	15.8
M-J-J-A-S	14.0	14.0	21.4	19.8	15.7	19.6	17.7	10.2	11.7

### 3.5.2.3 Passes Experiment

The purpose of this experiment was to observe the effects of changing the number of passes in a back-propagation algorithm, while keeping all other network parameters constant. Table 6 shows initial research using the preprocessed data with five-month skill scores, while Table 7 shows the weekly skill scores after the training and testing data bases were reconstructed.

TABLE 6  
PASSES EXPERIMENT

<u>Passes</u>	<u>Brier-based Skill Score</u>	<u>Time (hr:min:sec)</u>
5	+19.14	3.35
10	+20.19	7.12
20	+ 18.28	14.22
30	+ 14.98	21.34
40	+ 7.76	28.46
60	+ 1.74	43.08

TABLE 7  
WEEKLY SKILL SCORES FOR VARIOUS NUMBERS OF PASSES

	<u>NUMBER OF PASSES</u>					
<u>Summer-87</u>	<u>5</u>	<u>10</u>	<u>20</u>	<u>30</u>	<u>40</u>	<u>60</u>
June 7	20.1	18.1	30.3	24.9	22.7	17.0
14	32.8	32.4	27.5	29.0	15.0	27.9
21	57.1	62.1	55.9	58.2	56.3	52.7
28	30.8	40.2	26.5	39.8	47.5	40.7
July 5	20.2	30.6	37.7	37.7	33.9	33.8
12	6.1	8.9	12.4	14.7	27.7	23.3
19	22.3	28.4	7.6	9.0	6.7	-4.8
26	-9.6	-10.2	-19.5	-20.6	-24.3	-27.1
August 2	4.3	-4.3	-13.5	-23.9	-34.8	-34.1
9	10.9	17.3	-0.7	-17.7	-14.0	-4.8
16	14.5	-10.8	-11.8	-82.9	-144.7	-195.6
23	53.0	50.1	50.1	19.5	-102.4	-178.3
30	3.8	-7.5	-3.8	-16.3	-70.2	-152.4
Averages:	20.5	19.6	15.3	5.5	-13.9	-30.9
Combined Skill Scores:						
J-J-A	23.8	26.1	19.8	16.6	10.8	6.3
M-J-J-A-S	20.3	21.4	19.5	6.2	9.1	3.2

### 3.5.2.4 Momentum Experiment

The purpose of this experiment was to observe the effects of changing the momentum in a back-propagation algorithm, while keeping all other network parameters constant. Table 8 shows initial research using the preprocessed data with five-month skill scores.

<u>Momentum</u>	<u>Brier-based Skill Score</u>	<u>Time (hr:min:sec)</u>
.750	+ 16.98	7.11
.800	+ 17.96	7.11
.850	+ 19.04	7.11
.900	+ 20.19	7.11
.925	+ 19.79	7.11
.950	+ 19.90	7.11

### 3.5.2.5 Iterations Experiment

The purpose of this experiment was to observe the effects of changing the number of iterations in a back-propagation algorithm, while keeping all other network parameters constant. Table 9 shows initial research using the preprocessed data with five-month skill scores.

<u>Iterations</u>	<u>Brier-based Skill Score</u>	<u>Time (hr:min:sec)</u>
1	+ 20.19	7.11
2	+ 14.97	14.97
3	+ 9.22	21.05
5	- 8.99	34.58

### 3.5.2.6 Sigmoid Table Experiment

The purpose of this experiment was to observe the effects of obtaining the Sigmoid value from a table, and obtaining the value by calculation for a back-propagation algorithm, while keeping all other network parameters constant. Table 10 shows initial research using the preprocessed data with five-month skill scores.

<u>Sigmoid Value</u>	<u>Brier-based Skill Score</u>
Table	+ 20.19
Calculated	+ 20.19

### 3.5.2.7 Input-Output Layer Connection Experiment

The purpose of this experiment was to observe the effects of not connecting the input layer directly to the output layer in a back-propagation algorithm, while keeping all other network parameters constant. Table 11 shows initial research using the preprocessed data with five-month skill scores.

<u>Input-Output</u>	<u>Brier-based Skill Score</u>
Not Connected	+ 20.19
Connected	- 29.41

## 3.6 Evaluation and Comparisons Research

### 3.6.1 Overall Goals

This research sought to validate the previous research work by setting aside the preprocessed historical data base that was originally created to train the GOPAD-

ATLANTA-RIR, and reconstructing a new data base from the raw soundings provided by the National Climatic Data Center.

This research sought to develop a combination of BP forecasts models that could be compared to the GOPAD -E, -F, and -G models that comprise the GOPAD-ATLANTA-RIR model developed during Phase I.

This research sought to observe the degradation that would occur when a 12-24 hour forecast model was created rather than a 0-12 hour forecast model.

This research sought to determine whether the weighting factors on the interconnections in a BP model could be used to prioritize the relative contribution of the input variables.

### 3.6.2 General Approach

This research was performed during April-May 1989. A Hecht-Neilsen Anza Plus neurocomputer-board in an 80286-based microcomputer was used to perform the experiments. The training data base used was reconstructed from the original raw sounding data files.

Once the apparent optimal parameter settings (listed in Table 1) were found, the number of hidden nodes, the number of passes, and the learning rate parameters were selectively varied to observe the effect on weekly forecasting skill scores for the test period. This task was accomplished by setting all parameters to their optimal values, and then varying the settings for one parameter at a time. The ten-year historical data base was then processed through the network to create a forecast model.

Once a BP forecast model was created, the 5-month testing data base for 1987 was processed through this model one day at a time to produce the probability of rain for each day. The probability of rain for each of the 153 days in the test data base was then written to a forecast file. Each forecast file for each of the 24 models was overlaid onto a standard LOTUS™ spreadsheet, where the daily, weekly, and monthly Brier-based skill scores were immediately calculated. The results of these experiments are shown in Tables 3, 5, and 7.

### 3.6.3 Spreadsheet Calculation of Skill Score

Attached as Appendix A are samples of 3 of the 24 LOTUS™ spreadsheets that were used to calculate skill scores for the various BP models. These spreadsheets automatically calculated the performance of each experimental model when the BP output file was overlaid.

The Optimal Parameters column shows the optimal settings for BP-Atlanta-241. The column is the same on all spreadsheets.

The Variable Changed column shows which parameter was changed and its setting.

The Day # column is a day count number for each of the 153 days or records in the testing data base.

The Forecast Output column is the PoP for that day.

The Actual Rain column contains either a "1" or a "0" to designate whether it rained or did not rain on that particular day during the 12Z-24Z period.

The ANS column is the squared error between the probability forecast column and the Actual Rain column.

The Climatology column is the squared error between climatology for each month and the Actual Rain column. The climatology for rain in May was 27.7%; in June, it was 21.0%; in July, it was 24.9%; in August, it was 22.8%; and in September, it was 23.0%. A single climatology was used for all months in Phase I to compute skill scores for the GOPAD-ATLANTA-RIR model, so the skill scores prepared in Phase II are slightly different than those reported in the Phase I Final Report.

The Daily, Weekly, and Monthly columns compute the skill scores for the present day and the past seven days, and for the present day and the past 30 days, respectively.

The Brier-based skill score was computed according to the following formula:

$$SS = 1 - \frac{\sum(\text{ANS sq error})}{\sum(\text{climatology sq error})}$$

### 3.6.4 Comparative Performance Evaluations

#### 3.6.4.1 Objectives and Approaches

The objective of this research was to compare the performance of BP-ATLANTA models to the National Weather Service Forecast Office (NWSFO), the LFM/MOS, and the GOPAD-ATLANTA-RIR models created during Phase I. The approach was to create a series of BP-based forecast models that were similar in structure to the GOPAD-ATLANTA-RIR model developed in Phase I using a PC/AT with a Hecht-Neilsen neurocomputer board installed. The performance of these new models would then be compared to the performance of the GOPAD-ATLANTA-RIR, the NWSFO, and the LFM/MOS forecasts.

As an additional objective, CCI sought to verify the performance of the BP-ATLANTA-241 model by completely reprocessing the original rawinsonde training data base in-house. Consequently, all the preprocessed historical data files that were used to find the optimal parameter settings for BP-Atlanta-241 were discarded. In conjunction with the reconstruction of these data bases, all forecasts were consolidated into LOTUS™ spreadsheets so that all skill score computations would be calculated exactly the same.

#### 3.6.4.2 Research Results

Six BP forecast models were created with the optimal parameter settings used by the BP-ATLANTA-241 model. These models are designated BP-E241, BP-F241, BP-G241, BP-E32, BP-F32, and BP-G32. Each of these models was trained on a different combination of months. The E-model was trained on May-June-July data; F-model was trained on June-July-August data; and G-model was trained on July-August-September data. Although neither a D-model nor an H-model was developed, the D, E, and F-models would be polled to produce a forecast for June; the E, F, and G-models would be polled for July; and the F, G, and H-models would be polled for August in an operational environment.

The numbers 241 or 32 in a model's name indicate the number of input variables that were used in the training mode. The 32 variables were those that GOPAD selected out of all the 241 variables that were available as candidate predictor variables--a form of

dimensionality reduction. Thus, it was possible to measure how much information was contained in the variables that GOPAD1 (i.e., the BASIC language version) had selected.

The skill scores for these models were calculated using the Lotus™ spreadsheets described earlier so they could be compared to the GOPAD-ATLANTA-RIR, the WSFO, and LFM/MOS forecast models.

Table 12 summarizes the three-month combined skill scores. This table shows that the GOPAD1 selection process appears to lose some information as a result of dimensionality reduction.

TABLE 12  
THREE-MONTH SKILL SCORES  
USING BP-ATLANTA-241 PARAMETER SETTINGS

<u>Name</u>	<u>E-Models</u>	<u>F-Models</u>	<u>G-Models</u>	<u>Summer</u>
BP-241	25.0%	27.0%	22.0%	not computed
BP-32	17.5%	19.7%	15.6%	not computed
GOPAD-ATL	22.2%	10.0	18.8%	26.3*
LFM/MOS	n/a	n/a	n/a	16.1%
WSFO	n/a	n/a	n/a	21.7%
BP-241**	2.1%	5.9%	0.79%	not computed

\*This score represents the result of polling the E, F and G-models, and applying the Reliability Index Rule (RIRm) as modified. In Phase I, the skill score for the GOPAD-ATLANTA-RIR model used 22% as the climatology for all five months. In Phase II, the actual climatologies for each month were computed and used in the computation of skill scores. Consequently, there is a slight difference between the skill scores for GOPAD reported in the Phase I and Phase II final reports.

\*\*These models used the same OZ sounding that the LFM/MOS model used to make the 12-24Z forecast; whereas the other BP and GOPAD models used the 12Z sounding to make the 12-24Z forecast.

Table 13 shows the skill scores for each model for each month.

**TABLE 13**  
**MONTHLY SKILL SCORES**  
**USING BP-ATLANTA-241 PARAMETER SETTINGS**

<u>Name</u>	<u>June</u>	<u>July</u>	<u>August</u>	<u>Summer</u>
BP-E241	49.3%	6.9%	-0.8%	25.0%
BP-F241	46.5%	12.1%	7.6%	27.0%
BP-G24	38.1%	0.5%	10.8%	22.0%
BP-E32	41.0%	10.7%	-23.2%	17.5%
BP-F32	35.4%	11.1%	- 4.7%	19.7%
BP-G32	24.6%	7.1%	4.4%	15.6%
GOPAD-RIR	43.2%	22.4%	-0.6%	26.3%
LFM/MOS	26.0%	12.0%	3.0%	16.1%
WSFO	35.6%	11.3%	9.6%	21.7%

Table 14 shows the weekly skill scores using BP-Atlanta-241 parameter settings. The rain column shows the number of times it rained during each week.

**TABLE 14**  
**WEEKLY SKILL SCORES**  
**USING BP-ATLANTA-241 PARAMETER SETTINGS**

<u>Summer-87</u>	<u>WSFO</u>	<u>LFM/MOS</u>	<u>GOPAD-E</u>	<u>GOPAD-F</u>	<u>GOPAD-G</u>	<u>RIR</u>	<u>Rain</u>
June 7	-19.0	4.3	7.6	-21.7	15.5	5.4	1
14	2.7	14.3	40.8	25.2	35.4	27.3	2
21	61.3	39.2	64.5	48.4	40.8	5.6	6
28	34.1	18.3	20.6	13.7	47.9	29.3	3
July 5	24.7	24.2	49.0	1.1	36.4	54.9	3
12	-11.3	2.1	16.7	0.7	25.3	34.0	1
19	18.5	1.8	44.5	10.3	39.2	44.5	1
26	28.5	17.0	-24.5	6.8	-22.4	-22.4	2
August 2	6.8	5.4	-19.9	-37.7	-0.7	-7.4	2
9	13.9	11.6	-1.7	13.3	-1.7	-8.3	4
16	-36.5	-24.0	83.6	-50.6	15.1	54.3	0
23	17.0	52.4	64.4	83.6	67.1	75.4	0
30	1.9	-41.7	-204.0	-127.3	-220.4	-47.0	0
Averages	10.97	9.61	10.9	-2.6	6.0	23.5	
J-J-A	21.7	16.1	22.2	10.0	18.8	26.3	

Table 15 shows weekly skill scores using BP-Atlanta-241 Parameter Settings. The rain column shows the number of times it rained during each week.

Summer '7	E241	F241	G241	E32	F32	G32	Rain
June 7	22.7	21.2	10.8	-5.8	3.1	3.2	1
14	31.7	31.2	27.5	38.6	27.1	18.6	2
21	65.7	64.4	55.1	62.8	53.5	36.7	6
28	46.0	39.7	41.3	33.5	28.9	17.0	3
July 5	26.8	30.1	-4.7	24.1	22.3	20.3	3
12	-16.9	11.5	24.8	-4.1	4.3	5.2	1
19	44.3	28.9	34.0	51.1	42.4	35.7	1
26	-11.3	-9.1	-19.2	-3.4	-3.0	-13.2	2
August 2	-12.6	-6.4	-5.1	-7.5	-2.6	-6.1	2
9	16.2	22.2	1.0	17.6	24.6	19.4	4
16	22.0	-11.1	53.4	-50.6	-64.1	-28.1	0
23	65.8	52.6	72.3	-46.5	-14.1	23.7	0
30	-1.4	-20.8	39.7	-184.0	-56.0	17.7	0
Averages	23.0	19.6	25.4	-5.7	5.1	11.5	
J-J-A	25.0	27.0	22.0	17.5	19.7	15.6	
M-J-J-A-S	16.4	20.9	22.4	11.0	16.0	15.8	

### 3.6.5 Identification of Important Predictor Variables

#### 3.6.5.1 Objective

The objectives of the research are (1) to create a list of parameters sorted according to each parameter's relative weighting along the interconnection paths to the output node; and (2) to identify the 32 GOPAD selected parameters in this sorted list to determine if weights along the interconnections could be used to find important variables.

#### 3.6.5.2 Research Results

This research was conducted during April, 1989. An investigation was conducted to determine whether the BP learning algorithm could be used to identify the predictor variables that had the greatest influence on the forecast. This effort was thought to be useful because the most important ANS variables could be compared to those selected

by the statistical analysis process in GOPAD1. Since statistical analysis is the most time-consuming GOPAD process, it might be possible for the BP algorithm to perform dimensionality reduction because it appeared to be much faster than GOPAD1.

The BP-F241 model was used for this research. The weights between each input node and the output node for all interconnection paths were summed. These weights were then sorted. The 32 candidate predictor variables that GOPAD selected were identified in this sorted list to determine if they were bunched near the top, middle, or bottom of the list, or whether they were scattered evenly throughout. Appendix A shows the sorted list with all 241 variables, and the 32 variables that GOPAD selected as containing the most statistical information. This Appendix shows that the GOPAD-selected variables are scattered fairly evenly throughout this list. Table 16 is an extract from Appendix A showing just the 32 variables that GOPAD selected. Based on these results, simply summing the weights along the interconnections does not appear to provide any insight into which variables are most important.

TABLE 16  
SUMMARY OF WEIGHTS ALONG THE INTERCONNECTIONS  
FROM EACH INPUT NODE TO THE OUTPUT NODE  
FOR THE GOPAD SELECTED VARIABLES

<u>Ranking</u>	<u>Weighting</u>	<u>Input Variable</u>
7	2.541121	CA600U
22	2.350847	AA900D
25	2.340340	WA400U
33	2.296635	AA800U
42	2.250115	AA900V
50	2.207791	CA800V
65	2.160017	AA300D
69	2.137422	AA600U
77	2.088976	AA600T
90	2.061990	WA700T
94	2.058352	AA800V
98	2.039243	DAYCNT
103	2.031388	CA900V
104	2.030351	AA100U
107	2.024281	CA400U
122	1.982341	AA700D
127	1.974752	CA800U
129	1.961482	WA800V
139	1.938703	AA700U
145	1.930760	A400U
155	1.887024	AA100T
158	1.875487	CA200T
165	1.853136	A300T
186	1.769200	WA700V
188	1.760480	WA900V
190	1.748589	CA700V
191	1.745677	CA300U
204	1.692686	WA300T
211	1.658782	CA600D
221	1.596003	CA600T
232	1.440968	WA900U
233	1.435088	AA700V

#### 4.0 GOAL ORIENTED PATTERN DETECTION

##### 4.1 Background

Previously, CCI had investigated expert systems for creating tactical weather forecast models. During Phase I and II, standard and non-standard neural net approaches were

investigated. Through this effort, it was found that a proprietary algorithm, called **Goal Oriented Pattern Detection (GOPAD)**, developed by Dr. Kenneth Young at the Institute of Atmospheric Physics, University of Arizona, held the greatest potential to achieve Army objectives for tactical weather forecasting. During CCI's research, GOPAD was used to produce two experimental models--GOPAD-Atlanta-RIR and GOPAD-SHOOTOUT-89. The GOPAD-Atlanta-RIR was a Probability of Precipitation (PoP) model developed for Hartsfield International Airport in Atlanta, Georgia. The GOPAD-SHOOTOUT-89 model was a severe and significant weather forecast model that was independently tested by NOAA during a real-time severe and significant weather forecasting exercise called SHOOTOUT-89 that took place in the Boulder and Denver, Colorado, area. The forecasting skill of these GOPAD models appears to be very promising, in spite of the limited number of sources of candidate predictor variables for the former model, and the limited amount of input data that was available for the latter model.

#### 4.2 GOPAD Description

GOPAD is technically described as a statistical, optimizing, machine-learning, analogue, forecast model creation, software tool. GOPAD extends the multi-discriminant analysis (MDA) methods developed by Miller (1962), and the analogue forecasting method of Kruizinga and Murphy (1983). GOPAD uses a k-nearest neighbor search. GOPAD produces data that can be used to construct a mesoscale, real-time weather forecasting software program that executes in seconds.

In general, the GOPAD model development tool (1) creates optimal machine-derived indices from highly correlated variables; (2) identifies the optimal statistical relationships between all candidate predictor variables and indices using a very large, historical weather data set (i.e., 100 to 30,000 variables/indices per data point and 100 to 40,000 data points); and (3) optimizes the n-space scaling and neighborhood size to provide information that can be used to prepare a non-linear forecast model. GOPAD models are able to reveal the underlying physical relationships upon which the model is based in the form of exemplars--thus enabling a meteorologist to examine a model's forecast.

Appendix B is a paper that was presented at the 1989 EOSAEL/TWI Conference that describes how GOPAD operates, the types of tactical mesoscale forecast models that

could be developed, a method for defining forecast models, and how the GOPAD development process is used to create new forecast models.

#### 4.3 Conclusions

The full potential of the GOPAD development system to create mesoscale models that can provide accurate forecasting information to the Staff Weather Officer on the battlefield has not yet been determined. To date, GOPAD has been used to produce forecast models with very few sources of candidate predictor variables (i.e., rawinsonde and mesonet) and, in the SHOOTOUT-89 exercise, with a severely limited and inaccurate historical data base. The true potential of GOPAD cannot be fully documented until (a) all available sources of predictor variables are used, (b) an adequate historical training data base is provided, and (3) accurate records are available for the event to be predicted. These requirements also point out the Achilles heal for any neural net approach. However, when compared to the knowledge engineering problem for an expert systems approach to tactical weather forecasting, a machine learning approach still appears to offer the greatest long term cost-benefit to the Army.

### 5.0. MESOSCALE WEATHER FORECASTING EXERCISE--SHOOTOUT-89

#### 5.1 Background

At the conclusion of Phase I research, GOPAD1 (i.e., the BASIC language version) appeared to be a promising approach for automating the construction of mesoscale weather forecasting models for a tactical environment. However, GOPAD1 had several problems that appeared to limit its usefulness for more complex problems that would require many sources of predictor variables and larger data bases. Consequently, research with a more traditional neural net (i.e., the back-propagation learning algorithm) was undertaken for comparison purposes.

Between Phase I and Phase II, the GOPAD1 program was upgraded to a VAX FORTRAN version called GOPAD2. This new version appeared to overcome many of the problems perceived in GOPAD1. Since GOPAD2 appeared to have much more potential than GOPAD1, a decision was made to use GOPAD2 to construct a model that would

participate in the Forecast System Laboratory/NOAA-sponsored exercise called SHOOTOUT-89. The SHOOTOUT-89 model is referred to as GOPAD-RT89.

## 5.2 SHOOTOUT-89 Evaluations

### 5.2.1 NOAA/FSL Comparative Evaluation

A massively co-authored paper is being prepared by NOAA/FSL that evaluates all six models that participated in the SHOOTOUT-89 exercise and will be submitted for publication in the Bulletin of American Meteorological Society (BAMS) in 1990.

### 5.2.2 Performance Evaluation

Appendix C is a paper that quantitatively compares the performance of all models that participated in SHOOTOUT-89 in more detail.

## 5.3 Conclusions

There are many different ways to quantitatively and qualitatively compare the performance of the system that participated in the SHOOTOUT-89 exercise. We choose to summarize and caveat the quantitative performance in Table 17 and Table 18.

First, Table 17 shows the (Brier) skill scores for severe weather based upon the forecasts in which there was no statistically significant difference between reporting of severe weather between 1985/87 and 1989 (i.e., Regions II, III, and IV). This table eliminates the effect from seriously under-reporting significant weather in all regions, and from seriously under-reporting severe weather in region I. GOPAD and ALPS are most helped by this caveat.

TABLE 17  
SKILL SCORES FOR SEVERE WEATHER  
IN REGIONS II, III, AND IV

GOPAD1	+ 2.1%
GOPAD2	+ 1.9%
ALPS	- 0.7%
Willard	-11.9%
KASSPr	-17.0%
CONVEX	-24.0%
OCI	-32.3%

Second, Table 18 shows the skill scores only for region IV which was the only region that had an adequate number of events upon which to train a GOPAD model. This table mitigates the fact that there was not a large historical data base available to develop a GOPAD model. GOPAD is helped most by this caveat.

TABLE 18  
SKILL SCORES FOR SEVERE WEATHER  
IN REGION IV

GOPAD1	+13.8%
GOPAD2	+13.2%
ALPS	+ 1.8%
KASSPr	- 0.2%
OCI	- 3.1%
Willard	-12.6%
CONVEX	-40.9%

## 6.0 CLOUD IMAGE REPRESENTATION, RECOGNITION, AND UNDERSTANDING SOFTWARE

### 6.1 Background

**Cloud Image Representation, Recognition, and Understanding Software (CIRRUS-I)** autonomously tracks individual homogeneous temperature regions in GOES Infrared (IR) imagery, and intelligently derives cloud displacement vectors from the leading edges

of tracked cloud-objects. The CIRRUS-I vector file could be used as input to a vorticity modeling program to produce synoptic wind or stream flow fields over North America. The synoptic wind patterns would then be used as an important source of candidate predictor variables for a neural net or GOPAD.

## 6.2 CIRRUS-I Data Flow

Appendix D is a paper that was presented at the 1989 EOSAEL/TWI Conference. This paper describes how the CIRRUS algorithm operates.

## 6.3 CIRRUS-I Performance

Appendix E is a series of photographs that show examples of how CIRRUS-I performs.

## 6.4 Conclusions

CIRRUS-I was developed to provide yet another source of candidate predictor variables that would be processed by GOPAD to produce a more accurate forecast model. The ultimate test of the usefulness of CIRRUS-I for mesoscale forecasting is the quality of systematic information contained in its candidate predictor variables that can contribute to the forecast relative to the information available from other sources. Therefore, the best way to determine the value of the CIRRUS-I and the vorticity modeling program is to produce a multi-year historical synoptic wind flow data base, and measure the statistical contribution of CIRRUS-I as a source of predictor variables relative to the candidate predictor variables from other sources (e.g., rawinsonde, mesonet, NGM, barotropic, etc.).

CIRRUS-I lays the foundation for automating many tedious visual analysis tasks that are performed by a human, where shape, relative proximity of individual objects to each other, *a priori* knowledge, and inferencing are important for object recognition and image interpretation. In the weather domain, for example, CIRRUS-I could be extended to recognize features in GOES satellite imagery such as fronts, troughs, ridges, and areas of high and low pressure, and to speculate about the future state and location of these features.

For other applications, CIRRUS-I demonstrates the usefulness of a very innovative, non-digital, image representation scheme that makes it possible to develop software programs that can use the visual cues that a human uses to recognize objects. This approach to image processing mitigates many classical image understanding problems.

#### 7.0 PHASE II RECOMMENDATIONS

Artificial Intelligence techniques investigated during Phase I and II can be used to provide a new level of automated computer support to the Staff Weather Officer. In order to properly evaluate the capability of these technologies to support the SWO, a human forecaster who is using GOPAD models and/or CIRRUS should be directly compared to a second forecaster who is using the next best technology that might be available in a tactical environment. If it can be shown that the performance of the former forecaster is statistically higher than the latter, then the value of a system should be apparent.

**APPENDIX A**

**BRIER-BASED SKILL SCORES FOR BP-ATLANTA-241**

**USING OPTIMAL PARAMETERS**

Appendix A

BRIER-BASED SKILL SCORES FOR BP-ATLANTA-241  
USING OPTIMAL PARAMETERS

<u>Optimal Parameters</u>	<u>Variable Changed</u>	<u>Architectural Options</u>
2		# Slabs
30		# Hidden Nodes
10		# Passes
1		# Iterations
0.01		Learning Rate
0.9		Momentum
Table		Sigmoid Source
0.1		Random Seed
241		# Input parameters
no		Input slab connected to output

Overall Performance:

June-July-Aug Skill = 26.1%  
May-June-July-Aug-Sept Skill = 21.4%

<u>Day#</u>	<u>Forecast Output</u>	<u>Actual Rain</u>	<u>Squared-Errors</u>		<u>Skill Scores</u>			<u>Date</u>
			<u>ANS</u>	<u>Climatology</u>	<u>Daily</u>	<u>Weekly</u>	<u>Monthly</u>	
1	0.201184	1	0.638	0.522	-22.2%			May 1
2	0.499511	0	0.250	0.077	-224.2%			
3	0.305489	0	0.093	0.077	-21.3%			
4	0.345105	1	0.429	0.522	17.9%			
5	0.062103	0	0.004	0.077	95.0%			
6	0.209793	0	0.044	0.077	42.8%			
7	0.242564	0	0.059	0.077	23.5%	-6.1%		
8	0.231266	0	0.053	0.077	30.5%	5.3%		
9	0.080213	0	0.006	0.077	91.6%	30.0%		
10	0.203865	0	0.042	0.077	46.0%	35.2%		
11	0.528777	1	0.222	0.522	57.5%	56.3%		
12	0.494628	0	0.245	0.077	-217.9%	31.8%		
13	0.460046	0	0.212	0.077	-175.0%	14.8%		
14	0.736211	1	0.070	0.522	86.7%	40.6%		
15	0.650689	0	0.423	0.077	-450.2%	14.7%		
16	0.540196	0	0.292	0.077	-279.2%	-5.3%		
17	0.534855	0	0.286	0.077	-271.8%	-22.4%		
18	0.677047	0	0.458	0.077	-495.7%	-101.8%		
19	0.745583	1	0.065	0.522	87.6%	-26.4%		
20	0.316369	0	0.100	0.077	-30.1%	-18.5%		
21	0.548915	1	0.203	0.522	61.0%	-27.9%		
22	0.109134	0	0.012	0.077	84.5%	0.9%		
23	0.067608	0	0.005	0.077	94.1%	21.0%		

24	0.458348	0	0.210	0.077	-173.0%	26.3%	
25	0.054701	0	0.003	0.077	96.1%	58.2%	
26	0.038394	0	0.001	0.077	98.1%	45.7%	
27	0.025107	0	0.001	0.077	99.2%	55.8%	
28	0.050988	0	0.003	0.077	96.6%	56.5%	
29	0.103930	0	0.011	0.077	86.0%	56.7%	
30	0.043365	0	0.002	0.077	97.6%	57.2%	
31	0.077169	0	0.006	0.077	92.3%	95.1%	12.1%
32	0.125600	0	0.016	0.044	63.9%	92.3%	16.5%
33	0.025589	0	0.001	0.044	98.5%	91.9%	21.3%
34	0.175114	1	0.680	0.626	-8.7%	29.7%	18.3%
35	0.167490	0	0.028	0.044	35.7%	24.7%	18.5%
36	0.035914	0	0.001	0.044	97.0%	23.1%	18.0%
37	0.012747	0	0.000	0.044	99.6%	20.5%	18.3%
38	0.031232	0	0.001	0.044	97.8%	18.1%	19.0%
39	0.020138	0	0.000	0.044	99.1%	19.8%	19.6%
40	0.075721	0	0.006	0.044	86.9%	19.2%	19.0%
41	0.028571	0	0.001	0.044	98.1%	87.7%	19.3%
42	0.227640	1	0.597	0.626	4.7%	31.7%	12.9%
43	0.322525	0	0.104	0.044	-138.4%	20.2%	15.4%
44	0.587706	1	0.170	0.626	72.8%	40.2%	25.4%
45	0.340923	0	0.116	0.044	-166.3%	32.4%	16.6%
46	0.348644	1	0.424	0.626	32.2%	30.9%	25.5%
47	0.605566	1	0.156	0.626	75.1%	40.5%	35.1%
48	0.617858	1	0.146	0.626	76.7%	46.8%	43.1%
49	0.372276	0	0.139	0.044	-217.6%	52.4%	48.0%
50	0.590070	1	0.168	0.626	73.1%	59.0%	47.2%
51	0.606731	1	0.155	0.626	75.3%	59.5%	50.7%
52	0.496337	1	0.254	0.626	59.5%	62.1%	50.7%
53	0.500000	0	0.250	0.044	-472.9%	60.6%	47.0%
54	0.321672	1	0.460	0.626	26.5%	51.2%	44.8%
55	0.205455	0	0.042	0.044	3.3%	44.3%	46.8%
56	0.564338	1	0.190	0.626	69.7%	52.8%	48.1%
57	0.473900	1	0.277	0.626	55.8%	49.4%	48.2%
58	0.084266	0	0.007	0.044	83.7%	43.8%	48.0%
59	0.013363	0	0.000	0.044	99.6%	40.2%	47.8%
60	0.019568	0	0.000	0.044	99.1%	52.4%	47.7%
61	0.401452	0	0.161	0.044	-269.3%	53.9%	45.6%
62	0.516107	1	0.234	0.563	58.4%	56.3%	46.4%
63	0.538740	0	0.290	0.062	-366.2%	32.0%	43.1%
64	0.598312	1	0.161	0.563	71.4%	37.3%	44.7%
65	0.431104	1	0.324	0.563	42.5%	37.8%	44.4%
66	0.385837	0	0.149	0.062	-139.1%	30.6%	46.7%
67	0.324235	1	0.457	0.563	18.9%	26.6%	45.1%
68	0.518790	0	0.269	0.062	-332.4%	22.8%	42.6%
69	0.246714	0	0.061	0.062	2.2%	11.8%	42.0%
70	0.124851	0	0.016	0.062	75.0%	25.9%	42.0%
71	0.099996	0	0.010	0.062	83.9%	10.6%	42.0%
72	0.082845	0	0.007	0.062	89.0%	-3.3%	42.1%
73	0.185061	0	0.034	0.062	45.0%	8.9%	41.9%
74	0.134094	0	0.018	0.062	71.1%	4.8%	44.5%
75	0.200400	1	0.639	0.563	-13.5%	16.2%	42.1%
76	0.049912	0	0.002	0.062	96.0%	22.4%	40.4%
77	0.010091	0	0.000	0.062	99.8%	24.1%	41.7%

May 31  
June 1

June 30  
July 1

78	0.065186	0	0.004	0.062	93.2%	24.7%	42.8%
79	0.050237	0	0.003	0.062	95.9%	25.2%	40.7%
80	0.066873	0	0.004	0.062	92.8%	28.4%	38.2%
81	0.034068	0	0.001	0.062	98.1%	30.1%	40.2%
82	0.082919	0	0.007	0.062	89.0%	95.0%	37.7%
83	0.056340	0	0.003	0.062	94.9%	94.8%	34.7%
84	0.093677	0	0.009	0.062	85.9%	92.8%	32.7%
85	0.074432	0	0.006	0.062	91.1%	92.5%	36.9%
86	0.070176	1	0.865	0.563	-53.5%	4.5%	29.5%
87	0.166810	1	0.694	0.563	-23.2%	-10.2%	25.2%
88	0.073164	0	0.005	0.062	91.4%	-10.5%	21.2%
89	0.240061	0	0.058	0.062	7.4%	-14.0%	17.1%
90	0.095517	0	0.009	0.062	85.3%	-14.4%	17.3%
91	0.505859	0	0.256	0.062	-311.1%	-31.6%	12.9%
92	0.276299	1	0.524	0.563	7.0%	-24.3%	11.7%
93	0.213049	0	0.045	0.052	13.0%	-11.5%	13.8%
94	0.209307	1	0.625	0.595	-5.0%	-4.3%	7.8%
95	0.344002	1	0.430	0.595	27.7%	2.3%	13.1%
96	0.338295	1	0.438	0.595	26.5%	7.9%	9.3%
97	0.403096	0	0.162	0.052	-211.5%	1.4%	4.4%
98	0.419172	1	0.337	0.595	43.3%	16.0%	9.2%
99	0.171615	0	0.029	0.052	43.5%	18.5%	8.6%
100	0.208662	1	0.626	0.595	-5.2%	14.0%	10.6%
101	0.275129	0	0.076	0.052	-45.1%	17.3%	10.2%
102	0.081739	0	0.007	0.052	87.2%	16.0%	10.2%
103	0.145600	0	0.021	0.052	59.4%	13.3%	9.9%
104	0.172868	0	0.030	0.052	42.7%	22.4%	9.4%
105	0.103839	0	0.011	0.052	79.3%	11.9%	9.7%
106	0.062674	0	0.004	0.052	92.5%	14.7%	9.7%
107	0.326808	0	0.107	0.052	-104.7%	30.2%	10.9%
108	0.474874	0	0.226	0.052	-332.3%	-10.8%	7.1%
109	0.242026	0	0.059	0.052	-12.3%	-25.1%	5.9%
110	0.299719	0	0.090	0.052	-72.2%	-43.9%	4.4%
111	0.122418	0	0.015	0.052	71.3%	-39.8%	4.0%
112	0.049819	0	0.002	0.052	95.2%	-37.5%	3.9%
113	0.029958	0	0.001	0.052	98.3%	-36.7%	3.7%
114	0.023531	0	0.001	0.052	98.9%	-7.6%	3.7%
115	0.122103	0	0.015	0.052	71.4%	50.1%	3.3%
116	0.141637	0	0.020	0.052	61.5%	60.6%	2.9%
117	0.279434	0	0.078	0.052	-49.7%	63.9%	1.6%
118	0.108471	0	0.012	0.052	77.4%	64.7%	8.0%
119	0.116060	0	0.013	0.052	74.2%	61.7%	12.2%
120	0.241310	0	0.058	0.052	-11.6%	46.0%	11.0%
121	0.447218	0	0.200	0.052	-283.4%	-8.6%	7.9%
122	0.104385	0	0.011	0.052	79.1%	-7.5%	7.7%
123	0.548190	0	0.301	0.052	-476.1%	-84.3%	6.6%
124	0.397470	0	0.158	0.053	-196.1%	-105.5%	4.1%
125	0.304454	0	0.093	0.053	-73.7%	-126.8%	3.0%
126	0.109419	0	0.012	0.053	77.6%	-125.7%	5.3%
127	0.106783	0	0.011	0.053	78.6%	-112.3%	2.4%
128	0.341143	1	0.434	0.591	26.6%	-12.1%	2.4%
129	0.511472	1	0.239	0.591	59.6%	13.9%	14.2%
130	0.424650	0	0.180	0.053	-237.9%	22.2%	4.8%
131	0.119716	0	0.014	0.053	73.1%	32.2%	5.3%

July 31  
Aug 1

Aug 31  
Sept 1

132	0.280616	0	0.079	0.053	-47.6%	33.1%	6.5%
133	0.317637	0	0.101	0.053	-89.1%	27.0%	5.7%
134	0.717210	0	0.514	0.053	-864.0%	-7.7%	-12.7%
135	0.637933	0	0.407	0.053	-662.7%	-68.3%	-26.6%
136	0.294620	0	0.087	0.053	-62.7%	-270.1%	-28.6%
137	0.077867	0	0.006	0.053	88.6%	-223.5%	-28.4%
138	0.065246	0	0.004	0.053	92.0%	-220.8%	-28.4%
139	0.388849	0	0.151	0.053	-183.4%	-240.2%	-29.9%
140	0.347979	0	0.121	0.053	-126.9%	-245.6%	-26.1%
141	0.077378	0	0.006	0.053	88.8%	-109.5%	-24.1%
142	0.660391	1	0.115	0.591	80.5%	46.2%	-4.7%
143	0.147309	0	0.022	0.053	59.3%	53.3%	-4.8%
144	0.042324	0	0.002	0.053	96.6%	53.8%	-4.8%
145	0.194062	0	0.038	0.053	29.4%	50.1%	-5.8%
146	0.068787	0	0.005	0.053	91.1%	66.2%	-5.9%
147	0.070240	0	0.005	0.053	90.8%	78.9%	-5.6%
148	0.008985	0	0.000	0.053	99.8%	79.6%	-4.9%
149	0.009869	0	0.000	0.053	99.8%	81.0%	-2.6%
150	0.128415	0	0.016	0.053	69.1%	82.4%	-2.7%
151	0.169818	0	0.029	0.053	46.0%	75.1%	-3.1%
152	0.283186	0	0.080	0.053	-50.3%	63.8%	-3.7%
153	0.110087	0	0.012	0.053	77.3%	61.8%	2.0%

Sept 30

BRIER-BASED SKILL SCORES FOR BP-ATLANTA-241  
USING LEARNING RATE = .005

<u>Optimal Parameters</u>	<u>Variable Changed</u>	<u>Architectural Options</u>
2		# Slabs
30		# Hidden Nodes
10		# Passes
1		# Iterations
0.01	.005	Learning Rate
0.9		Momentum
Table		Sigmoid Source
0.1		Random Seed
241		# Input parameters
no		Input slab connected to output

Overall Performance:

June-July-Aug Skill = 23.9%  
May-June-July-Aug-Sept Skill = 19.0%

<u>Day#</u>	<u>Forecast Output</u>	<u>Actual Rain</u>	<u>Squared-Errors</u>			<u>Skill Scores</u>		<u>Date</u>
			<u>ANS</u>	<u>Climatology</u>	<u>Daily</u>	<u>Weekly</u>	<u>Monthly</u>	
1	19%	1	0.657	0.522	-25.8%			May 1
2	46%	0	0.213	0.077	-176.5%			
3	28%	0	0.077	0.077	0.5%			
4	31%	1	0.477	0.522	8.6%			
5	10%	0	0.011	0.077	86.1%			
6	19%	0	0.035	0.077	54.6%			
7	22%	0	0.050	0.077	35.1%	-6.3%		
8	29%	0	0.085	0.077	-10.9%	3.7%		
9	10%	0	0.009	0.077	87.7%	24.4%		
10	19%	0	0.036	0.077	52.7%	28.4%		
11	42%	1	0.333	0.522	36.2%	43.1%		
12	52%	\	0.267	0.077	-246.5%	17.1%		
13	44%	0	0.192	0.077	-149.4%	1.1%		
14	67%	1	0.108	0.522	79.4%	27.9%		
15	57%	0	0.321	0.077	-317.0%	11.4%		
16	54%	0	0.292	0.077	-279.2%	-8.3%		
17	50%	0	0.251	0.077	-225.8%	-23.3%		
18	58%	0	0.334	0.077	-333.4%	-79.2%		
19	71%	1	0.081	0.522	84.4%	-10.4%		
20	41%	0	0.166	0.077	-115.1%	-8.6%		
21	57%	1	0.183	0.522	64.9%	-13.9%		
22	17%	0	0.028	0.077	63.2%	6.6%		
23	15%	0	0.022	0.077	71.2%	25.5%		
24	47%	0	0.226	0.077	-193.1%	27.3%		

25	13%	0	0.018	0.077	76.8%	49.3%	
26	9%	0	0.008	0.077	90.0%	33.9%	
27	7%	0	0.005	0.077	93.7%	50.2%	
28	11%	0	0.012	0.077	83.9%	40.8%	
29	19%	0	0.035	0.077	54.1%	39.5%	
30	6%	0	0.004	0.077	95.4%	43.0%	
31	19%	0	0.035	0.077	53.9%	78.2%	9.6%
32	19%	0	0.036	0.044	16.5%	73.1%	13.7%
33	7%	0	0.005	0.044	88.7%	71.8%	17.7%
34	25%	1	0.560	0.626	10.5%	32.6%	17.1%
35	28%	0	0.081	0.044	-85.6%	23.4%	17.0%
36	8%	0	0.006	0.044	85.6%	23.7%	16.5%
37	2%	0	0.000	0.044	98.9%	21.3%	16.7%
38	5%	0	0.002	0.044	94.4%	22.1%	17.1%
39	4%	0	0.002	0.044	95.8%	26.0%	18.4%
40	11%	0	0.011	0.044	73.7%	25.2%	17.7%
41	6%	0	0.004	0.044	91.5%	64.9%	17.8%
42	39%	1	0.373	0.626	40.5%	55.1%	18.8%
43	32%	0	0.105	0.044	-139.6%	44.0%	21.8%
44	56%	1	0.196	0.626	68.6%	52.9%	30.3%
45	46%	0	0.211	0.044	-382.9%	38.7%	20.7%
46	31%	1	0.478	0.626	23.6%	32.9%	26.1%
47	59%	1	0.170	0.626	72.9%	41.7%	35.5%
48	58%	1	0.175	0.626	72.0%	46.9%	42.4%
49	49%	0	0.237	0.044	-444.2%	40.3%	43.6%
50	57%	1	0.186	0.626	70.3%	48.6%	42.9%
51	63%	1	0.138	0.626	77.9%	50.4%	47.9%
52	58%	1	0.177	0.626	71.8%	58.9%	48.8%
53	54%	0	0.294	0.044	-573.5%	57.2%	44.7%
54	31%	1	0.471	0.626	24.8%	47.8%	42.7%
55	11%	0	0.012	0.044	71.4%	42.5%	45.3%
56	48%	1	0.272	0.626	56.5%	51.8%	45.9%
57	46%	1	0.293	0.626	53.2%	48.5%	46.1%
58	19%	0	0.035	0.044	19.1%	41.0%	45.5%
59	5%	0	0.002	0.044	95.2%	32.8%	45.4%
60	4%	0	0.002	0.044	95.7%	47.0%	45.6%
61	47%	0	0.219	0.044	-401.0%	43.1%	42.8%
62	51%	1	0.240	0.563	57.5%	46.6%	43.7%
63	57%	0	0.321	0.062	-415.1%	22.1%	40.4%
64	53%	1	0.217	0.563	61.5%	24.1%	41.8%
65	44%	1	0.310	0.563	45.0%	30.5%	41.8%
66	39%	0	0.150	0.062	-140.6%	23.4%	42.6%
67	28%	1	0.520	0.563	7.7%	18.4%	41.2%
68	50%	0	0.247	0.062	-296.1%	17.9%	38.9%
69	32%	0	0.101	0.062	-62.9%	3.8%	38.0%
70	22%	0	0.049	0.062	21.1%	17.8%	37.7%
71	20%	0	0.040	0.062	35.0%	1.4%	37.4%
72	12%	0	0.014	0.062	77.9%	-19.7%	37.5%
73	14%	0	0.019	0.062	70.1%	-5.7%	37.5%
74	12%	0	0.013	0.062	78.4%	-10.9%	37.5%
75	20%	1	0.634	0.563	-12.5%	7.1%	35.5%
76	8%	0	0.007	0.062	88.9%	17.2%	33.6%
77	2%	0	0.000	0.062	99.5%	22.4%	36.0%
78	6%	0	0.004	0.062	94.0%	26.3%	37.3%

May 31  
June 1

June 30  
July 1

79	8%	0	0.006	0.062	90.6%	27.1%	35.0%
80	12%	0	0.013	0.062	78.6%	27.7%	32.3%
81	8%	0	0.006	0.062	90.6%	28.5%	35.5%
82	14%	0	0.018	0.062	70.4%	87.5%	32.8%
83	13%	0	0.016	0.062	74.4%	85.4%	28.9%
84	17%	0	0.029	0.062	53.2%	78.8%	24.7%
85	16%	0	0.025	0.062	59.5%	73.9%	29.4%
86	10%	1	0.806	0.563	-43.0%	2.5%	23.1%
87	17%	1	0.685	0.563	-21.5%	-10.2%	18.9%
88	9%	0	0.008	0.062	86.8%	-10.4%	15.7%
89	27%	0	0.072	0.062	-15.2%	-14.1%	11.0%
90	10%	0	0.010	0.062	83.2%	-13.7%	11.8%
91	40%	0	0.159	0.062	-155.0%	-22.7%	9.2%
92	24%	1	0.581	0.563	-3.1%	-19.7%	7.4%
93	24%	0	0.060	0.052	-14.3%	-10.3%	10.2%
94	27%	1	0.535	0.595	10.1%	2.4%	5.8%
95	34%	1	0.442	0.595	25.7%	6.7%	11.6%
96	28%	1	0.514	0.595	13.6%	8.9%	7.5%
97	37%	0	0.140	0.052	-168.3%	3.4%	2.5%
98	39%	1	0.369	0.595	38.0%	13.4%	7.1%
99	25%	0	0.064	0.052	-23.4%	16.3%	6.8%
100	19%	1	0.649	0.595	-9.0%	11.9%	8.2%
101	24%	0	0.056	0.052	-7.1%	12.0%	8.7%
102	10%	0	0.011	0.052	79.2%	9.6%	9.2%
103	19%	0	0.038	0.052	27.7%	8.6%	9.1%
104	20%	0	0.039	0.052	24.9%	15.5%	8.6%
105	15%	0	0.023	0.052	56.4%	3.2%	8.4%
106	11%	0	0.013	0.052	75.7%	8.9%	8.2%
107	24%	0	0.057	0.052	-10.1%	35.2%	10.0%
108	36%	0	0.128	0.052	-146.0%	15.4%	7.8%
109	24%	0	0.059	0.052	-13.5%	2.2%	6.7%
110	27%	0	0.072	0.052	-37.5%	-7.2%	5.4%
111	24%	0	0.057	0.052	-9.8%	-12.1%	4.4%
112	10%	0	0.010	0.052	80.0%	-8.7%	4.3%
113	5%	0	0.002	0.052	95.5%	-5.9%	4.2%
114	5%	0	0.003	0.052	95.0%	9.1%	4.3%
115	11%	0	0.012	0.052	77.4%	41.0%	4.2%
116	14%	0	0.021	0.052	59.9%	51.5%	4.2%
117	24%	0	0.060	0.052	-14.8%	54.8%	3.4%
118	16%	0	0.025	0.052	52.7%	63.7%	8.7%
119	20%	0	0.041	0.052	21.4%	55.3%	12.3%
120	24%	0	0.059	0.052	-12.3%	39.9%	11.1%
121	41%	0	0.166	0.052	-219.2%	-5.0%	9.0%
122	21%	0	0.045	0.052	14.2%	-14.0%	8.1%
123	53%	0	0.278	0.052	-432.0%	-84.3%	5.5%
124	46%	0	0.216	0.053	-304.2%	-126.2%	2.8%
125	29%	0	0.084	0.053	-57.6%	-141.6%	2.3%
126	16%	0	0.025	0.053	53.6%	-136.5%	1.8%
127	17%	0	0.030	0.053	43.6%	-128.0%	-1.9%
128	34%	1	0.434	0.591	26.7%	-22.1%	0.5%
129	45%	1	0.301	0.591	49.1%	5.6%	10.2%
130	38%	0	0.143	0.053	-168.7%	15.0%	2.3%
131	13%	0	0.017	0.053	67.5%	28.7%	3.8%
132	24%	0	0.057	0.053	-5.9%	30.6%	6.4%

July 31  
Aug 1

Aug 31  
Sept 1

133	29%	0	0.082	0.053	-53.9%	26.6%	5.5%
134	68%	0	0.464	0.053	-768.8%	-3.3%	-10.9%
135	61%	0	0.372	0.053	-596.2%	-57.5%	-23.0%
136	30%	0	0.092	0.053	-71.8%	-228.3%	-24.8%
137	11%	0	0.012	0.053	77.5%	-193.1%	-24.4%
138	9%	0	0.008	0.053	84.7%	-190.6%	-24.1%
139	38%	0	0.143	0.053	-167.1%	-213.7%	-27.2%
140	40%	0	0.161	0.053	-201.7%	-234.8%	-28.3%
141	10%	0	0.011	0.053	79.6%	-113.6%	-26.5%
142	62%	1	0.142	0.591	76.0%	37.7%	-8.0%
143	22%	0	0.047	0.053	12.7%	42.6%	-7.6%
144	6%	0	0.004	0.053	93.0%	43.5%	-7.4%
145	18%	0	0.033	0.053	37.2%	40.7%	-8.3%
146	11%	0	0.012	0.053	77.8%	55.1%	-8.5%
147	7%	0	0.006	0.053	89.6%	72.1%	-8.3%
148	2%	0	0.000	0.053	99.3%	73.3%	-7.6%
149	2%	0	0.001	0.053	98.8%	72.6%	-5.8%
150	17%	0	0.028	0.053	47.8%	77.6%	-5.9%
151	17%	0	0.030	0.053	43.2%	70.5%	-5.5%
152	24%	0	0.060	0.053	-11.6%	63.6%	-5.5%
153	20%	0	0.039	0.053	26.3%	56.2%	-1.6%

Sept 30

BRIER-BASED SKILL SCORES FOR BP-ATLANTA-241  
USING NUMBER OF PASSES = 20

<u>Optimal Parameters</u>	<u>Variable Changed</u>	<u>Architectural Options</u>
2		# Slabs
30		# Hidden Nodes
10	20	# Passes
1		# Iterations
0.01		Learning Rate
0.9		Momentum
Table		Sigmoid Source
0.1		Random Seed
241		# Input parameters
no		Input slab connected to output

Overall Performance:

June-July-Aug Skill = 19.8%  
May-June-July-Aug-Sept Skill = 19.5%

<u>Day#</u>	<u>Forecast Output</u>	<u>Actual Rain</u>	<u>Squared-Errors</u>		<u>Skill Scores</u>			
			<u>ANS</u>	<u>Climatology</u>	<u>Daily</u>	<u>Weekly</u>	<u>Monthly</u>	<u>Date</u>
1	0.185356	1	0.664	0.522	-27.1%			May 1
2	0.548190	0	0.301	0.077	-290.5%			
3	0.299924	0	0.090	0.077	-16.9%			
4	0.410637	1	0.347	0.522	33.5%			
5	0.020944	0	0.000	0.077	99.4%			
6	0.125600	0	0.016	0.077	79.5%			
7	0.255900	0	0.065	0.077	14.9%	-3.8%		
8	0.091058	0	0.008	0.077	89.2%	15.9%		
9	0.052037	0	0.003	0.077	96.5%	46.1%		
10	0.200088	0	0.040	0.077	48.0%	51.2%		
11	0.637933	1	0.131	0.522	74.9%	73.2%		
12	0.426560	0	0.182	0.077	-136.5%	54.7%		
13	0.343781	0	0.118	0.077	-53.6%	44.3%		
14	0.617397	1	0.146	0.522	72.0%	56.0%		
15	0.561455	0	0.315	0.077	-309.7%	34.5%		
16	0.487551	0	0.238	0.077	-208.9%	18.1%		
17	0.319970	0	0.102	0.077	-33.0%	13.7%		
18	0.655997	0	0.430	0.077	-459.2%	-55.7%		
19	0.683208	1	0.100	0.522	80.8%	-1.5%		
20	0.056236	0	0.003	0.077	95.9%	6.5%		
21	0.471466	1	0.279	0.522	46.5%	-2.8%		
22	0.027480	0	0.001	0.077	99.0%	19.2%		
23	0.020274	0	0.000	0.077	99.5%	35.8%		
24	0.497070	0	0.247	0.077	-221.1%	25.7%		

25	0.020824	0	0.000	0.077	99.4%	55.8%	
26	0.005905	0	0.000	0.077	100.0%	46.0%	
27	0.007232	0	0.000	0.077	99.9%	46.3%	
28	0.020884	0	0.000	0.077	99.4%	53.7%	
29	0.036459	0	0.001	0.077	98.3%	53.6%	
30	0.012206	0	0.000	0.077	99.8%	53.7%	
31	0.013299	0	0.000	0.077	99.8%	99.5%	24.2%
32	0.050424	0	0.003	0.044	94.2%	99.1%	30.8%
33	0.017934	0	0.000	0.044	99.3%	98.9%	36.9%
34	0.217836	1	0.612	0.626	2.2%	39.6%	33.4%
35	0.058131	0	0.003	0.044	92.3%	37.3%	34.0%
36	0.016308	0	0.000	0.044	99.4%	35.2%	33.5%
37	0.001824	0	0.000	0.044	100.0%	32.8%	33.3%
38	0.012883	0	0.000	0.044	99.6%	30.3%	34.3%
39	0.009312	0	0.000	0.044	99.8%	30.6%	34.0%
40	0.037856	0	0.001	0.044	96.7%	30.5%	33.5%
41	0.011008	0	0.000	0.044	99.7%	98.2%	33.9%
42	0.180106	1	0.672	0.626	-7.4%	24.0%	23.5%
43	0.453019	0	0.205	0.044	-370.3%	0.9%	22.4%
44	0.633183	1	0.135	0.626	78.5%	31.0%	30.5%
45	0.228328	0	0.052	0.044	-19.5%	27.5%	25.3%
46	0.199619	1	0.641	0.626	-2.4%	16.8%	27.0%
47	0.587470	1	0.170	0.626	72.8%	28.8%	35.2%
48	0.736400	1	0.069	0.626	88.9%	39.5%	41.5%
49	0.177668	0	0.032	0.044	27.7%	50.5%	47.6%
50	0.649801	1	0.123	0.626	80.4%	62.0%	48.2%
51	0.594080	1	0.165	0.626	73.7%	61.1%	50.0%
52	0.310903	1	0.475	0.626	24.1%	55.9%	47.9%
53	0.420361	0	0.177	0.044	-304.9%	62.4%	45.1%
54	0.212395	1	0.620	0.626	0.9%	48.4%	40.8%
55	0.154184	0	0.024	0.044	45.5%	38.7%	43.6%
56	0.588416	1	0.169	0.626	72.9%	45.5%	45.3%
57	0.280813	1	0.517	0.626	17.4%	33.2%	42.8%
58	0.019700	0	0.000	0.044	99.1%	24.7%	42.5%
59	0.003090	0	0.000	0.044	100.0%	26.5%	42.3%
60	0.007815	0	0.000	0.044	99.9%	35.1%	42.1%
61	0.338076	0	0.114	0.044	-161.9%	43.9%	40.5%
62	0.488527	1	0.262	0.563	53.6%	46.6%	41.3%
63	0.484623	0	0.235	0.062	-277.3%	20.9%	38.6%
64	0.722527	1	0.077	0.563	86.3%	49.5%	41.2%
65	0.437342	1	0.317	0.563	43.8%	46.7%	41.1%
66	0.423457	0	0.179	0.062	-188.1%	37.7%	42.2%
67	0.332201	1	0.446	0.563	20.8%	32.7%	40.7%
68	0.555435	0	0.309	0.062	-395.6%	25.2%	37.7%
69	0.155590	0	0.024	0.062	61.1%	18.2%	37.6%
70	0.074298	0	0.006	0.062	91.1%	30.0%	37.7%
71	0.045777	0	0.002	0.062	96.6%	10.8%	37.8%
72	0.037047	0	0.001	0.062	97.8%	-3.2%	37.9%
73	0.181118	0	0.033	0.062	47.3%	12.4%	37.7%
74	0.095181	0	0.009	0.062	85.4%	12.0%	41.0%
75	0.078925	1	0.848	0.563	-50.6%	1.4%	37.6%
76	0.021125	0	0.000	0.062	99.3%	4.0%	35.3%
77	0.005992	0	0.000	0.062	99.9%	4.5%	36.0%
78	0.084795	0	0.007	0.062	88.4%	4.0%	39.0%

May 31  
June 1

June 30  
July 1

79	0.023757	0	0.001	0.062	99.1%	4.1%	36.9%
80	0.015573	0	0.000	0.062	99.6%	7.6%	33.3%
81	0.007800	0	0.000	0.062	99.9%	8.5%	33.8%
82	0.032191	0	0.001	0.062	98.3%	97.8%	30.3%
83	0.018404	0	0.000	0.062	99.5%	97.8%	26.9%
84	0.045310	0	0.002	0.062	96.7%	97.4%	27.9%
85	0.029367	0	0.001	0.062	98.6%	98.8%	31.0%
86	0.031828	1	0.937	0.563	-66.4%	-0.6%	25.0%
87	0.118895	1	0.776	0.563	-37.8%	-19.5%	19.5%
88	0.037116	0	0.001	0.062	97.8%	-19.6%	14.7%
89	0.138694	0	0.019	0.062	69.1%	-20.9%	15.0%
90	0.032405	0	0.001	0.062	98.3%	-20.9%	15.3%
91	0.581778	0	0.338	0.062	-443.7%	-44.3%	9.4%
92	0.280813	1	0.517	0.563	8.2%	-33.6%	8.6%
93	0.153549	0	0.024	0.052	54.8%	-17.5%	10.3%
94	0.130174	1	0.757	0.595	-27.1%	-13.5%	2.5%
95	0.187578	1	0.660	0.595	-10.9%	-16.2%	4.0%
96	0.356670	1	0.414	0.595	30.5%	-7.3%	-0.7%
97	0.464658	0	0.216	0.052	-313.9%	-16.3%	-7.5%
98	0.311740	1	0.474	0.595	20.4%	-0.4%	-3.3%
99	0.061480	0	0.004	0.052	92.8%	-0.4%	-4.7%
100	0.134775	1	0.749	0.595	-25.7%	-6.2%	-2.9%
101	0.202285	0	0.041	0.052	21.6%	-0.7%	-3.3%
102	0.033399	0	0.001	0.052	97.9%	4.9%	-3.4%
103	0.075448	0	0.006	0.052	89.1%	-2.6%	-3.6%
104	0.083890	0	0.007	0.052	86.5%	11.8%	-3.9%
105	0.045310	0	0.002	0.052	96.1%	10.9%	-3.5%
106	0.026455	0	0.001	0.052	98.7%	11.3%	-3.6%
107	0.226099	0	0.051	0.052	2.0%	70.2%	0.8%
108	0.583678	0	0.341	0.052	-553.1%	-11.8%	-4.9%
109	0.269517	0	0.073	0.052	-39.2%	-31.4%	-6.3%
110	0.308815	0	0.095	0.052	-82.8%	-56.0%	-8.0%
111	0.026205	0	0.001	0.052	98.7%	-54.2%	-8.1%
112	0.010997	0	0.000	0.052	99.8%	-53.7%	-8.3%
113	0.013808	0	0.000	0.052	99.6%	-53.6%	-8.5%
114	0.009831	0	0.000	0.052	99.8%	-39.6%	-8.7%
115	0.114467	0	0.013	0.052	74.9%	50.1%	-9.1%
116	0.165727	0	0.027	0.052	47.3%	62.5%	-9.7%
117	0.386763	0	0.150	0.052	-186.7%	47.6%	-12.4%
118	0.070367	0	0.005	0.052	90.5%	46.5%	-5.8%
119	0.069163	0	0.005	0.052	90.8%	45.2%	-1.1%
120	0.143067	0	0.020	0.052	60.8%	39.6%	-1.7%
121	0.404036	0	0.163	0.052	-212.9%	-5.0%	-4.8%
122	0.092114	0	0.008	0.052	83.7%	-3.8%	-5.2%
123	0.493164	0	0.243	0.052	-366.2%	-62.9%	-3.5%
124	0.418696	0	0.175	0.052	-228.5%	-69.4%	-7.7%
125	0.177810	0	0.032	0.052	40.7%	-76.1%	-7.9%
126	0.066326	0	0.004	0.053	91.8%	-75.4%	-3.5%
127	0.056340	0	0.003	0.053	94.1%	-70.1%	-0.6%
128	0.282591	1	0.515	0.591	13.0%	-7.9%	-3.8%
129	0.518546	1	0.232	0.591	60.8%	16.9%	10.4%
130	0.328960	0	0.108	0.053	-102.8%	26.2%	6.7%
131	0.112697	0	0.013	0.053	76.2%	37.5%	6.5%
132	0.371820	0	0.138	0.053	-159.1%	30.1%	10.2%

July 31  
Aug 1

Aug 31  
Sept 1

133	0.314050	0	0.099	0.053	-84.8%	23.6%	8.2%
134	0.791821	0	0.627	0.053	-1075.0%	-19.4%	-14.5%
135	0.688259	0	0.474	0.053	-787.7%	-85.4%	-31.4%
136	0.221350	0	0.049	0.053	8.2%	-303.6%	-32.8%
137	0.110183	0	0.012	0.053	77.2%	-277.9%	-33.1%
138	0.035310	0	0.001	0.053	97.7%	-274.8%	-33.1%
139	0.353762	0	0.125	0.053	-134.5%	-271.3%	-35.7%
140	0.335677	0	0.113	0.053	-111.2%	-275.0%	-27.4%
141	0.039158	0	0.002	0.053	97.1%	-107.6%	-24.8%
142	0.769080	1	0.053	0.591	91.0%	61.0%	-3.2%
143	0.090654	0	0.008	0.053	84.6%	65.5%	-3.4%
144	0.040313	0	0.002	0.053	97.0%	66.7%	-3.4%
145	0.176387	0	0.031	0.053	41.7%	63.4%	-4.3%
146	0.032805	0	0.001	0.053	98.0%	77.0%	-4.3%
147	0.035577	0	0.001	0.053	97.6%	89.2%	-3.9%
148	0.001396	0	0.000	0.053	100.0%	89.4%	-3.0%
149	0.000851	0	0.000	0.053	100.0%	88.4%	1.6%
150	0.049634	0	0.002	0.053	95.4%	89.9%	1.7%
151	0.184179	0	0.034	0.053	36.4%	81.3%	0.8%
152	0.210766	0	0.044	0.053	16.8%	77.7%	0.1%
153	0.027350	0	0.001	0.053	98.6%	77.8%	5.1%

Sept 30

NWSFO POP FORECAST SKILL SCORE  
0-12 HRS POP FORECASTER FOR HARTSFIELD INTERNATIONAL AIRPORT

June-July-August Skill Score = 22.2%

Day#	Forecast Output	Actual Rain	Squared-Errors			Skill Scores		Date
			ANS	Climatology	Daily	Weekly	Monthly	
32	30%	0	0.090	0.044	-106.2%			June 1
33	30%	0	0.090	0.044	-106.2%			
34	20%	1	0.640	0.626	-2.3%			
35	50%	0	0.250	0.044	-472.9%			
36	0%	0	0.000	0.044	100.0%			
37	0%	0	0.000	0.044	100.0%			
38	0%	0	0.000	0.044	100.0%	-20.5%		
39	0%	0	0.000	0.044	100.0%	-10.4%		
40	0%	0	0.000	0.044	100.0%	-0.3%		
41	20%	0	0.040	0.044	8.3%	5.1%		
42	10%	1	0.810	0.626	-29.4%	4.2%		
43	40%	0	0.160	0.044	-266.6%	-13.8%		
44	60%	1	0.160	0.626	74.4%	20.4%		
45	50%	0	0.250	0.044	-472.9%	3.4%		
46	50%	1	0.250	0.626	60.1%	18.6%		
47	70%	1	0.090	0.626	85.6%	33.2%		
48	60%	1	0.160	0.626	74.4%	41.6%		
49	60%	0	0.360	0.044	-724.9%	45.7%		
50	50%	1	0.250	0.626	60.1%	52.7%		
51	60%	1	0.160	0.626	74.4%	52.7%		
52	60%	1	0.160	0.626	74.4%	62.4%		
53	50%	0	0.250	0.044	-472.9%	55.5%		
54	30%	1	0.490	0.626	21.7%	43.1%		
55	30%	0	0.090	0.044	-106.2%	33.2%		
56	50%	1	0.250	0.626	60.1%	48.7%		
57	50%	1	0.250	0.626	60.1%	48.7%		
58	0%	0	0.000	0.044	100.0%	43.4%		
59	0%	0	0.000	0.044	100.0%	35.2%		
60	0%	0	0.000	0.044	100.0%	47.4%		
61	10%	0	0.010	0.044	77.1%	59.2%	36.6%	June 30
62	50%	1	0.250	0.563	55.6%	61.8%	37.8%	July 1
63	70%	0	0.490	0.062	-687.1%	29.9%	32.7%	
64	60%	1	0.160	0.563	71.6%	33.3%	35.7%	
65	40%	1	0.360	0.563	36.1%	32.6%	36.3%	
66	50%	0	0.250	0.062	-301.6%	20.1%	36.7%	
67	20%	1	0.640	0.563	-13.6%	10.8%	36.1%	
68	40%	0	0.160	0.062	-157.0%	5.3%	34.6%	
69	20%	0	0.040	0.062	35.7%	-8.3%	34.3%	
70	20%	0	0.040	0.062	35.7%	14.9%	34.0%	
71	20%	0	0.040	0.062	35.7%	-6.4%	33.7%	
72	20%	0	0.040	0.062	35.7%	-29.2%	33.5%	
73	20%	0	0.040	0.062	35.7%	-6.8%	33.6%	

74	30%	0	0.090	0.062	-44.6%	-3.3%	37.2%
75	20%	1	0.640	0.563	-13.6%	0.7%	35.7%
76	5%	0	0.003	0.062	96.0%	4.7%	33.5%
77	0%	0	0.000	0.062	100.0%	9.0%	36.3%
78	0%	0	0.000	0.062	100.0%	13.3%	35.1%
79	0%	0	0.000	0.062	100.0%	17.5%	31.8%
80	0%	0	0.000	0.062	100.0%	21.8%	28.9%
81	0%	0	0.000	0.062	100.0%	31.4%	33.7%
82	0%	0	0.000	0.062	100.0%	99.4%	31.9%
83	0%	0	0.000	0.062	100.0%	100.0%	28.6%
84	5%	0	0.003	0.062	96.0%	99.4%	24.5%
85	20%	0	0.040	0.062	35.7%	90.2%	28.2%
86	20%	1	0.640	0.563	-13.6%	27.1%	25.0%
87	40%	1	0.360	0.563	36.1%	27.5%	26.8%
88	30%	0	0.090	0.062	-44.6%	21.2%	22.6%
89	40%	0	0.160	0.062	-157.0%	10.1%	16.2%
90	30%	0	0.090	0.062	-44.6%	3.8%	14.8%
91	20%	0	0.040	0.062	35.7%	1.2%	14.4%
92	20%	1	0.640	0.563	-13.6%	-4.2%	11.1%
93	30%	0	0.090	0.052	-72.5%	-3.0%	9.9%
94	50%	1	0.250	0.595	58.0%	6.8%	10.4%
95	40%	1	0.360	0.595	39.5%	18.2%	19.7%
96	40%	1	0.360	0.595	39.5%	27.6%	17.0%
97	50%	0	0.250	0.052	-379.2%	20.9%	11.9%
98	40%	1	0.360	0.595	39.5%	24.2%	17.3%
99	40%	0	0.160	0.052	-206.7%	27.9%	18.3%
100	20%	1	0.640	0.595	-7.5%	22.8%	17.6%
101	30%	0	0.090	0.052	-72.5%	12.5%	16.7%
102	30%	0	0.090	0.052	-72.5%	2.2%	15.8%
103	30%	0	0.090	0.052	-72.5%	-15.7%	14.9%
104	40%	0	0.160	0.052	-206.7%	-9.5%	13.0%
105	20%	0	0.040	0.052	23.3%	-39.8%	12.9%
106	20%	0	0.040	0.052	23.3%	-26.6%	13.5%
107	5%	0	0.003	0.052	95.2%	-40.3%	16.7%
108	20%	0	0.040	0.052	23.3%	-26.7%	15.9%
109	20%	0	0.040	0.052	23.3%	-13.0%	15.1%
110	40%	0	0.160	0.052	-206.7%	-32.1%	12.3%
111	20%	0	0.040	0.052	23.3%	0.7%	11.5%
112	2%	0	0.000	0.052	99.2%	11.6%	11.4%
113	2%	0	0.000	0.052	99.2%	22.4%	11.2%
114	2%	0	0.000	0.052	99.2%	23.0%	11.1%
115	20%	0	0.040	0.052	23.3%	23.0%	10.3%
116	5%	0	0.003	0.052	95.2%	33.3%	10.1%
117	20%	0	0.040	0.052	23.3%	66.1%	9.9%
118	20%	0	0.040	0.052	23.3%	66.1%	12.5%
119	20%	0	0.040	0.052	23.3%	55.3%	9.9%
120	40%	0	0.160	0.052	-206.7%	11.6%	8.3%
121	20%	0	0.040	0.052	23.3%	0.7%	10.6%
122	10%	0	0.010	0.052	80.8%	8.9%	12.0%
123	50%	0	0.250	0.052	-379.2%	-58.8%	7.6%

July 31  
Aug 1

Aug 31

LFM/MOS POP FORECAST SKILL SCORE  
0-12 HRS POP FORECASTER FOR HARTSFIELD INTERNATIONAL AIRPORT

June-July-August Skill Score = 16.6%

Day#	Forecast Output	Actual Rain	Squared-Errors			Skill Scores		
			ANS	Climatology	Daily	Weekly	Monthly	Date
32	20%	0	0.040	0.044	8.3%			June 1
33	30%	0	0.090	0.044	-106.2%			
34	20%	1	0.640	0.626	-2.3%			
35	30%	0	0.090	0.044	-106.2%			
36	0%	0	0.000	0.044	100.0%			
37	0%	0	0.000	0.044	100.0%			
38	0%	0	0.000	0.044	100.0%	3.1%		
39	0%	0	0.000	0.044	100.0%	7.6%		
40	0%	0	0.000	0.044	100.0%	17.8%		
41	2%	0	0.000	0.044	99.1%	70.4%		
42	20%	1	0.640	0.626	-2.3%	27.9%		
43	30%	0	0.090	0.044	-106.2%	17.7%		
44	60%	1	0.160	0.626	74.4%	39.4%		
45	60%	0	0.360	0.044	-724.9%	14.9%		
46	30%	1	0.490	0.626	21.7%	15.2%		
47	60%	1	0.160	0.626	74.4%	27.9%		
48	40%	1	0.360	0.626	42.5%	29.7%		
49	50%	0	0.250	0.044	-472.9%	29.0%		
50	50%	1	0.250	0.626	60.1%	36.9%		
51	50%	1	0.250	0.626	60.1%	34.1%		
52	30%	1	0.490	0.626	21.7%	40.8%		
53	50%	0	0.250	0.044	-472.9%	37.5%		
54	20%	1	0.640	0.626	-2.3%	22.6%		
55	20%	0	0.040	0.044	8.3%	17.6%		
56	40%	1	0.360	0.626	42.5%	29.1%		
57	40%	1	0.360	0.626	42.5%	25.7%		
58	0%	0	0.000	0.044	100.0%	18.8%		
59	0%	0	0.000	0.044	100.0%	19.6%		
60	0%	0	0.000	0.044	100.0%	31.8%		
61	20%	0	0.040	0.044	8.3%	45.6%	27.1%	June 30
62	40%	1	0.360	0.563	36.1%	43.7%	27.6%	July 1
63	60%	0	0.360	0.062	-478.3%	21.5%	24.1%	
64	50%	1	0.250	0.563	55.6%	25.9%	26.1%	
65	40%	1	0.360	0.563	36.1%	27.2%	27.2%	
66	40%	0	0.160	0.062	-157.0%	19.5%	27.9%	
67	20%	1	0.640	0.563	-13.6%	10.4%	26.2%	
68	20%	0	0.040	0.062	35.7%	11.1%	25.9%	
69	20%	0	0.040	0.062	35.7%	4.6%	25.7%	
70	20%	0	0.040	0.062	35.7%	21.1%	25.4%	
71	20%	0	0.040	0.062	35.7%	8.2%	25.1%	
72	20%	0	0.040	0.062	35.7%	-6.8%	24.9%	
73	20%	0	0.040	0.062	35.7%	6.1%	24.6%	

74	20%	0	0.040	0.062	35.7%	35.7%	26.5%
75	10%	1	0.810	0.563	-43.8%	-12.1%	23.1%
76	10%	0	0.010	0.062	83.9%	-8.9%	20.1%
77	10%	0	0.010	0.062	83.9%	-5.7%	23.9%
78	10%	0	0.010	0.062	83.9%	-2.5%	24.5%
79	5%	0	0.003	0.062	96.0%	1.5%	21.3%
80	0%	0	0.000	0.062	100.0%	5.8%	20.2%
81	0%	0	0.000	0.062	100.0%	10.1%	23.6%
82	2%	0	0.000	0.062	99.4%	92.4%	21.1%
83	0%	0	0.000	0.062	100.0%	94.7%	18.2%
84	20%	0	0.040	0.062	35.7%	87.9%	18.0%
85	20%	0	0.040	0.062	35.7%	81.0%	21.7%
86	20%	1	0.640	0.563	-13.6%	23.1%	20.9%
87	30%	1	0.490	0.563	13.0%	15.8%	20.3%
88	20%	0	0.040	0.062	35.7%	13.0%	18.1%
89	20%	0	0.040	0.062	35.7%	10.3%	15.5%
90	20%	0	0.040	0.062	35.7%	7.5%	15.1%
91	20%	0	0.040	0.062	35.7%	7.5%	14.6%
92	20%	1	0.640	0.563	-13.6%	0.5%	11.3%
93	30%	0	0.090	0.052	-72.5%	3.3%	10.6%
94	30%	1	0.490	0.595	17.7%	5.5%	9.0%
95	40%	1	0.360	0.595	39.5%	14.7%	16.4%
96	30%	1	0.490	0.595	17.7%	14.9%	13.1%
97	50%	0	0.250	0.052	-379.2%	6.2%	7.6%
98	40%	1	0.360	0.595	39.5%	12.1%	12.0%
99	30%	0	0.090	0.052	-72.5%	16.1%	13.7%
100	20%	1	0.640	0.595	-7.5%	13.0%	11.6%
101	30%	0	0.090	0.052	-72.5%	10.2%	10.7%
102	20%	0	0.040	0.052	23.3%	1.7%	10.6%
103	30%	0	0.090	0.052	-72.5%	-7.5%	9.7%
104	40%	0	0.160	0.052	-206.7%	-1.3%	7.7%
105	20%	0	0.040	0.052	23.3%	-26.6%	7.6%
106	10%	0	0.010	0.052	80.8%	-17.8%	7.9%
107	20%	0	0.040	0.052	23.3%	-28.7%	12.8%
108	20%	0	0.040	0.052	23.3%	-15.0%	12.2%
109	20%	0	0.040	0.052	23.3%	-15.0%	11.5%
110	20%	0	0.040	0.052	23.3%	-1.3%	10.9%
111	20%	0	0.040	0.052	23.3%	31.5%	10.1%
112	2%	0	0.000	0.052	99.2%	42.4%	10.0%
113	2%	0	0.000	0.052	99.2%	45.0%	9.8%
114	2%	0	0.000	0.052	99.2%	55.9%	9.7%
115	20%	0	0.040	0.052	23.3%	55.9%	8.8%
116	20%	0	0.040	0.052	23.3%	55.9%	8.7%
117	30%	0	0.090	0.052	-72.5%	42.2%	7.7%
118	20%	0	0.040	0.052	23.3%	42.2%	10.0%
119	20%	0	0.040	0.052	23.3%	31.3%	9.8%
120	30%	0	0.090	0.052	-72.5%	6.8%	8.6%
121	30%	0	0.090	0.052	-72.5%	-17.8%	7.4%
122	30%	0	0.090	0.052	-72.5%	-31.4%	6.2%
123	50%	0	0.250	0.052	-379.2%	-89.0%	1.7%

July 31  
Aug 1

Aug 31

SUM OF WEIGHTS ALONG THE INTERCONNECTIONS  
FROM EACH INPUT NODE TO THE OUTPUT NODE

<u>Ranking</u>	<u>Weighting</u>	<u>Input Variable</u>	
	1	2.911733	CP500V
	2	2.711369	AP700U
	3	2.668178	CA150V
	4	2.602760	CA800T
	5	2.555386	P800U
	6	2.543929	WP400V
GOPAD	7	2.541121	CA600U
	8	2.530459	AA300V
	9	2.525478	AP700V
	10	2.504251	CP150V
	11	2.498630	CP700D
	12	2.441557	CA200D
	13	2.406791	AA600D
	14	2.405581	AP500T
	15	2.391812	CA100D
	16	2.378694	CA800D
	17	2.374402	AP300D
	18	2.366579	CA700T
	19	2.364362	AP300U
	20	2.364124	WP100V
	21	2.359408	CA150T
GOPAD	22	2.350847	AA900D
	23	2.344415	CP200U
	24	2.343939	AP200D
GOPAD	25	2.340340	WA400U
	26	2.328331	WA600V
	27	2.326402	WP200U
	28	2.316905	AA200T
	29	2.312125	WP900U
	30	2.310261	WA900T
	31	2.306701	WP300D
	32	2.297834	WA600T
GOPAD	33	2.296635	AA800U
	34	2.296424	CP200D
	35	2.295634	CP200T
	36	2.278786	WP800U
	37	2.268543	AP150D
	38	2.264325	CP700U
	39	2.255943	WP500V
	40	2.254840	CA500U
	41	2.254013	WP600U
GOPAD	42	2.250115	AA900V
	43	2.246739	WA600U
	44	2.245973	AP800U
	45	2.242491	AP600D
	46	2.239413	WA200V
	47	2.235012	WP700V

	48	2.226358	CP700T
	49	2.213338	CP600D
GOPAD	50	2.207791	CA800V
	51	2.207051	CP600T
	52	2.204367	AP150V
	53	2.197721	WA500V
	54	2.193971	WA600D
	55	2.192145	WP300T
	56	2.186021	CP600V
	57	2.184488	WA900D
	58	2.181702	AP400V
	59	2.178080	AA400D
	60	2.175112	WA800D
	61	2.173228	CP700V
	62	2.169908	CP900D
	63	2.163131	WP800D
GOPAD	64	2.162275	WA400V
	65	2.160017	AA300D
	66	2.159704	AA500D
	67	2.145610	AP900V
GOPAD	68	2.142212	WP800V
	69	2.137422	AA600U
	70	2.124437	AP800V
	71	2.122836	CP150D
	72	2.107995	AP300T
	73	2.107691	CP150U
	74	2.104243	AP600V
	75	2.099675	AA400V
GOPAD	76	2.089873	WA500U
	77	2.088976	AA600T
	78	2.086111	WP700U
	79	2.081774	CP100V
	80	2.081373	CA100U
	81	2.078511	CA400D
	82	2.07268	CA150D
	83	2.070478	AA300U
	84	2.070300	WA300U
	85	2.069681	AP300V
	86	2.069205	CP900T
	87	2.066138	AA200U
	88	2.066046	AA600V
GOPAD	89	2.065295	WP150V
	90	2.061990	WA700T
	91	2.061002	CP900U
	92	2.060100	AP600T
	93	2.060040	WA700U
GOPAD	94	2.058352	AA800V
	95	2.049728	WP400D
	96	2.048078	CP800D
	97	2.042189	WP300V
GOPAD	98	2.039243	DAYCNT
	99	2.039145	WP900T
	100	2.039141	WA100U
	101	2.034025	WP800T

	102	2.032360	AA100V
GOPAD	103	2.031388	CA900V
GOPAD	104	2.030351	AA100U
	105	2.029932	WP400T
	106	2.026695	WA400D
GOPAD	107	2.024281	CA400U
	108	2.023258	AP400D
	109	2.021585	AP600U
	110	2.019581	CP400D
	111	2.014587	WA400T
	112	2.013900	WP700T
	113	2.012967	AP500V
	114	2.008278	AA500T
	115	2.007701	AP100U
	116	2.006664	AA400T
	117	2.005505	CP800T
	118	2.002861	CA300T
	119	2.002381	WA800U
	120	2.000854	WA200T
	121	1.999283	WP300U
GOPAD	122	1.982341	AA700D
	123	1.982100	AP900U
	124	1.981929	AA800T
	125	1.979996	CP300T
	126	1.974905	WA150V
GOPAD	127	1.974752	CA800U
	128	1.966168	CA200U
GOPAD	129	1.961482	WA800V
	130	1.959604	AP200U
	131	1.959304	AP500U
	132	1.956458	WP100T
	133	1.955483	AA150D
	134	1.948286	CP200V
	135	1.941446	AA900U
	136	1.941157	WP900V
	137	1.940861	WA500T
	138	1.940551	WP150U
GOPAD	139	1.938703	AA700U
	140	1.938693	WA150U
	141	1.934963	CA100V
	142	1.934620	CA500T
	143	1.931488	AP800T
	144	1.931081	WA100D
GOPAD	145	1.930760	AA400U
	146	1.929377	CA200V
	147	1.916327	AP150T
	148	1.912604	CP100U
	149	1.911037	CP150T
	150	1.910569	CA100T
	151	1.910101	CP500T
	152	1.909751	AP100D
	153	1.903888	AP700D
	154	1.887930	AP500D
GOPAD	155	1.887024	AA100T

	156	1.878347	CP600U
	157	1.875954	CP500U
GOPAD	158	1.875487	CA200T
	159	1.874961	AP100V
	160	1.869607	AP200V
	161	1.860836	WA100T
	162	1.859771	CP300U
	163	1.857536	AP800D
GOPAD	164	1.853144	WA200U
	165	1.853136	AA300T
	166	1.851860	CA150U
	167	1.848877	WA150D
	168	1.846307	CA300D
	169	1.844337	WP200D
	170	1.840719	AP100T
	171	1.839105	WA800T
	172	1.836656	CP800V
	173	1.834760	CP400T
	174	1.833024	WP150D
	175	1.832038	WP500T
	176	1.824288	WP600D
	177	1.823195	AA500V
	178	1.823091	AA150T
	179	1.821531	CA700D
	180	1.820413	WA300D
	181	1.807886	CP500D
	182	1.803082	CA400T
	183	1.785021	AP700T
	184	1.783709	WP500U
GOPAD	185	1.783413	AA150V
	186	1.769200	WA700V
	187	1.761752	WP600V
GOPAD	188	1.760480	WA900V
	189	1.755016	WP200T
GOPAD	190	1.748589	CA700V
GOPAD	191	1.745677	CA300U
	192	1.741396	CP400U
	193	1.736056	WP100D
	194	1.729476	AA800D
	195	1.723241	CP400V
	196	1.722183	AA200D
	197	1.720485	AA150U
	198	1.714073	WA200D
	199	1.711676	WP200V
	200	1.708119	CA900D
	201	1.704934	WA300V
	202	1.692764	CA900T
	203	1.692764	WA100V
GOPAD	204	1.692686	WA300T
	205	1.691195	WP150T
	206	1.689967	AA200V
	207	1.683903	WA700D
	208	1.674008	CP300V
	209	1.673079	AP900D

	210	1.665392	CP300D
GOPAD	211	1.658782	CA600D
	212	1.543406	AA500U
	213	1.637009	WP400U
	214	1.636141	AA700T
	215	1.629690	WA150T
	216	1.627893	AP150U
	217	1.627503	CA500D
	218	1.615998	WA500D
	219	1.614467	CA900U
	220	1.611934	AP200T
GOPAD	221	1.596063	CA600T
	222	1.573736	AP400U
	223	1.571156	CP100T
	224	1.569651	AA900T
	225	1.568914	WP900D
	226	1.541798	WP700D
	227	1.534481	CA700U
	228	1.499521	WP500D
	229	1.498209	CA400V
	230	1.479125	CA500V
	231	1.459406	CP900V
GOPAD	232	1.440968	WA900U
GOPAD	233	1.435088	AA700V
	234	1.434691	CP100D
	235	1.393521	CA600V
	236	1.368853	AP900T
	237	1.329901	AA100D
	238	1.281635	WP600T
	239	1.236936	WP100U
	240	1.174124	CA300V
	241	1.129619	AP400T

**APPENDIX B**

**GOAL-ORIENTED PATTERN DETECTION (GOPAD)  
FOR TACTICAL MESOSCALE WEATHER FORECASTING**

**GOAL-ORIENTED PATTERN DETECTION (GOPAD)  
FOR TACTICAL MESOSCALE WEATHER FORECASTING**

**Kenneth Young  
ThinkNet, Inc.  
and  
Paul D. Lampru, Jr.  
Consultant's Choice, Inc.**

**Paper presented at the Tenth Annual  
EOSAEL/TWI Conference  
28-30 November 1989  
Las Cruces, New Mexico**

**ABSTRACT**

The wide dispersion of Army forces on the modern battlefield and the complexity of current weapons systems have increased the need for forecasted weather data that could be used as input to Tactical Decision Aids. The Integrated Meteorological System (IMETS) will enable the Staff Weather Officer (SWO) to support Division and Corp staffs who are primarily engaged in planning. These staffs and other operational units need a diverse set of weather parameters on-demand for specific locations and specific time frames. Research and development work investigated the potential of a software program called Goal Oriented Pattern Detection (GOPAD) to produce tactical weather forecasting models. This paper describes: (1) how GOPAD operates, (2) the types of tactical mesoscale forecast models that could be developed, (3) a method for defining forecast models, and (4) the GOPAD development process used to create new forecast models.

**1. THE ROLE OF AUTOMATED WEATHER  
FORECASTING ON THE BATTLEFIELD**

The wide dispersion of Army forces on the modern battlefield and the complexity of current weapons systems have increased the need for forecasted weather data that could be used as input to Tactical Decision Aids (TDA) that perform weather effects analysis. Weather conditions affect various types of military units in different ways, depending upon the type of unit, the mission, the enemy situation, and the terrain. Since weather varies with time and locality, weather forecasting and effects analysis must be constantly reappraised to retain its usefulness as combat intelligence. The complexity of this analysis process, the premium placed on timeliness, and the availability of tactical computers requires that the forecasting, analysis, and display techniques be automated. Consequently, research and development is ongoing to devise new ways of automating mesoscale weather parameter forecasting in the battlefield environment.

We believe that weather parameter forecasting is one of the fundamental functional requirements for the Integrated Meteorological System (IMETS) because IMETS will support Division and Corps staffs who are primarily engaged in planning. These staffs need a diverse set of forecasted weather parameters on-demand for specific locations and times frames. The

incorporation of automated weather forecasting models in IMETS is therefore crucial to the Staff Weather Officer's (SWO) ability to provide forecasted weather parameters for input to a myriad of Tactical Decision Aids (TDA).

The Required Operational Capability<sup>1</sup> (ROC) states that IMETS will provide the commander with weather forecasts in the operational area. These documents reflect the critical importance of automated weather parameter forecasting to IMETS. Clearly, IMETS must enable the SWO to supervise, control, understand, and subsequently brief the current and projected weather to the commander. But IMETS must also enable the SWO to provide forecasts for a diverse set of weather parameters that will be used as input to many TDAs. The SWO cannot be expected to manually produce individual forecasts for all the weather parameters required by all Corps/division/Brigade staffs and operational units, as needed, for specific locations and time frames.

In addition, the SWO and his staff may not be very familiar with local conditions for the area of interest. Consequently, the forecasting performance of humans in a tactical situation might be highly variable when positive skill and consistent performance are crucial. Thus, automated weather forecast models are essential to a SWO-based forecasting process and should be considered as yet another type of decision aid. For example, the SWO would use automated forecast models just as the National Weather Service forecasters use the Limited Fine Mesh/Model Output Statistics (LFM/MOS) models.

Assuming that there is a critical need for a highly automated process which is under the control of the SWO, then the next question is how do we produce these weather forecast models? Should these models be based upon statistical modeling techniques, expert system, neural nets, chaos theory, satellite-based image understanding, or some appropriate combination? What are the expected time and resource costs to produce these weather forecast models using any approach versus the potential performance of each approach? The answers to these types of questions is one of the goals of our research.

## 2. OVERVIEW OF GOPAD

CCI is investigating the potential of a neural net approach to produce tactical weather forecast models. This neural net research is based upon a proprietary algorithm, called **Goal Oriented Pattern Detection (GOPAD)**, developed by Dr. Kenneth Young at the Institute of Atmospheric Physics, University of Arizona. GOPAD has been used to produce two research models--GOPAD-Atlanta-RIR and GOPAD RT-89. The GOPAD-Atlanta-RIR was a Probability of Precipitation (PoP) model developed for Hartsfield International Airport in Atlanta, Georgia. The GOPAD RT-89 was a severe and significant weather forecast model developed for the SHOOTOUT-89 exercise sponsored by NOAA/FSL in Boulder, Colorado.

In general, GOPAD first identifies the optimal statistical relationships between the variables and indices from an arbitrarily large, correlated weather data set, and then develops a non-linear forecast model. This model development process is also able to reveal the underlying physical relationships between the predictor variables in the form of exemplars. GOPAD extends the multi-discriminant analysis (MDA) methods developed by Miller (1962) and the analogue forecasting method of Kruizinga and Murphy (1983). The

---

<sup>1</sup>Letter, Department of the Army, ATSI-CD-AS, Subject: Revised Integrated Meteorological System (IMETS) Required Operational Capability (ROC), dated July 31, 1989.

GOPAD approach is a k-nearest neighbor search which is similar to Leon Cooper's Reduced Coulomb Energy (RCE) algorithm.

The GOPAD model development software is actually a set of three separate programs called FUZAN, FUZPICK, and FUZUP. The first two programs are the statistical front-end to the third, which is a neural net type of program.

The first program (FUZAN) analyzes all the candidate predictor variables one at a time to determine their individual potential contribution of information to the forecast model to be developed. Once this is completed, it creates linear combinations of the variables that are considered by the developer to be highly correlated (e.g., all temperature variables, etc.). FUZAN systematically creates increasingly complex indices from all the specified variables until the Chi-square value cannot be increased by a more complex index. The creation of indices from highly correlated variables serves to improve the signal-to-noise ratio and sharpen the overall forecast ability of the model.

In the GOPAD RT-89 model there were approximately 1400 candidate rawinsonde and mesonet predictor variables for three years--1983, 1985, and 1987. FUZAN used these variables to automatically create about 120 candidate predictor indices. FUZAN then analyzed all 1520 candidate variables and indices to choose a subset of 400-500 variables and indices for further processing by the second program.

The second program called FUZPICK selects the optimal combination of variables and indices that contain virtually all the predictive information in the original data set. In the GOPAD RT-89 six sub-models, there were 3 to 6 variables/indices that were ultimately selected. All together there are about 40 individual predictor variables that are required to run the GOPAD RT-89 model (indices may combine up to 10 individual predictor variables).

The third program called FUZUP optimizes the n-space scaling and the neighborhood size to maximize a measure of forecast performance (e.g., Brier-based skill score). One major advantage of this process is that it allows direct access to all the other forecast parameters that were not used in training the model. This enables a GOPAD forecast model to display a wide variety of forecast parameters derived from the data variables.

The forecast model is based on the output of FUZUP which includes the historical data base of the predictor variables chosen by FUZPICK. Forecasts are made using analogs selected from the historical data set. The number of analogs is the neighbor size as optimized by FUZUP. The forecast model can also be used to generate exemplars to illustrate the patterns leading to a particular forecast.

There are three versions of the GOPAD software--GOPAD I, GOPAD II, and GOPAD III. GOPAD I operates on an IBM-compatible 8386 type computer. GOPAD I was used to produce the GOPAD-Atlanta Probability of Precipitation model. GOPAD II operates on a VAX 3200. GOPAD II was used to produce the GOPAD RT-89 severe/significant weather forecasting model. GOPAD III (presently in development) operates on a VAX 3200 which is a host for Interstate Electronics' Quen supermini-computer rated at 150 Megaflops. GOPAD III is the latest version. Each subsequent version of GOPAD is able to process more sources of raw weather parameters and larger data bases.

### 3. TACTICAL MESOSCALE FORECAST MODELS

The GOPAD development software can be used to automate the creation of a wide variety of tactical forecast models. Four of the most difficult tactical mesoscale forecasting problems are (1) fog as it is related to visibility and ceiling; (2) precipitation amounts and type; (3) severe weather such as tornadoes, hail, lightning, and wind gusts; and (4) cloud distributions, types, and coverage. The following paragraphs describe the type of information that a GOPAD model for each of these forecasting problems could provide.

A GOPAD based **fog model** would forecast formation and dissipation times, and graphically display visibility and ceiling. The operator would be able to specify the probability that visibility or ceilings would be below a specified value on a time axis. The operator would be able to produce maps showing regions of visibility or ceiling using a zoom capability. The user would be able to display a wide variety of exemplar conditions to help explain, confirm, modify, or reject a computer-generated forecast. Fog models might use terrain information, the output from a model of wind flow over complex terrain, local rawinsonde data, low-level cloud information from a satellite, and output from a synoptic scale forecast model. Ground truth would be derived from hourly surface observations from a variety of locations.

A GOPAD based **precipitation model** would display isopleths of expected amounts and types (e.g., rain, snow, freezing rain, etc.). The user would be able to selectively display the probability of precipitation greater than a specified amount in a specified period. A user would be able to display the expected total cumulative amount of precipitation expected within a specified period. The user would be able to predict rain intensities as a function of time and within a specified confidence interval. The user would be able to display a wide variety of exemplar conditions to help explain, confirm, modify, or reject a computer-generated forecast. These models might use the output from a synoptic scale numerical model, local rawinsonde data, and satellite-derived cloud track winds, total ozone measurements, precipitable water, etc. Ground truth would be obtained from archived records.

A GOPAD based **severe/significant weather model** would forecast the probabilities of occurrence of severe weather events such as tornadoes, hail, lightning, and high winds as a function of time. However, spatial resolution of severe weather phenomena greater than one hour in advance on a scale of ten kilometers or less is unlikely. The user would be able to display a wide variety of exemplar conditions to help explain, confirm, modify, or reject a computer-generated forecast. These models might use the output from a synoptic scale numerical model, local rawinsonde data, conventional and Doppler radar data, wind profiler data, surface meso-net data, mesoscale models, and satellite-derived cloud track winds, total ozone measurements, precipitable water, etc. Ground truth data would be obtained from conventional surface observations, meso-net data, and severe weather studies like the real-time exercises conducted every two years by NOAA/ERL in northeast Colorado.

A GOPAD based **cloud model** would forecast a three-dimensional distribution of clouds over time. Volumes will have an assigned "expected fraction of cloud" and an indication of basic cloud type (e.g., cumuloform or stratiform). The display would use this fraction to randomly distribute clouds within each volume. Typical cloud sizes would be estimated from the forecasted cloud type and climatology. Sophisticated display techniques would enable the user to specify an arbitrary point and direction of sight, and display a cloud-free line-of-sight view. The capability would also be applied to non-visible wavelengths such

as infrared. Consequently, forecast models would also be developed to predict parameters like temperature and water vapor profiles that affect non-visual wavelength visibilities. The user would be able to display a wide variety of exemplar conditions to help explain, confirm, modify, or reject a computer-generated forecast. These models might use the output from a synoptic scale numerical model, satellite-derived cloud track winds, cloud types, heights, and amounts derived from satellites, and local rawinsonde data. Ground truth would be obtained from surface observations and satellites.

#### 4. WEATHER FORECAST MODEL DEFINITION

In order to completely describe a forecast model at least four components should be specified: (1) the meteorological event to be forecasted; (2) the sources of historical input variables and ground truth; (3) the lead time and forecast period; (4) the size of the forecast region. Each of these four components are described in the following paragraphs.

##### 4.1 THE EVENT TO BE FORECASTED

###### PRECIPITATION

- (a) PoP by type (rain, snow, freezing rain)
- (b) estimate of precipitation amount with confidence limits
- (c) probability of precipitation (PoP) greater than specified amount

###### TEMPERATURE

- (a) expected temperature with confidence limits
- (b) probability of temperature above or below specified value

###### WINDS

- (a) expected wind direction, speed, and gusts with confidence limits
- (b) probability of winds above or below specified speed

###### CLOUD COVER, CEILING, AND VISIBILITY

- (a) expected cloud cover, ceiling, and visibility with confidence limits
- (b) probability of an event above or below specified values
- (c) expected cloud types and coverage with confidence limits

###### SEVERE WEATHER

- (a) probabilities of funnel cloud or tornado
- (b) probabilities of hail larger than specified sizes
- (c) probability of wind gusts greater than specified speed
- (d) probability of cloud-to-ground lightning within specified grids

Although there are many environmental events that can be predicted, the GOPAD model development process requires a fairly accurate training set (i.e., a historical data base) in order to develop a model to forecast the desired event. We have found that as a minimum these data bases should include about 100 data points for climate forecasters or about 500 data points for shorter term forecasters.

Another important criteria for determining how well an event can be forecasted is that there must be a minimum number of occurrences of that event in the historical data base. For example, a rare event (e.g., a tornado) may occur with a frequency of 0.1%. A data set containing 500 data points would contain only 5 tornado events. We find that at least 10

or more occurrences are required to accurately forecast a rare event. If the historical data set does not contain a sufficient number of occurrences of an event, then more data and/or "multiplexing" may be required.

In order to achieve the optimal level of performance given a limited number of ground truth events in the training set, we experimented with two techniques to mitigate this problem which we refer to as the "rare event" problem. First, a new technique, called **multiplexing** (plexing), was developed to enable different sets of ground truth events to be used in the creation of a model thereby increasing the number of occurrences of the event in the training set. The concept of multiplexing was tested on a very small scale using geographically similar contiguous regions during SHOOTOUT-89. GOPAD RT-89 used multiplexing to extend a historical training set that contained only three years of ground truth data for forecasting severe storm parameters and two years of ground truth data for forecasting significant storm parameters. GOPAD RT-89 is composed of six submodels. One submodel is single-plexed, four are two-plexed, and one is three-plexed. By comparison, a site-specific scenario model might require as many as 20-plexes. Methods for selecting the optimal number of plexes for a given problem have been addressed only in a preliminary manner. It is also fair to note that greater plexing will be more computationally expensive.

Second, a **self-adapting** forecast model that learns as it is being used was also developed for SHOOTOUT-89 to evaluate the potential of this technique for mitigating the lack of ground truth data. We are presently evaluating the skill of our self-adapting model compared to an identical but static model to estimate the potential learning curve.

#### 4.2. SOURCES OF PREDICTOR VARIABLES

- |  |  |
|--|--|
| A. Mesonet or other surface data             | F. Satellite derived cloud track winds           |
| B. Rawinsonde data                           | G. Other satellite derived variables             |
| C. Barotropic model output                   | H. Topographic or terrain data                   |
| D. Nested Grid Model (NGM) output            | I. Worldwide monthly average temperatures        |
| E. Mesoscale primitive equation model output | J. Worldwide monthly average sea level pressures |

This list shows many, but not all, of the possible sources of predictor variables that could be used to construct a model. The selection of the variables to use depends upon many factors. One of the major cost factors in developing a model is the number of new historical data bases that must be developed for a particular site or region. Often these historical data bases can be formed one time for very large regions (e.g., several states in size) and, subsequently, be used to produce a variety of models in the same region or in different areas of the same region. After the data bases are developed and organized for processing, GOPAD model construction is primarily man-out-of-the-loop.

Generally, the best models will be produced when the widest possible variety of input variables are used to develop a forecast model. This variety should include variables that may never have been thought to be important enough to consider in a model. The number of individual candidate variables that can be included in a GOPAD model could number from 100 to 8,000 or more. It also makes no difference whether these variables are highly correlated or not. The GOPAD model development process creates a near optimal model for a given data set, no matter how much redundancy is present in the training set. Normally, the redundant variables are automatically combined by GOPAD to form optimal machine-derived

indices which usually contain much more predictive information than any of the individual candidate variables from which they were derived. We find that these indices are often so complex that they cannot be easily explained. Nevertheless, the indices that are selected have extremely high Chi-square values (e.g., over 100) indicating very high predictive power.

The only limitation pertaining to these input variables is that they should be continuous, rather than binary or discrete, with few possible values. For example, discrete variables with relatively few values (i.e., less than 10) do not facilitate optimization of the separation between these multi-dimensional data points. In the weather domain, the raw variables are generally continuous variables, so this limitation is usually not important.

Finally, the size of the training set should be as large as possible. For example, these data base should contain 1,000 or more data points. Consequently, the size of these data bases are usually on the order of 10-500 megabytes in size. For example, the NGM historical data base for just the past four years is about 5-7 gigabytes in size, but only about 500 MB of candidate predictor variables will be extracted for processing.

#### 4.3. FORECAST LEAD TIMES AND VALID PERIODS

<u>FORECAST TYPES</u>	<u>LEAD TIMES</u>	<u>MINIMUM VALID PERIODS</u>
Immediate-range	0 to 4 hours	1 hour
Short-range	6 to 24 hours	3 hours
Mid-range	24 to 96 hours	12 hours
Long-range	4 to 9 days	1 day
Extended-range	10 to 30 days	5 days
Short-climate	1 to 3 months	10 days
Mid-climate	3 to 9 months	30 days
Long-climate	9 to 24 months	3 months

The **lead time** is the amount of lag between the time that the forecast model produces a forecast and the time that the valid period begins. The **valid period** is the timeframe within which the forecast is valid. For example, an Immediate-range forecast model may produce a forecast at 12Z which is valid for 15Z-16Z. In this example, the lead time is three hours and the valid period is one hour. The valid period may be equal to or longer than the temporal resolution of the ground truth data used to train the model. Valid periods shorter than those listed are not recommended, but valid periods may be longer than those listed.

A forecast model with a short valid period could be very important to the battlefield planning process. If a series of hourly forecast models were run at the same time and if their forecasts were graphically displayed on the same time line, then one could see the temporal evolution of the weather event being forecasted. We refer to this type of combined forecast model as a **scenario model**. A scenario model will make it possible for one to see breaks or windows in the weather. In addition, a scenario model would support the tactical planning and decision-making process at Division and Corps by making forecast information readily available for any combination of lead time and valid period that might be required by a myriad of the Tactical Decision Aids (TDA).

#### 4.4. SIZE OF FORECAST REGION

##### FIXED POINT MODELS

- (a) Single-Site Model--one model forecasts for one site.
- (b) Multi-Site Model--one model forecasts for several sites.

##### REGIONAL MODELS

- (a) Low-Res Single Region Model--one model provides a forecast to cover a single geographical region.
- (b) Multi-Region Model--one model forecasts in several regions that may be meteorologically very similar and/or relatively close geographically.

##### FULL RESOLUTION MODELS

- (a) Hi-Res Single Region Model--one model forecasts for any/all specified points within the given geographical region.
- (b) Generic Model--one model forecasts for any/all specified points in a variety of meteorologically or geographically similar regions.

**Fixed point forecast models** are trained on the ground truth information that is specific to one or more sites. A probability of precipitation (PoP) model trained on the amount of rain received in one rain gauge is a good example of a **single-site model**. A **multi-site model** would be trained on the data from several locations and therefore could be used to make predictions for any of those sites. In either case, a point model generally will provide useful forecasts only for the specific locations where it was trained.

A **low-res single region model** will make predictions for a region rather than for one or more sites within a region. The resolution of the ground truth data is the region as a whole. Consequently, the output of a regional model only indicates the probabilities that a specific event will occur within the region but will not localize the event within the region.

A **multi-region model** is a concept designed to reduce the cost of creating many regional models when these areas are meteorologically similar and relatively close geographically. This concept suggests that when models are required for large regions, it is possible to multiplex the ground truth data from several smaller portions of the larger region to create a multi-region model. For example, the ground truth data base for a mesoscale weather forecasting model, developed for four regions around Boulder, Colorado, contained a record of whether or not severe/significant weather had occurred anywhere within the region.

The **hi-res single region model** combines the advantage of the point and regional models to provide point forecasts for any or all of the points in the region, whether or not there is ground truth data available for the desired region. In order to make this model useful, non-meteorological information (e.g., terrain elevation data, direction of slope, vegetation type, surface roughness, lat-long, distance to ocean, etc.) must be used in addition to the meteorological data.

The **hi-res generic model** takes the high resolution model one step farther. A **generic model**, in concept, would be portable to geographic locations where insufficient historical data was available to construct a model. This concept suggests that it might be possible to create a model using the historical data from a variety of geographically-different, but meteorologically-similar locations. Thus, a region-specific model for an overseas area might be initially developed for a similar region in the United States for example, and once

constructed it would be used in the overseas location. Such a model would be designed to self-adapt using real-time data and post-forecast ground truth information. Eventually it would transform itself into a site-specific forecast model with a greater level of skill than when it was first placed into service. A generic model could enclose a region of almost any size (e.g., the State of Georgia, or Georgia and Alabama) and it would also be trained with meteorological data and non-meteorological data. It is appropriate to note that the development of a generic model will require exploration and the development of new production techniques.

Finally, all of these high resolution regional models would isopleth their forecasts (e.g., expected amount of precipitation) over the region. A zoom capability would enable regions of interest to be isoplethed at any desired resolution. Similar isopleth maps could be constructed, for example, for the minimum expected amounts of precipitation with any user-specified confidence limit. In this way, isopleths maps could also show the probability that precipitation would exceed any user-specified amount. The list of possibilities is extensive.

## 5. GOPAD MODEL DEVELOPMENT PROCESS

This section describes how the GOPAD development software would be used to develop a new weather forecast model for **cloud cover, ceiling, and visibility** for an overseas country where the developer has no prior knowledge about the weather patterns and where he must create all new historical data bases. As these time estimates will show, the majority of the man-hours required is in formatting, correcting, and organizing the historical data bases. The development procedure would be organized into three ordered phases. Upon completion of each phase, an operational model would be available that could be fielded.

### 5.1 DEVELOP A SINGLE-SITE, SCENARIO MODEL

In Phase I, the objective would be to develop, test, and deliver a single-site, 12-month, scenario model for *City, Country* (e.g., some city in a Latin American country). The model developed in Phase I would use either one, two, or three sources of predictor variables. Obviously, a model that uses more variable sources will take more time, but its accuracy would also be greater. So a trade-off decision must be made by selecting from the available sources of predictor variables that may be used to develop the Phase I model. Although we would fully expect the performance of this simple model to surpass climatology, we cannot know how much of an increase is possible.

If only **one source** of predictor variables could be used, then rawinsonde data from five to ten stations in and around the country would be used. It would take about 10 weeks to develop this model.

If **two sources** of predictor variables could be used, then rawinsonde and barotropic model data would be used. The historical barotropic data base would be constructed from scratch for a 10-year period. Obviously, this option will produce a better forecast model, but it will take an additional effort to create the barotropic data base. Nevertheless, the production of this data base for a country needs to be done only once, but it can be used many times. It would take about **26 weeks** to develop this model from scratch. This option probably offers the best trade-off between cost and development time versus the potential for increased performance.

If **three sources** of predictor variables could be used, then this model would be developed using satellite-based imagery to derive cloud-tracked winds, barotropic, and rawinsonde data as predictor variables. In addition to the rawinsonde data and the development of the barotropic historical data base, this option would include the development of a cloud-tracked winds historical data base using GOES imagery, CIRRUS I, and a vorticity model to derive synoptic scale wind patterns. It would take about 45 weeks to develop this model from scratch.

## 5.2 DEVELOP MULTI-SITE, MULTI-SOURCE, SCENARIO MODEL

In Phase II, a multi-site, multi-source, scenario model would be developed for up to ten specified sites in a country in three-hour increments out to 24 hours. This model would use the predictor variable data sets produced in the Phase I (i.e., rawinsonde only; rawinsonde and barotropic only; or rawinsonde, barotropic, and synoptic scale wind flow). The multiplexing concept would be used to create this model. Although the selection of these 10 sites may be somewhat arbitrary, each site selected must have about 10 years' worth of historical ground truth information available. It would take about **5 weeks** to develop this model.

## 5.3 DEVELOP A HIGH RESOLUTION, MULTI-SOURCE, SCENARIO MODEL

In Phase III, a high-resolution, scenario model would be developed to produce forecasts anywhere in a country. This model would be constructed using all the historical data bases created in Phases I and II, and at least one new historical data base of non-meteorological variables (e.g., terrain elevation, direction and amount of slope, etc.). The multiplexing concept would be used to create this model. Once this model has been completed, other forecast models (e.g., precipitation, temperature, etc.) would be able to use many of the same historical data bases that were developed for the first time. Therefore, the costs of additional models would be significantly less. It would take about **16 weeks** to develop this model.

## 6. SUMMARY

The Army and other services need a high technology initiative in mesoscale weather forecasting for high-, medium-, and low-intensity combat situations. Rapid weather forecasting is critical to the planning cycle. Forecasting, which is a difficult task in peacetime, will be even more difficult on the battlefield. The number of weather parameters required for a new generation of Tactical Decision Aids and automated systems has placed increased importance on the requirement for the Army to develop a highly automated, tactical weather forecasting system. New technologies and hardware are now available that may make this possible. Therefore, bold research is needed to develop a technical foundation to achieve this goal.

## ACKNOWLEDGMENT

The authors gratefully acknowledge the outstanding assistance provided by Joan Pruett, Kathie Speas, and Susan Winkler. This paper could not have been completed without their editing and publication support.

## REFERENCES

- Kruizinga, S., and A. H. Murphy, (1983): Use of an Analogue Procedure to Formulate Objective Probabilistic Temperature Forecasts in The Netherlands, Monthly Weather Review, Vol. 111, 2244-2254.
- Miller, R. G., (1962): Statistical Prediction by Discriminant Analysis, Meteor. Monogr., 4, 54.
- Shuman, F., (1978): Numerical Weather Prediction, Bull Amer. Meteor. Soc., 59, 5-17.

**APPENDIX C**

**A QUANTITATIVE COMPARISON OF FORECAST MODELS  
THAT PARTICIPATED IN NOAA/FSL SHOOTOUT-89 EXERCISE**

# **A QUANTITATIVE COMPARISON OF FORECAST MODELS THAT PARTICIPATED IN NOAA/FSL SHOOTOUT-89 EXERCISE**

Kenneth Young  
ThinkNet, Inc.  
Tucson, Arizona 85711, USA

Paul D. Lampru, Jr.  
Consultant's Choice, Inc.  
Atlanta, Georgia 30350, USA

## **1.0 ABSTRACT**

During the summer of 1989, the Forecast Systems Laboratory, NOAA, sponsored an evaluation of Artificial Intelligence systems that forecast convective storms taking place within a 110-mile radius of Boulder, Colorado. This exercise was called SHOOTOUT-89 and was designed to be an exploratory study of the effectiveness of a variety of AI systems in the weather forecasting process. Data gathered during the forecast phase of the exercise was used to evaluate the performance of the participating systems. The systems participating included: (1) Knowledge Augmented Severe Storms Predictor (KASSPr); (2) Goal Oriented Pattern Detection (GOPAD); (3) NOAA/NESDIS CONVEX; (4) Additive Linear Prediction System (ALPS); (5) WILLARD; and (6) Objective Convective Index (OCI). The goal of SHOOTOUT-89 is to provide AI system designers with feedback so they can design future systems that will support the overall weather forecasting process. This paper summarizes the results and discusses some of the lessons learned from this exercise.

## **2.0 INTRODUCTION**

During the summer of 1989, the Forecast Systems Laboratory (FSL) of the National Oceanic and Atmospheric Administration (NOAA) conducted an exercise that was designed to evaluate Artificial Intelligence (AI) systems that forecast significant and severe weather over four regions in the northeastern Colorado plains. This exercise, called SHOOTOUT-89, took place in Boulder, Colorado. Previous real-time (RT) exercises were conducted during the summers of 1983, 1985, and 1987, in northeast Colorado by the Program for Regional Observations and Forecasting Services (PROFS). PROFS operates an extensive network of sensors, maintains historical data bases, and facilitates advanced research studies in mesoscale forecasting.

The SHOOTOUT-89 was an exploratory, quantitative, and qualitative comparison of AI systems that forecast severe weather. Although each system required different predictor variables, all systems received real-time data at approximately the same time, and were required to produce a forecast for the 11:00 A.M. weather briefing. Thus, the unique format for the SHOOTOUT exercises made it possible to directly compare and contrast the performance of AI-based forecasting systems in a laboratory setting. Data gathered during the exercise will be used to evaluate the tasks, rules, and regulations of the study, as well as to evaluate the participating systems. System evaluation included testing the robustness of the systems in an operational situation, comparing the effectiveness of different AI approaches, determining the need for expert human input, evaluating the sensitivity of a system given different operators, soliciting user comments, and stimulating collaboration among researchers. In this paper, we focus on the effectiveness of the systems that participated.

### 3.0 PARTICIPATING SYSTEMS

There were six AI systems that participated in the SHOOTOUT-89 exercise. A few of the systems required no more than a few keystrokes to initiate the forecast model. Other systems required extensive interaction with a human expert, and some systems interrogated the meteorologist. A brief review of these systems follows:

- 1) **KASSPr** (Knowledge Augmented Severe Storm Predictor) was developed by the Atmospheric Environment Service of Canada, Department of the Environment, in cooperation with Digital Equipment Corporation. KASSPr is a traditional expert system written in OPS-5. Rule firing is controlled by the forward-chaining OPS-5 production system. The knowledge base was derived from John Bullas, an expert in severe weather forecasting, and Bruno deLorenzis (1988), the developer, from Atmospheric Environment Service of Canada.

KASSPr requires both NGM numerical model output, and extensive input from the meteorologist running the system. The meteorologist identifies and draws the forecasted positions of numerous meteorological features, such as troughs and ridges, on the computer screen (deLorenzis, 1988). Once this task has been completed, the system generates forecasts without further interaction.

- 2) **GOPAD** (Goal Oriented Pattern Detection) was developed by Dr. Kenneth Young with the help of Paul Lampru of Consultant's Choice, Inc. GOPAD is a combination of a front-end program which uses multiple discriminant analysis (MDA) to screen a large number of potential predictor variables and to create indices, which are linear combinations of these variables. The forecast model is then developed using a non-linear k-nearest neighbor approach, based on the predictor variables selected by MDA. The forecast model was developed using PROFS mesonet data for 1200Z through 1555Z, and 1200Z rawinsonde data from Denver and seven surrounding stations.

GOPAD is designed to run autonomously. During the exercise, the necessary mesonet and rawinsonde information was provided in a file created by the PROFS computer system, and the forecast program was initiated by the human operator. In addition to the standard probability forecasts required, GOPAD forecasts the probability of tornados and/or funnel clouds, the probability distributions of expected maximum hailstone sizes, and the probability distributions of expected peak wind gusts.

Two versions of GOPAD were run. The "learning version" received verification data for the previous day which, along with the forecast parameters for that day, were added to its historical data base. The "static" version received no updated verification data and so did not alter the historical data base from which it made forecasts.

- 3) **CONVEX** was developed by John Weaver, NOAA/NESDIS, who provided the severe storm forecasting experience, and by R. Phillips from NOAA/NESDIS, who was the knowledge engineer (Weaver and Phillips, 1987; Weaver and Phillips, 1989). CONVEX relies heavily on a sounding analysis package which determines the instability of the host airmass and its likelihood of initiating convection over the front range. It also requires the operator to predict the surface temperatures and dew points for each forecast region, which form the basis for the sounding analysis package.

In addition to the Denver morning sounding and surface mesonet data, CONVEX requires reasonably knowledgeable responses from a meteorologist to several questions regarding synoptic scale conditions.

- 4) **ALPS** (Adaptive Linear Prediction System) was developed by Tom Stewart of the State University of New York at Albany, and Cynthia Lusk of the University of Colorado at Boulder. ALPS is a linear model developed using the methods of judgment analysis from the field of cognitive science. The foundation for this theory is the belief that linear models are robust prediction systems that are more consistent than human judgment in certain situations. This theory suggests that simple algebraic models can capture the skill in the judgments of an expert in tasks that involve a high degree of uncertainty, intercorrelated variables, and monotonic relationships between variables and the observed event.

Meteorological expertise was required only in the selection of variables, estimating their relative weights, and calibrating the output. The six key variables used by ALPS are positive buoyancy, wind shear, surface temperature, humidity, wind direction, and wind speed. Some of the values are read automatically from the PROFS mesonet data, while others are determined by the operator from the Denver morning sounding.

- 5) **WILLARD** was developed originally by Steve Zubrick at Radian Corporation. WILLARD is an expert system where rules were developed using an induction algorithm in Rulemaster (Zubrick and Riese, 1985). WILLARD was originally designed and developed to forecast the potential of severe thunderstorms in the central United States. The system's forecasts are designed to be similar to the Convective Outlooks issued three times a day by the National Severe Storm Forecast Center.

WILLARD is an expert system that is composed of a hierarchy of about 30 modules at least containing one decision rule. For SHOOTOUT-89, additional rules were added to WILLARD, based on the expertise of forecasters and the Denver NWS Forecast Office. WILLARD might ask the operator up to forty questions before making a forecast. These questions pertain to current synoptic and mesoscale features, as well as numerical forecast guidance. Relatively few questions might be asked if the situation is not promising for severe weather.

- 6) **OCI** (Objective Convective Index) was developed by Robert Shaw with considerable input from Thomas Corona, Denise Walker, and many participants of the PROFS Real-Time 1987 experiment (RT-87). A long list of potential predictor variables was developed, using many Boulder-area meteorologists as experts. OCI uses proven severe weather forecasting principles to answer the question, "What are the chances of severe weather this afternoon in the PROFS mesonet region?"

Many Boulder-area meteorologists were consulted to identify a comprehensive list of potential predictor variables. However, the amount of archived data and number of potential predictor variables were too large for effective regression equations to be generated. Consequently, predictors were subjectively weighted to build a linear model. Heuristic rules were added to identify relationships among the variables that might inhibit convection. Both observed data and NGM forecast model data were included for each of the four basic weather elements: temperature, pressure, moisture, and wind. Since the OCI is based

on universal convective forecasting principles, it can be modified for any climate. OCI requires the operator to input surface observations, Denver sounding data, and NGM forecast model data for Denver and Cheyenne. Forecasts are produced without further interaction.

#### 4.0 EXERCISE PERIOD AND REGION

SHOOTOUT-89 ran from May 17 through August 16, 1989. On each day of the exercise, all systems were to generate forecasts of the mutually exclusive and exhaustive probabilities of occurrence of each of three weather categories, in each of four designated zones in northeast Colorado. The choice of the forecast zones was based on work by Weaver et al., (1987). The four forecast regions are shown on the map in Figure 1.

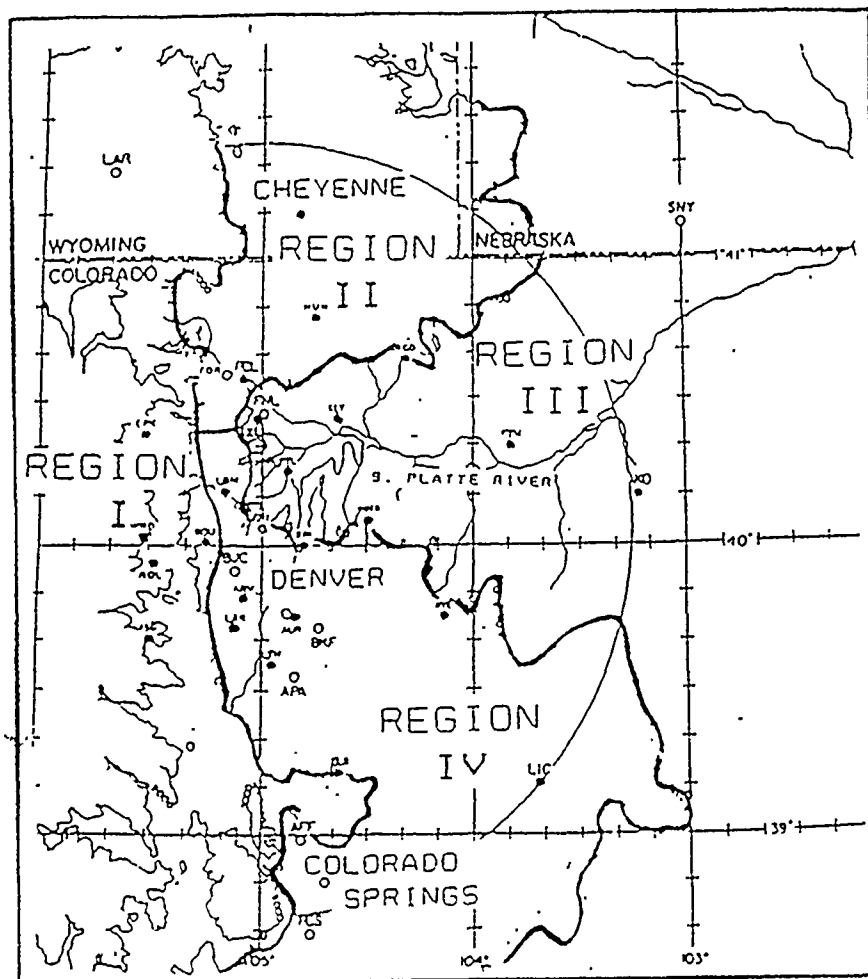


Figure 1. Forecast Regions for SHOOTOUT-89. (Roberts et al., 1989)

## 5.0. DEFINITION OF WEATHER CATEGORIES

The weather categories are listed as follows:

Category 0: Nonsignificant (Nil) weather is the absence of category 1 or category 2 weather.

Category 1: Significant weather is the absence of category 2 weather, with the occurrence of any of the following: (a) hail at least 0.25 inches but less than 0.75 inches diameter, (b) surface winds between 35 and 49 kts, (c) a rainfall rate of 2 inches/hour or more, based on 5-minute measurements, and/or (d) a funnel cloud.

Category 2: Severe weather is the occurrence of any of the following: (a) hail with a diameter of at least 0.75 inches, (b) wind gusts of 50 kts or greater, and/or (c) a tornado.

## 6.0 FORECAST LEAD TIME AND VALID PERIOD

Forecasts were required by 11:15 A.M. (1715Z) to be valid from 1:00 P.M. (1900Z) to 8:00 P.M. (0200Z). Due to the amount of manual input required, forecasts for OCI were run in the early afternoon, based on data available that morning. Not all forecast models produced forecasts for all four regions for all operational days of the exercise. WILLARD generated only a single forecast for the entire region. This forecast was assumed to be the same for each region. OCI did not generate forecasts for Region I.

Most of the data required by the systems was available by 10:15 A.M. Forecasts for all systems except OCI were completed by 11:15 A.M. (1715Z) and presented at the FSL daily weather briefing at 11:25 A.M. Not all the forecast models were operational on the first day of the exercise.

## 7.0 NUMBER OF OPERATIONAL DAYS

The starting dates and number of days each system was operated are shown in Table 1. Forecasts were not met when a program crashed (programming problems), or when required input data was not available. OCI did not produce forecasts for Region I. Since GOPAD and ALPS are totally objective systems, they were rerun for the days that were missed during the exercise.

TABLE 1  
NUMBER OF DAYS EACH SYSTEM WAS OPERATIONAL

	<u>Starting Date</u>	<u>#Days Operational</u>
KASSPr	17 May 1989	60 days
GOPAD learning	17 May 1989	53 days
GOPAD static	24 May 1989	50 days
CONVEX	19 May 1989	57 days
ALPS	7 Jun 1989	48 days
OCI	30 May 1989	45 days*
WILLARD	30 May 1989	54 days

\* The number of operational days for Regions II, III and IV.

After the exercise was completed, the objective systems were allowed to generate offline forecasts for the days they were not operational. The purpose was to obtain the largest number of common days in which forecasts were available for comparative evaluations. As a result of this effort, there were 48 common days for Region I, and 45 common days for Regions II, III and IV.

## 8.0 VERIFICATION DATA

### 8.1 Verification During SHOOTOUT-89

The collection of verification data is a crucial aspect of SHOOTOUT-89. A full-time Verification Coordinator (VC) was responsible for gathering and documenting the verification data for the exercise. These data are also used by the Denver WSFO in its own forecast verification studies. The VC was stationed at the Denver WSFO, where real-time radar data was readily available. When radar or other data suggested possible significant or severe weather, the VC called cooperative observers in the affected regions. The VC also received reports that were phoned in to the Denver WSFO, and made follow-up phone calls on the day following a possible weather event.

The following sources provided verification data: (1) a volunteer spotter network, and a paid cooperative observer network sponsored by the NWS; (2) police and fire stations, county emergency preparedness staffs, and highway road crews; (3) a network of amateur radio operators; (4) weather service offices in Colorado Springs and Cheyenne, in addition to the Denver WSFO; (5) automated mesonet stations (PROFS) that provide information on wind gusts and rainfall rates; (6) daily weather observations recorded by a network of approximately 30 specially recruited weather observers with observations mailed in monthly; and (7) volunteer chase teams consisting of research meteorologists who maintain contact with the VC by cellular phones, or who report after the fact. In spite of this extensive list of possible observers, it was nonetheless very difficult to obtain verification data with sufficient accuracy to make absolute measures of skill or performance highly reliable.

## 8.2 Stationarity of Historical Validation Data

Table 2 contrasts the frequencies of severe and significant/severe weather events observed in 1989 with those observed in previous years for each of the four forecast regions. With the exception of Region I, the observed frequencies of severe weather for 1989 were similar to the frequencies observed for three previous exercises. Table 2 also suggests that significant weather was greatly over-reported in 1989, or at least significantly different than during 1985 and 1987. Note that we did not have access to significant weather information collected in 1983. The observed frequencies in 1989 are probably more reflective of the true climatology for each region. The probability that the observed frequencies for 1989 occurred by chance, given the averages for 1985 and 1987, is less than 0.1%; that is, this is not a chance occurrence. Obviously, the methods of reporting significant weather events dramatically changed in 1989 as compared to previous years.

TABLE 2  
OBSERVED FREQUENCY OF EVENTS BY REGION

	Severe Weather Frequency			
	I	II	III	IV
Observed (1989)	8.3%	4.4%	13.3%	17.8%
Observed (1983,1985,1987)	2.9%	5.5%	8.8%	18.4%

	Significant or Severe Weather Frequency			
	I	II	III	IV
Observed (1989)	45.8%	37.8%	33.3%	55.6%
Observed (1985,1987)	9.4%	14.9%	15.8%	29.2%

Serious over-reporting, (or under-reporting), of significant weather adversely affects the performance of all the models, but it especially impacts GOPAD and ALPS, since the historical data sets for RT-83, RT-85, and RT-87 were essential to the development of these models. Although this situation might occur when tactical forecast models are developed for one region and used in another region, or whenever one year is abnormal from all other years, it should not vary so much that it is statistically significant. Thus, the possibility that past exercises seriously under-reported significant weather is a critical issue in properly comparing the performance of all the models that participated in the SHOOTOUT-89 exercise. In order to investigate this issue in depth, a Markov chain simulation was performed to compare the reporting of significant and severe weather events in 1985 and 1987 to 1989.

## 8.3 Markov Chain Simulation

The fraction of significant weather events reported during the RT-89 experiment, shown in Table 3, is markedly higher than the fraction reported during the RT-85 and RT-87

experiments as shown in Table 4. The fraction of Nil weather events was likewise much lower in 1989. However, the fraction of severe weather events appears to be quite similar.

TABLE 3  
1989 REPORTED NIL, SIGNIFICANT, AND SEVERE WEATHER

	Nil	Sig	Sev	
I	35 (56%)	23 (37%)	4 (6%)	62
II	39 (63%)	20 (32%)	3 (5%)	62
III	42 (68%)	13 (21%)	7 (11%)	62
IV	31 (50%)	20 (32%)	11 (18%)	62
Sum	147 (59%)	76 (31%)	25 (10%)	248

TABLE 4  
1985 AND 1987 REPORTED NIL, SIGNIFICANT, AND SEVERE WEATHER

	Nil	Sig	Sev	
I	183 (91%)	15 (7%)	4 (2%)	202
II	172 (85%)	18 (9%)	12 (6%)	202
III	170 (84%)	14 (7%)	18 (9%)	202
IV	143 (71%)	23 (11%)	36 (18%)	202
Sum	668 (83%)	70 (9%)	70 (9%)	808

Note: Frequencies may vary from those in Table 2 because only 1985 and 1987 severe events are included in this Table.

This situation raises a question: Is the larger fraction of significant weather reports during 1989 within expected statistical fluctuations? In order to answer this question, Markov chain simulations were conducted for each of the four regions. These simulations assumed that the probabilities of significant or severe weather are influenced by the occurrence or non-occurrence of significant or severe weather on the preceding day only. This situation represents a first-order Markov chain.

The Null hypothesis assumed the true population of significant and severe weather events was that observed in the RT-85 and RT-87 experiments. The transition matrices used for the Markov chain simulations are shown in Table 5. In region IV, for example, the transition probability for a severe weather occurrence to occur on the next day,

given a significant weather event, is 0.250. The transition probabilities were assumed to be stationary; that is, they do not change throughout the experiments (from May through August).

TABLE 5  
MARKOV CHAIN TRANSITION PROBABILITIES

	<u>Region I</u>			<u>Region II</u>			
	Nil	Sig	Sev	Nil	Sig	Sev	
Nil	.922	.061	.017	Nil	.860	.087	.052
Sig	.733	.200	.067	Sig	.765	.176	.059
Sev	1.000	.000	.000	Sev	.833	.000	.167
	<u>Region III</u>			<u>Region IV</u>			
	Nil	Sig	Sev	Nil	Sig	Sev	
Nil	.851	.065	.083	Nil	.710	.099	.191
Sig	.786	.143	.071	Sig	.583	.167	.250
Sev	.778	.056	.167	Sev	.722	.139	.139

The RT-89 experiment was conducted on 62 days within a 92-day span from May 17 through August 16. Thus, a simulated sequence of 92 days was conducted and then analyzed by removing the 30 days on which the RT-89 experiment was not conducted. Each sequence was initiated using the stationary probabilities for Nil, Significant, and Severe weather. The number of Nil, Significant, and Severe weather days was determined for each of 10,000 trials. Cumulative distributions of the fraction of trials that yielded "n" or fewer Nil, Significant, and Severe days were prepared.

These cumulative distributions were developed for each of the four regions. The probabilities that the fractions of Nil, Significant, and Severe weather events reported for 1989 could have occurred by chance (P-values), given the transition probabilities based on the 1985 and 1987 experiments, are readily derived from these cumulative distributions.

For example, Table 6 shows the cumulative distribution of the fraction of trials that yielded "n" or fewer Nil, Significant, and Severe weather events for Region IV based on the Markov chain simulations. During 1989, there were 31 Nil weather events reported for Region IV. Using the cumulative distribution shown in Table 6, the probability of having 31 or fewer Nil weather events is 0.12%. Similarly, the probability of having 20 or more significant weather events is less than 0.01%, and the probability of having 11 or fewer severe weather events is 49%. Thus, we conclude that there is no difference in the frequency of severe weather events reported for Region IV, but the frequency of

significant weather events is significantly higher and the frequency of Nil weather events is significantly lower in 1989.

TABLE 6  
CUMULATIVE DISTRIBUTIONS FROM MARKOV CHAIN SIMULATIONS  
FOR REGION IV

n	Nil	Sig	Sev	n	Nil
0	0.00%	0.02%	0.00%	31	0.12%
1	0.00	0.51	0.00	32	0.23
2	0.00	2.57	0.02	33	0.50
3	0.00	7.24	0.05	34	1.17
4	0.00	15.68	0.37	35	2.05
5	0.00	27.55	1.23	36	3.84
6	0.00	42.73	3.31	37	6.50
7	0.00	57.67	7.39	38	10.07
8	0.00	71.63	14.18	39	15.37
9	0.00	82.24	23.39	40	22.57
10	0.00	89.83	36.09	41	31.66
11	0.00	94.58	49.06	42	42.19
12	0.00	97.53	62.32	43	52.65
13	0.00	98.86	74.23	44	62.81
14	0.00	99.59	83.37	45	72.37
15	0.00	99.84	89.90	46	81.07
16	0.00	99.94	94.22	47	87.75
17	0.00	99.97	97.20	48	92.62
18	0.00	99.99	98.67	49	95.90
19	0.00	99.99	99.40	50	98
20	0.00	100.00	99.80	51	99.04
21	0.00		99.94	52	99.65
22	0.00		99.99	53	99.84
23	0.00		99.99	54	99.94
24	0.00		100.00	55	99.99
25	0.00			56	99.99
26	0.00			57	100.00
27	0.00			58	100.00
28	0.01			59	100.00
29	0.01			60	100.00
30	0.03			61	100.00

The P-values representing the probabilities that the numbers of Nil, Significant, and Severe weather events reported in 1989 are within the expected range of natural variability based on the 1985 and 1987 experiments, as shown in Table 7. The pattern discussed above for Region IV is quite similar for the other three regions. Region I does show an increased frequency of severe weather events in addition to the increased frequency of significant weather events.

TABLE 7  
P-VALUES LIKELIHOOD RANGE

	Nil	Sig	Sev
I	<0.01%	<0.01%	3.3%
II	<0.01%	<0.01%	50%
III	0.20%	0.03%	33%
IV	0.12%	<0.01%	50%

#### 8.4 Conclusions

Therefore, it may be concluded that the observed frequency of severe weather events for 1989 is within the range of natural variability given by the 1985 and 1987 observations, whereas the frequency of significant weather events for 1989 is certainly not within the expected range. This situation suggests that the verification procedures used in RT-89 were significantly different than those used in RT-85 and RT-87 in detecting the occurrence of significant weather. Note that the increase in significant weather events is balanced by a decrease in the Nil weather events with virtually no effect on the severe weather events. This would not be expected if the changes were due to natural variability.

The primary difference between the RT-85/RT-87 exercises and the RT-89 exercise appears to be the method of validating severe and significant weather events. For example, the RT-85/RT-87 exercises used chase teams to verify severe weather events while none were used during RT-89. These chase teams confined their efforts to Regions II, III, and IV and did not pursue storms in Region I. During RT-89, the validation coordinator actively used radar information to identify where severe and significant weather might be occurring. Aggressive telephone calls were then initiated to sheriff's departments, fire departments, highway crews, and other agencies located in areas where the radar showed activity.

These differences suggest that the RT-89 verification methods were:

- (a) equivalent to using chase teams to determine the incidence of severe weather in Regions II, III, and IV;
- (b) superior to the chase teams in determining the incidence of severe weather in Region I;
- (c) superior to the chase teams in determining the incidence of significant weather in all regions.

#### 9.0. PERFORMANCE COMPARISONS

All forecasts models that participated in the SHOOTOUT-89 exercise produced three forecasts--the probability of Nil weather, significant weather, and severe weather--for

each day for each region, except OCI which did not forecast for Region I. Evaluations were done for Nil versus Non-Nil, and severe versus non-severe weather.

The GOPAD forecast models used in RT-89 were developed on the basis of reports of significant and severe weather reports obtained in RT-83, RT-85, and RT-87. There were virtually no reports of significant weather available for RT-83. The incidence of significant weather reports for RT-85 and RT-87 were substantially lower than in RT-89. Thus, one may expect that the skill scores for GOPAD based on the significant weather forecasts will be much lower than if the "training" data had shown a similar frequency of significant weather events. Likewise, the skill scores for severe weather in Region I should be adversely affected as well.

### 9.1 Skill Scores

The individual forecasts for each system, for each region, and for each of the common days for which all systems produced forecasts, are presented in Attachments 1 to 9. The event outcome for each day is coded as follows: **E0 means Nil weather; E1 means significant weather; and E2 means severe weather.** The Brier scores and the Brier-based skill scores are also given for each region and each system.

#### 9.1.1 Regional Climatological Brier Scores

The Brier score is a cumulative form where the probability that the event will occur is P. If the event occurs, then the contribution to the Brier score is  $1 - (1-P)^2$ . If the event does not occur, then the contribution to the Brier score is  $1-P^2$ . The climatological Brier score is determined in the same manner using the long-term frequency as the forecast probability (1983, 1985, and 1987 for severe weather; 1985 and 1987 for significant weather). The long-term frequencies on which the climatological Brier scores are based are listed in Table 8.

TABLE 8  
LONG-TERM FREQUENCIES USED FOR  
CLIMATOLOGICAL BRIER SCORE CALCULATIONS

	<u>I</u>	<u>II</u>	<u>III</u>	<u>IV</u>
Non-Nil	9.41%	14.85%	15.84%	29.21%
Severe	3.68%	5.52%	8.82%	15.38%

#### 9.1.2 Brier-Based Skill Scores

A Brier-based skill score is calculated from the observed Brier score for the actual forecasts and the climatological Brier score. Attachments 1 to 4 show the calculation of Brier scores for severe weather. Attachments 1 to 8 show the Brier scores for severe and non-Nil weather. For example, Attachment 4, severe weather forecasts for Region IV, shows the Brier score for GOPAD1 to be 39.332. Using the long-term frequencies for those same forecasts, the climatological Brier score is 38.421. The maximum

possible Brier score is 45 (i.e., no error in any of the forecasts). Thus, the Brier-based skill score is calculated as follows:

$$SS = (39.332 - 38.421) / (45 - 38.421) = +13.9\%$$

This formulation of the Brier score makes it easy to combine the scores from each of the four regions to determine the overall forecast skill. Attachment 9 shows the Brier scores for (1) severe weather, (2) non-Nil, and (3) combined forecasts. For example, the Brier scores for GOPAD1 in each of the four regions are 44.019, 43.012, 39.164, and 39.332, totaling 165.527. The corresponding climatological Brier scores are 44.229, 43.084, 39.709, and 38.421, totaling 165.443. The corresponding perfect score is 48 + 45 + 45 + 45, totaling 183. Thus, the severe weather skill score for the four regions combined is calculated as follows:

$$SS = (165.527 - 165.443) / (183 - 165.443) = + 0.5\%$$

The analysis of severe weather forecasts appears to be a better indicator of the forecasting skill than an analysis that is based upon non-Nil weather forecasts. This opinion is based upon the fact that there appears to be a significant difference in the observed frequency of significant weather in 1985 and 1987 compared to 1989. It is difficult to reconcile this difference when no similar difference appears in severe weather.

### 9.1.3 Conclusions

There are many different ways to compare the performance of the system that participated in the SHOOTOUT-89 exercise. We choose to rank the models in two ways.

First, Table 9 shows the (Brier) skill scores for severe weather based upon the forecasts in which there was no statistically significant difference between reporting of severe weather between 1985/87 and 1989 (i.e., Regions II, III, and IV). This table eliminates the effect from seriously over-reporting significant weather in all regions and from over-reporting severe weather in Region I. GOPAD and ALPS should be helped by this caveat since they were trained on the 1985 and 1987 data.

TABLE 9  
SKILL SCORES FOR SEVERE WEATHER  
IN REGIONS II, III, AND IV

GOPAD1	+ 2.1%
GOPAD2	+ 1.9%
ALPS	- 0.7%
WILLARD	-11.9%
KASSPr	-17.0%
CONVEX	-24.0%
OCI	-32.3%

Second, Table 10 shows the skill scores only for Region IV, which was the only region that had an adequate number of events upon which to train a GOPAD model. This

table mitigates the lack of a large historical data base that is needed in order to develop a GOPAD or ALPS model.

TABLE 10  
SKILL SCORES FOR SEVERE WEATHER  
IN REGION IV

GOPAD1	+13.8%
GOPAD2	+13.2%
ALPS	+ 1.8%
KASSPr	- 0.2%
OCI	- 3.1%
WILLARD	-12.6%
CONVEX	-40.9%

9.2 Relative Operating Characteristic

A good forecast system should be able to "detect" or correctly forecast the event without giving too many "false alarms." Consider the following tables for GOPAD1 forecasts of severe weather for Region IV. Consider that forecast probabilities above the threshold (18% and 40%, respectively) represent a forecast for severe weather, whereas forecast probabilities below the threshold are forecasts that severe weather will not occur.

TABLE 11  
SEVERE WEATHER FORECASTS FOR REGION IV  
(GOPAD1)

	Pr <=18%	Pr >18%	Sum		Pr <=40%	Pr >40%	Sum
EO/E1	27	10	37	EO/E1	35	2	37
E2	3	5	8	E2	6	2	8
Sum	30	15	45	Sum	41	4	45

Consider the first table with a threshold of 18%. GOPAD1 forecast severe weather on 15 occasions with severe weather occurring 5 times. Note that five of the eight severe weather occurrences were "detected," or the probability of detecting severe weather

(POD) is 5/8 or 0.625. There were ten forecasts for severe weather which were not followed by severe weather, i.e., false alarms. The false alarm rate (FAR) is 10/37, or 0.270.

One may improve (decrease) the FAR by increasing the probability threshold. If this threshold is increased to 40% (Table 10), the FAR drops to 2/37, or 0.054. The probability of detecting severe weather events also decreases (i.e., the forecast will miss more occurrences of severe weather). Now the POD is 2/8, or 0.250.

The relative operating characteristic (ROC) combines the FAR and POD into a single diagram over the entire range of thresholds. A forecast system with positive skill will consistently show a larger POD than a FAR. The ROC plot will lie above the diagonal between (0,0) and (1,1). The further above the diagonal the ROC plot lies, the better the discrimination between severe and non-severe weather. Note that this measures the discrimination ability of the forecast model and it is not affected by bias.

The ROC plots shown in Figures 4 and 5 show a much smaller spread among the different forecast systems than do the ROC plots in Figures 2 and 3. Clearly, this difference is a result of using a larger number of forecasts to determine the ROC plot. The significant + severe weather (Figure 4) ROC plots suggest CONVEX, KASSPr, and GOPAD exhibit the greatest skill, whereas WILLARD and ALPS demonstrate the least skill, with substantial portions of their ROC plots lying below the diagonal. These findings are not inconsistent with the conclusions given by the Brier score analysis.

The forecast systems did better forecasting severe weather, according to Figure 5. Here, only WILLARD shows a portion of its ROC plot below the diagonal. GOPAD exhibits relatively smooth ROC plots, suggesting it produces useful forecasts over its entire range. The OCI forecast system does a much better job in the upper right region of its ROC plot, suggesting it does a better job identifying those days on which severe weather will occur (lower left) somewhat better than it identifies days on which severe weather will not occur.

### 9.3 Measure of Forecast Sharpness

A **sharp** forecast model tends to issue, for example, either rain or no-rain forecasts. Obviously, the ideal forecast model would be very sharp (i.e., totally categorical) and perfectly accurate. However, such a perfect model is far beyond current technology.

Since the state of the art in weather forecasting is far less than perfect, a non-categorical or probabilistic model is the best means for providing information on-demand to a myriad of Tactical Decision Aids (TDA). If a TDA is designed to use a categorical type of forecast, then that TDA should receive the probabilistic forecast and convert it to a categorical forecast, based upon a criteria tailored for its individual tolerance for false alarms, and/or probability of detecting the event. Each TDA may be expected to have its own tolerance level, and thus its own interpretation of the probabilistic forecast.

The distribution of forecast probabilities for each of the models is presented in Tables 12, 13, and 14. The models are arranged, in increasing order of sharpness, from ALPS, which produces forecasts that deviate little from climatology, to KASSPr, which produces nearly categorical forecasts. Forecasts that are overly sharp may be expected to show decreases in skill.

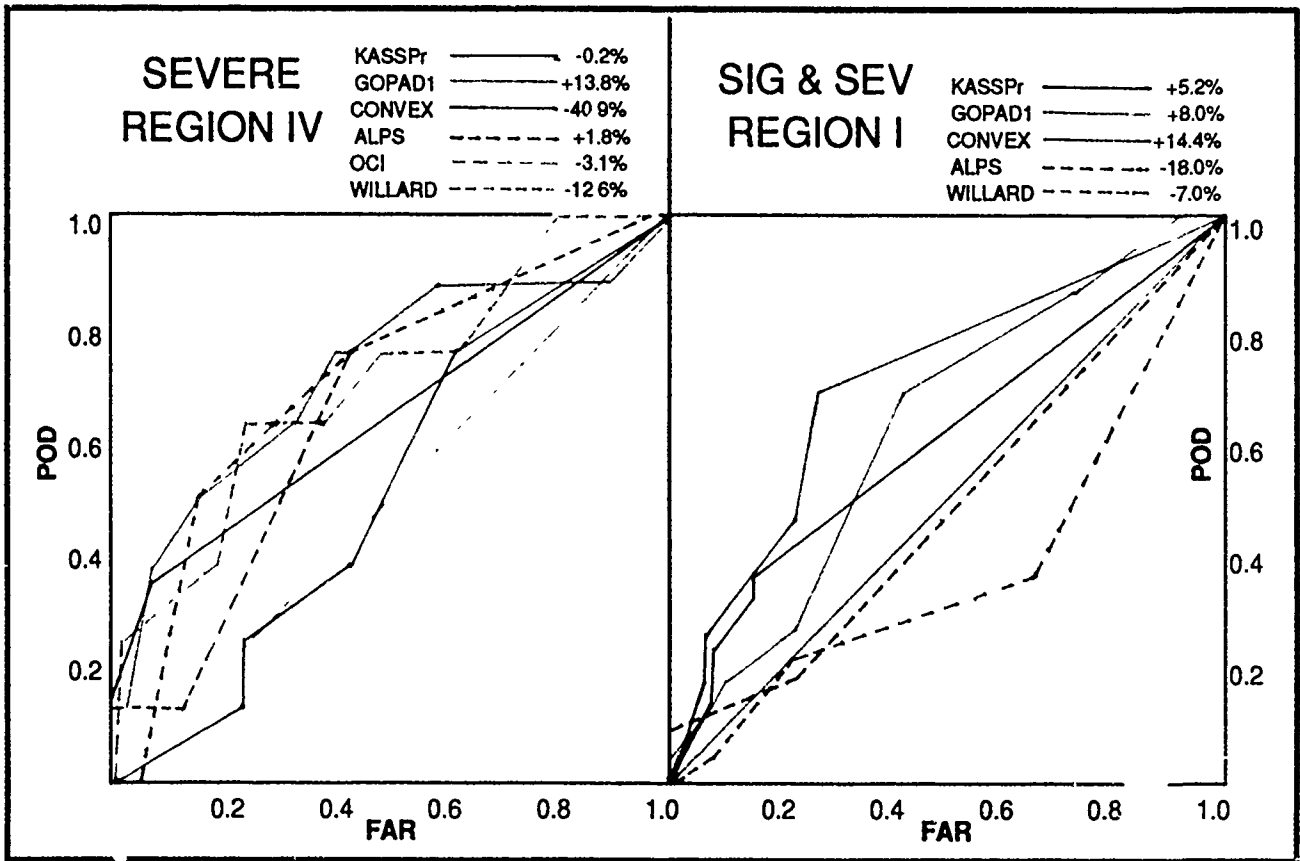


Figure 2. Relative Operating Characteristic for Severe Weather in Region IV

Figure 3. Relative Operating Characteristic for Significant and Severe Weather in Region I

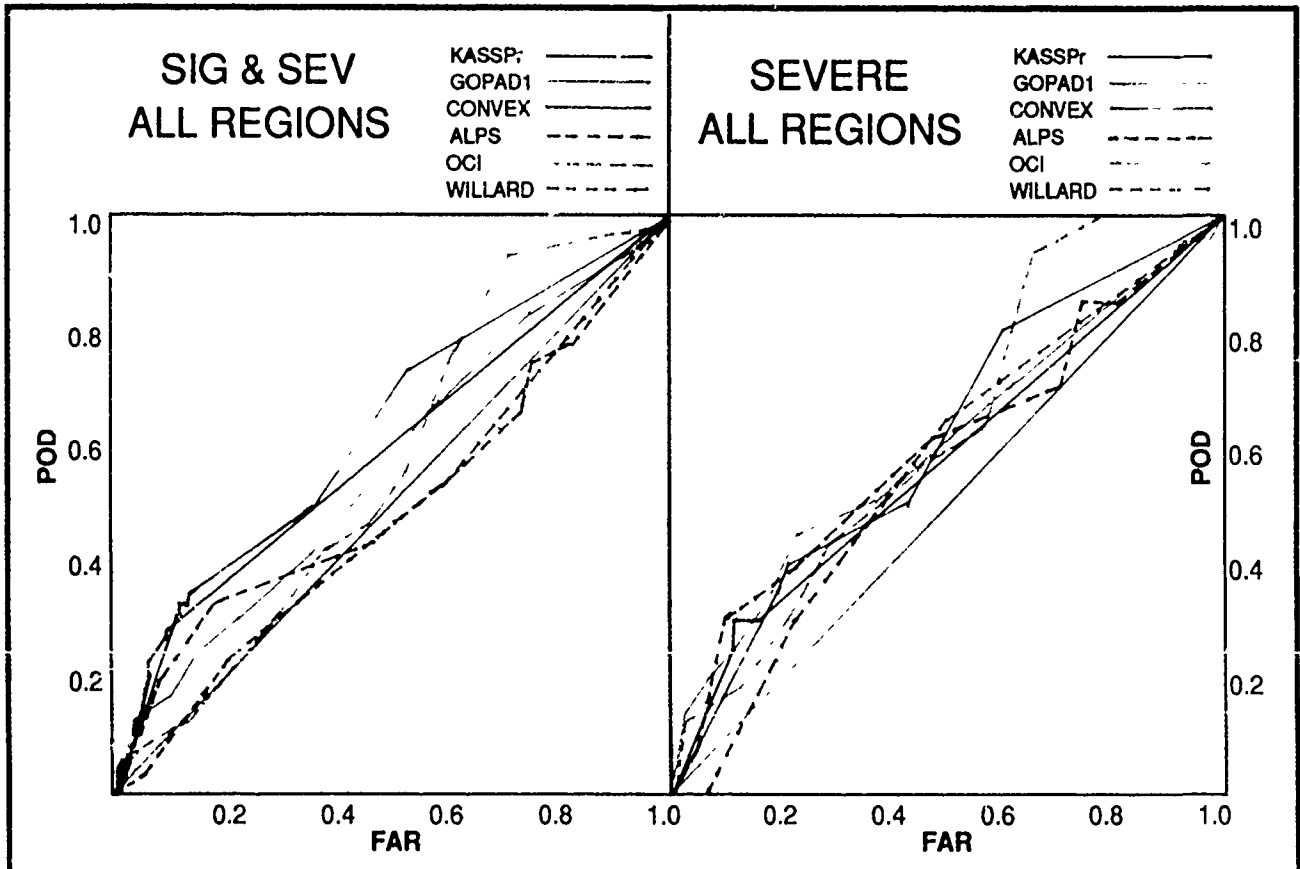


Figure 4. Relative Operating Characteristic for Significant and Severe Weather in All Regions

Figure 5. Relative Operating Characteristic for Severe Weather in All Regions

GOPAD, ALPS, and OCI were capable of producing virtually any probability between 0 and 100%; KASSPr, CONVEX, and WILLARD were rule-based systems that provided for a relatively limited number of options for probability forecasts. To a certain extent, the three models with the greatest sharpness, CONVEX, KASSPr, and WILLARD, were designed to be categorical in nature because they were intended to assist human forecasters in issuing severe weather watches. Tables 12 and 13 list the systems in increasing order of sharpness.

TABLE 12  
DISTRIBUTION OF SEVERE FORECASTS  
ALL REGIONS COMBINED

Forecasted Probability of Severe Weather

Model	0-9%	10-19%	20-39%	40-69%	70-100%	Total	Sharpness
ALPS	76%	24%				192	0.22
GOPAD	73%	15%	8%	3%		212	0.30
OCI	56%	11%	18%	11%	4%	129	0.43
WILLARD	80%	15%	6%			216	0.80
CONVEX	80%	13%	2%		5%	228	0.83
KASSPr	93%	1%	1%	1%	4%	240	0.95

TABLE 13  
DISTRIBUTION OF NON-NIL FORECASTS  
ALL REGIONS COMBINED

Forecasted Probability of Non-Nil Weather

Model	0-9%	10-19%	20-39%	40-69%	70-100%	Total	Sharpness
ALPS	54%	34%	11%			192	0.19
GOPAD*	41%	33%	18%	7%	1%	212	0.22
OCI	21%	27%	21%	21%	10%	129	0.31
WILLARD	50%	29%		17%	4%	216	0.56
CONVEX	40%	19%	20%	3%	18%	228	0.64
KASSPr	84%		1%	5%	10%	240	0.93

#### 9.4 Examination of Bias

Another desirable characteristic for a weather forecasting model is that the model should produce forecasts whose average for a season is very close to the observed frequency of the event being forecasted (i.e., an unbiased model). Bias is defined as the average event forecast probability divided by the observed event frequency. A bias less than one indicates under-forecasting (i.e., forecasted probabilities are too low); whereas a forecast greater than one indicates over-forecasting.

Tables 14 and 15 show the forecast bias for each region and the overall bias for each forecast model. The models in Tables 14 and 15 are listed in order from least overall bias to greatest overall bias. Since GOPAD was trained and optimized on the observed frequencies for the past three exercises, GOPAD should have very little bias, unless ground truth reporting methods are altered. OCI was the only system that consistently over-predicted severe weather. All the other systems tended to under-predict both non-Nil and severe weather.

Bias in a model's forecast may be expected to decrease the skill scores. If the forecast is determined, the model's forecasting skill can be improved by correcting for the bias. The model with the greatest bias tend also to be the models exhibiting the least skill (i.e., KASSPr and WILLARD).

TABLE 14  
SEVERE WEATHER FORECAST BIASES

	I	II	III	IV	Overall Bias
GOPAD2	.52	1.04	.64	1.02	0.812
GOPAD1	.48	1.04	.63	1.01	0.798
OCI	x	3.06	1.40	1.20	(1.509)*
CONVEX	.40	.70	.75	.43	0.569
ALPS	.04	.88	.47	.75	0.544
KASSPr	.86	1.06	.06	.12	0.339
WILLARD	.40	.65	.22	.16	0.273

\*OCI is ranked by 1/1.509 since there is an inverse relation between under-forecasting and over-forecasting.

TABLE 15  
NON-NIL FORECAST BIASES

	I	II	III	IV	Overall Bias
CONVEX	.45	.78	1.09	.53	0.668
OCI	x	.59	.95	.66	0.714*
GOPAD2	.28	.29	.47	.47	0.382
GOPAD1	.27	.29	.47	.46	0.372
WILLARD	.30	.34	.39	.23	0.304
KASSPr	.38	.34	.29	.17	0.284
ALPS	.02	.22	.31	.36	0.229

\*OCI is ranked by comparison to biases for the other systems based on Regions II, III, and IV (non-show).

## 10.0 CONCLUSIONS

Accurate verification of severe and significant weather events plays a very important role in evaluating the performance of those forecast models. Verification of weather events for a region rather than a single point depends upon a network of diligent and cooperative observers. The verification data received for RT-89 reflects a substantial change in verification, especially in recognizing significant weather. This change may be a result of a more active procedure for gathering verification data.

The valid periods and regions for the SHOOTOUT-89 exercise did not match those used for operational forecasts by the Denver WSFO, so direct comparisons of performance to the forecasts issued by operational meteorologists were not possible. One recommendation for future improvement in the format for the SHOOTOUT exercises is that a human forecaster should be used as a benchmark so that it might be possible to estimate the potential these AI-based systems offer for improving human forecasting skill.

Another desirable characteristic is that a tactical forecast model should forecast each event individually (e.g., hail size, high winds, funnel cloud/tornado) rather than forecasting a weather phenomenon (e.g., convection-induced severe or significant weather) that is a combination of events. Clearly, the Attack Helicopter Battalion is interested in forecasts of high winds, whether they are convection induced or non-convection induced.

In addition, probability forecasts should also include a confidence level to measure the degree of certainty in the forecast and, thereby, enable a TDA to provide even more tailored information. Although none of the models had this feature, it is an important feature that should be required in tactical forecast models.

The rich variety of forecast models has provided a source of information that makes it possible to better understand the nature of our forecast modeling approach. We have

provided the reader with a general overview of how the SHOOTOUT-89 exercise was conducted.

The very fact that six AI-systems were brought together in one location to make the same forecasts on the same day in an operational setting, and that each system produced forecasts for a majority of the operational days, is sufficient to deem the RT-89 experiment a success. The nature of SHOOTOUT-89 made it possible for different developers to discuss their approaches in a very cooperative spirit. The SHOOTOUT exercises are important to advancing the state of the art in mesoscale event forecasting. The exceptional effort provided by NOAA/FSL, the chief meteorologist, Woody Roberts, and Bill Moninger are major factors in this success.

## 11.0 REFERENCES

- deLorenzis, B., 1988: Interactive Graphics Editor. Preprints, 4th International Conference on Interactive Information and Processing Systems for Meteorology, Oceanography, and Hydrology, American Meteorological Society, Boston, Massachusetts, pp. 143-145.
- Roberts, W. F., W. R. Moninger, B. deLorenzis, E. Ellison, J. Flueck, J. C. McLeod, C. Lusk, P. D. Lampru, R. Shaw, T. R. Stewart, J. Weaver, K. C. Young, S. Zubrick, 1989: A Field Test of Artificial Intelligence Systems Applied to the Problem of Severe Weather Forecasting: SHOOTOUT-89. Twelfth Conference on Weather Analysis and Forecasting, American Meteorological Society, Boston, Massachusetts, pp. J59-J64.
- Weaver, J. F. and R. S. Phillips, 1987a: Mesoscale Thunderstorm Forecasting Using RAOB Data, Surface Mesonet Observations, and an Expert System Shell. Preprints, Symposium on Mesoscale Analysis and Forecasting Incorporating 'Nowcasting', American Meteorological Society, Boston, Massachusetts, pp. 327-331.
- Weaver, J. F. and R. S. Phillips, 1989: Mesoscale Thunderstorm Forecasting Using an Expert System. Preprints, 12th Conference on Weather Analysis and Forecasting, American Meteorological Society, Boston, Massachusetts.
- Weaver, J. F., F. P. Kelly, M. Klitch, and T. Bonder Haar, 1987: Cloud Climatologies Constructed from Satellite Imagery. Preprints, Third International Conference on Interactive Information and Processing Systems for Meteorology, Oceanography, and Hydrology, American Meteorological Society, Boston, Massachusetts, pp. 169-172.
- Young, K. and P. Lampru, 1989: Goal Oriented Pattern Detection (GOPAD) for Mesoscale Weather Forecasting. In Proceedings from the Tenth Annual EOSAEL/TWI Conference, November 29-30 and December 1, 1989, to be published.
- Zubrick, S. M. and C. E. Riese, 1985: An Expert System to Aid in Severe Thunderstorm Forecasting. Preprints, 14th Conference on Severe Local Storms, American Meteorological Society, Boston, Massachusetts, pp. 117-122.

**APPENDIX D**

**CLOUD TRACKED WINDS DERIVED FROM SATELLITE  
IMAGERY USING AN IMAGE UNDERSTANDING APPROACH**

# CLOUD TRACKED WINDS DERIVED FROM SATELLITE IMAGERY USING AN IMAGE UNDERSTANDING APPROACH

Paul D. Lampru, Jr.  
Lee A. Atkinson  
Consultant's Choice, Inc.

Paper presented at the Tenth Annual  
EOSAEL/TWI Conference  
28-30 November 1989  
Las Cruces, New Mexico

## ABSTRACT

A LISP program called Cloud Image Representation, Recognition, and Understanding Software (CIRRUS I) autonomously tracks individual homogeneous temperature regions and intelligently derives displacement vectors for the leading edges of cloud-objects from GOES IR imagery. CIRRUS I processes use AI methods and rules--but it is not an expert system. Essential to this processing is the transformation of the digital image into a "symbolic" representation defined as a width-encoded medial axis. The symbolic image representation scheme makes it possible to apply image understanding by perceptual grouping concepts. The output from CIRRUS I is called the Cloud-Tracked Forward-Displacement Vector File (CT-FD-VF). This vector file could be used as input to a vorticity modeling program that would produce the synoptic wind or stream flow fields over North America. CIRRUS I lays the foundation for automating many tedious visual analysis tasks that are performed by a human where shape and relative proximity information are important to object recognition. For example, CIRRUS I could be extended to recognize weather related features such as fronts, troughs, ridges, areas of high and low pressure, and to speculate about the future state and location of these features.

## 1. CIRRUS I DATA FLOW OVERVIEW

A data flow overview for CIRRUS I, shown in fig. 1, depicts a satellite receiver collecting multi-temporal GOES IR images at one hour intervals. These digital images (DT+1 and DT+2) are cut, filtered, and sliced into eight binary images--or temperature levels of which only five are actually processed. We refer to the grayscale shapes as **cloud-regions**. Each of the five levels is differenced to produce a third set of images (DT1-0). Then, each image set is transformed into "symbolic" image sets, referred to as ST+1, ST+0, and ST1-0. A **symbolic-cloud-region** corresponds to a **width-encoded medial axis (WEMA)** of segmented regions in an image. The WEMA is composed of data that is organized into LISP lists for the individual cloud-regions. Once these GOES images are in this particular type of symbolic representation, the symbolic-cloud-regions in ST+1 and ST+0 are initialized as **cloud-objects**.

Once initialization is completed, intelligent cloud-object tracking is performed. This process treats all the cloud-objects in the ST+0 image set as **target-clouds** which must be found or

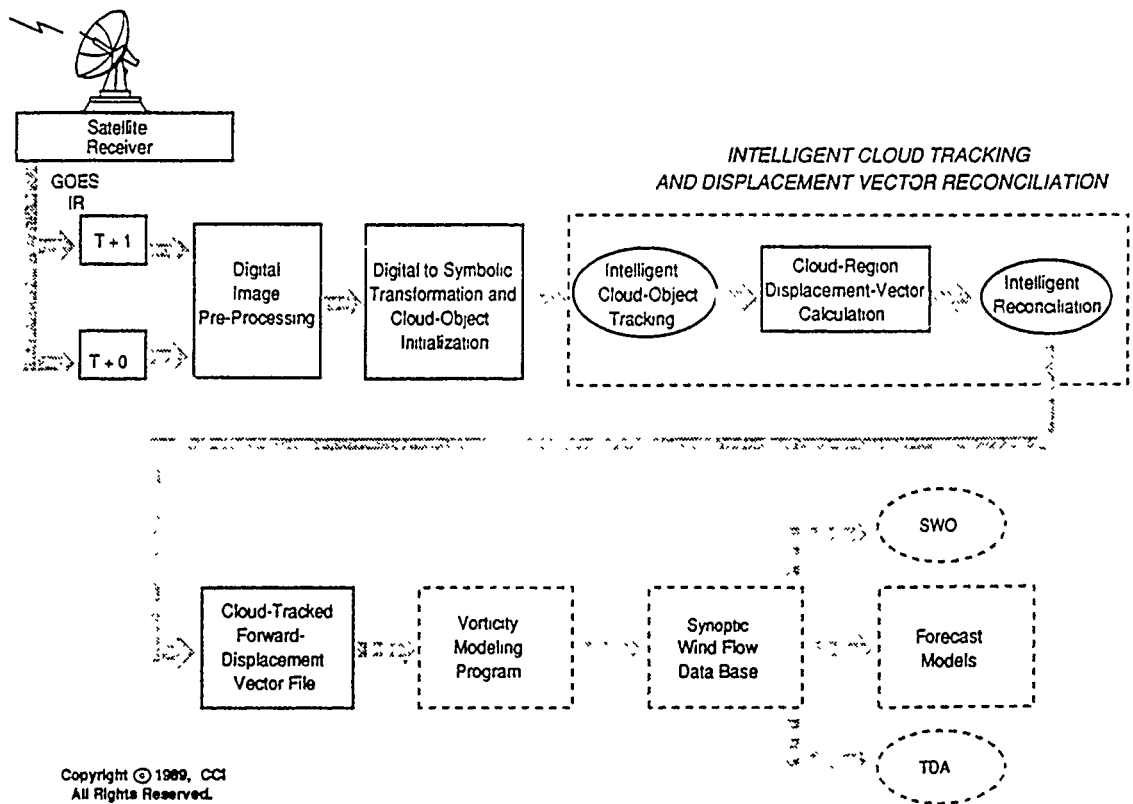


FIGURE 1. CIRRUS I overview.

matched in the ST+1 image set. The cloud-objects in the ST+1 image set are potential **candidate-clouds** that may or may not correspond to one or more target-clouds. The tracking process first identifies a finite set of candidate-clouds for each target-cloud. Then the tracking process proceeds to reduce the number of candidate-clouds until it selects one or more **matched-clouds** for each target-cloud, thus completing the tracking process. A target-cloud that has been tracked to one or more matched-clouds is now referred to as a **tracked-cloud**.

Once the tracking process is completed, cloud-region displacement vectors are computed from the differenced image set ST1-0. The difference calculation is performed on binary images DT+1 and DT+0 to produce an image array with values +1, 0, and -1. The +1 represents the non-overlapping leading edges of clouds-regions. The 0 represents the overlapping areas. The -1 represents the non-overlapping trailing edges of cloud-regions. Only the leading edge regions are transformed into the ST1-0 image and, subsequently, used to calculate cloud-region displacement vectors. Since these vectors only indicate magnitude and orientation, they are referred to as **orientation-vectors**.

Finally, a reconciliation procedure uses knowledge about the tracked-clouds and matched-clouds to determine the sign or direction of the orientation-vectors. The result is the **Cloud-Tracked Forward-Displacement Vector File (CT-FD-VF)**, thus completing the CIRRUS I processing.

Once the CT-FD-VF is composed, it could be used as input to a vorticity modeling program that computes the synoptic wind or stream flow fields for North America. This stream flow data could then be accessed on-demand by the Staff Weather Officer, a weather forecast model, or any Tactical Decision Aid (TDA).

## 2. DIGITAL IMAGE PRE-PROCESSING (DIPP)

The digital image pre-processing steps are shown in more detail in fig. 2. The GOES IR image is 640 x 480 pixels with 256 gray levels. The image is cut to a 256 x 256 pixel window. The smaller window retains most of North America while eliminating portions of the image where curvature of the earth is great. The image is then processed by a 5 x 5 median filter to reduce noise. The image is "thick-sliced" into eight equal gray levels (i.e., a 32 gray scale range).

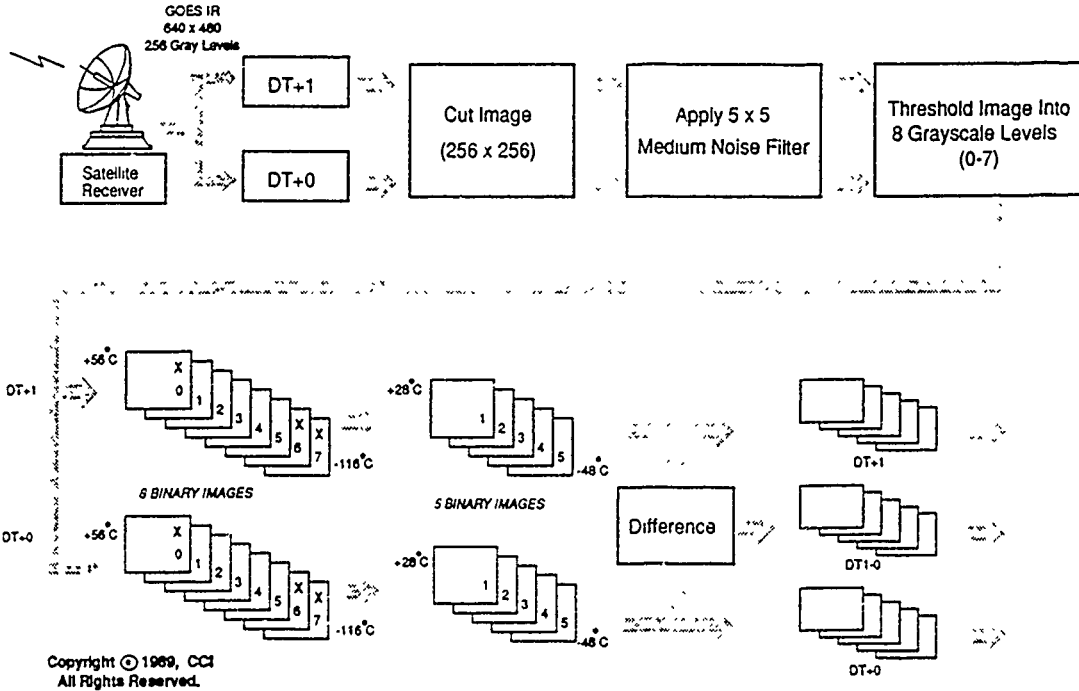


FIGURE 2. Digital image pre-processing.

Since there appears to be little information in the warmest gray level (i.e., range 0-31) and the two coldest levels (i.e., range 192-256), these three levels are discarded. Five gray levels are left that range in temperature between +28°C and -48°C. Table 1 shows each gray level and its associated temperature range. (Parke, 1998).

TABLE 1  
TEMPERATURE RANGES ASSOCIATED  
WITH THE FIVE LEVELS BEING PROCESSED

Gray scale Level	Sliced Range	Temperature Range (°C)
1	32 - 64	+28 to +16
2	65 - 96	+16 to + 8
3	97 - 128	+ 8 to -12
4	129 - 160	-12 to -24
5	161 - 192	-24 to -48

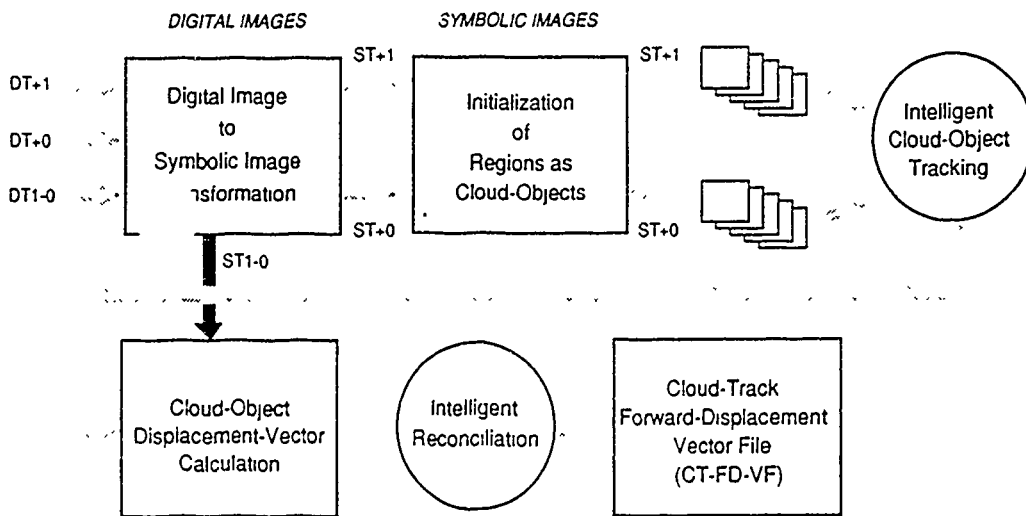
Once the first and second Digital image at Time plus ZERO (DT+0) and ONE (DT+1) are processed to this point, all five levels in each image are subtracted to produce a differenced image set (DT1-0) for each of the five levels. The difference image set contains only regions that do not overlap. These are the leading edges of cloud-objects that are moving. When completed, these three sets of digital images are ready to be transformed into a symbolic representation.

### 3. DIGITAL TO SYMBOLIC IMAGE TRANSFORMATION AND INITIALIZATION OF CLOUD-OBJECTS

Illustrated in fig. 3 is the transformation of all three sets of digital images into symbolic-cloud-regions and the initialization of two image sets (ST+1 and ST+0) as cloud-objects.

All gray levels from each digital image set (i.e., DT+1, DT+2, and DT1-0) are passed through a FORTRAN algorithm called the Digital-to-Symbolic-Transformation Algorithm (DSTA) to transform each level from a digital image into three Symbolic image sets (ST+1, ST+2, and ST1-0). These symbolic image sets are composed of numerical data in a LISP list format (i.e., they are bounded by parenthesis). The data defines the width-encoded medial axis for each cloud-region (i.e., homogeneous temperature region) at each of the five levels.

Each individual symbolic-cloud-region in each of the five levels in image sets ST+1 and ST+2 are then "initialized" in a LISP environment as a cloud-object with attribute slots and default information. After initialization, each thick-sliced level in the first image set is paired with its corresponding level in the second image set. The cloud-objects in both levels are then processed through a tracking process, an attribute calculation process, and a reconciliation process to ultimately produce the Cloud-Tracked Forward-Displacement Vector File (CT-FD-VF).



Copyright © 1989, CCI  
All Rights Reserved.

FIGURE 3. Image transformation and initialization.

#### 4. CLOUD-TRACKED FORWARD-DISPLACEMENT VECTOR FILE (CT-FD-VF)

Shown in fig. 4 are the remaining processing steps needed to produce the CT-FD-VF. In the following sections, each of these steps is described in detail.

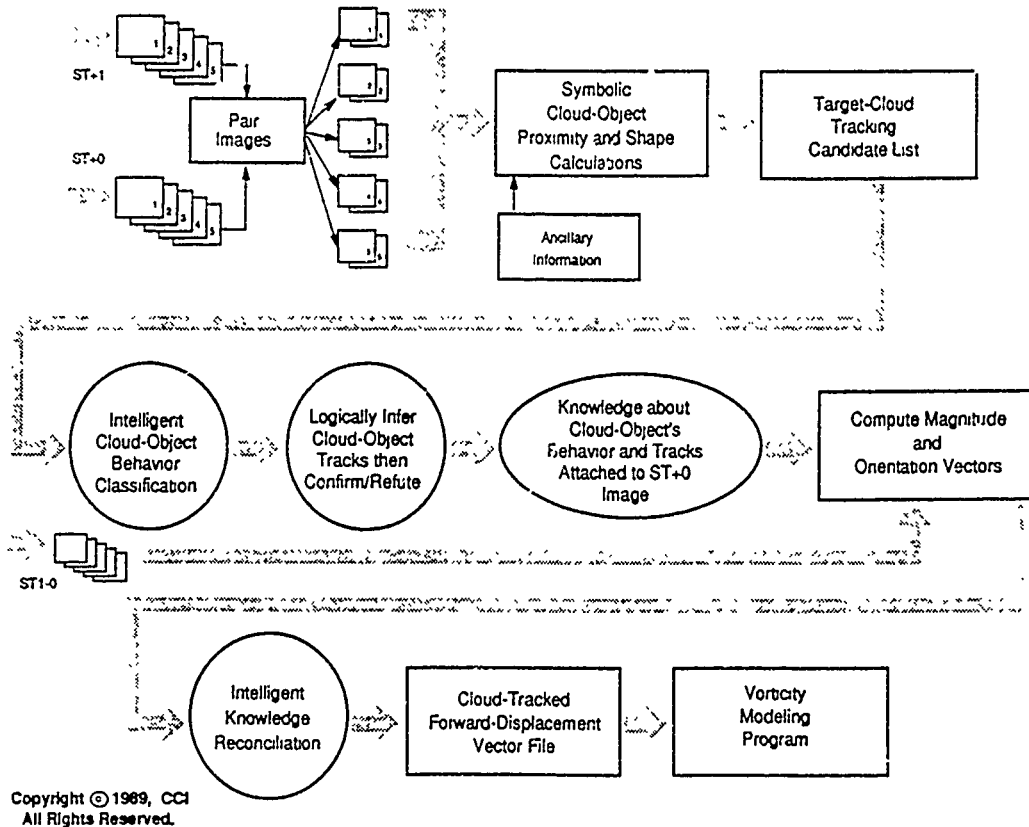


FIGURE 4. Intelligent cloud tracking and displacement vector reconciliation.

##### 4.1. CLOUD-OBJECT ATTRIBUTE CALCULATIONS

This algorithm identifies all possible candidate-clouds in image set ST+1 that are in close proximity to a target-cloud in image set ST+0. Close proximity is determined in the following manner. During initialization, a framing box is created from the WEMA that encloses the target-cloud within some tolerance to allow for maximum displacement. Similarly, another framing box is created that just encloses each candidate-cloud. Then, all the cloud-objects in the ST+1 image that overlap the target-cloud box are candidate-clouds.

The size and length of candidate-clouds are computed using the WEMA. The size of a cloud-object is defined as a diagonal between the upper-left-most corner and the lower-right-most corner of the frame box that encloses the WEMA skeleton. The length of a cloud-object is defined as the summation of all arcs in the WEMA.

The gross overlapping area between the remaining candidate-clouds and the target-cloud is the difference between the box that encloses the target-cloud and the box that encloses one of its candidate-clouds. The area of overlap is normalized by the area of the target-cloud box and then the area of the candidate-cloud box, thus producing two measures of the gross overlap for each candidate-cloud. These measures are then attached to the cloud-objects for use during the behavior classification process.

#### 4.2 INTELLIGENT CLOUD-OBJECT BEHAVIOR CLASSIFICATION

The next processing step is to determine the behavior of the cloud-objects.<sup>1</sup> The objective here is to classify how a target-cloud might be evolving so that it can be used to select by logical inference the correct candidate-cloud(s) when possible, and to logically infer the most relevant cloud-candidate(s) when necessary.

Cloud behavior is determined by using ancillary information and a dozen or so rules to classify the target-clouds into one of five categories (i.e., Sub-Cloud, Super-Cloud, Hyper-Cloud, Meta-Cloud, and Null). The distinction between behavior classes is illustrated in figs. 5-9. The region labeled "A" is the target-cloud and the region labeled "D" is the correctly tracked cloud-candidate (i.e., the tracked-cloud).

Cloud Behavior-1 (CB-1) is illustrated in fig. 5 where all of D is a subset of A. CB-1 is the situation where target cloud A is breaking up into one or more subclouds (i.e., one-to-one or one-to-many). In other words, D is a Sub-Cloud of A. CB-2 is illustrated in fig. 6 where D is a superset of all of A. CB-2 is the situation where candidate cloud D has been formed by the merging of more than one cloud (i.e., many-to-one). In other words, D is a Super-Cloud of A. CB-3 is illustrated in fig. 7 where part of D is a subset of A. CB-3 is the situation where candidate cloud D has been formed by the breaking up of target cloud A and the merging with one or more other clouds (i.e., few-to-many) to form cloud D. In other words, D is a Hyper-Cloud of A. CB-4 is illustrated in fig. 8 where D is a superset of part of A. CB-4 is the situation where candidate cloud D has been formed by the merging of part of cloud A with other clouds (i.e., many-to-few). In other words, D is a Meta-Cloud of A. CB-5 is the Null category to account for those candidates that do not have any relevant behavior.

When the behavior of the target-clouds is finally determined, it is attached to the target-clouds in the ST+0 image set. The behavioral knowledge can then be used to logically infer which candidate-cloud(s) are the matched-cloud(s). When the target-cloud is matched to its candidates (i.e., matched-clouds), the target-cloud is referred to as the tracked-cloud.

#### 4.3 CLOUD-OBJECT DISPLACEMENT VECTOR FILE

The symbolic differenced image set ST1-0 is used to compute the orientation-vectors for leading edges of the cloud-regions in ST+1 and ST+0. Typically, the WEMA for a leading edge is distinctly elongated. In this case, the cloud-region orientation-vector is perpendicular to each of the major WEMA arcs. However, no attempt is made to determine which direction the orientation-vectors are actually pointing (i.e., the sign). This problem is resolved by the reconciliation process described in the next section.

---

<sup>1</sup>Examples of typical cloud behavior are as follows: growing, merging, converging, diverging, shrinking, dissipating, and breaking-up without dissipating. In CIRRUS I these behaviors are grouped into five categories as follows: breaking-up, merging, breaking-up-and-merging, and merging-and-breaking-up, and no discernable behavior (i.e., null).

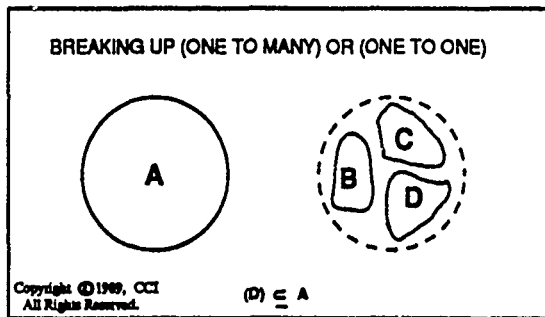


FIGURE 5. Cloud behavior 1: sub-cloud

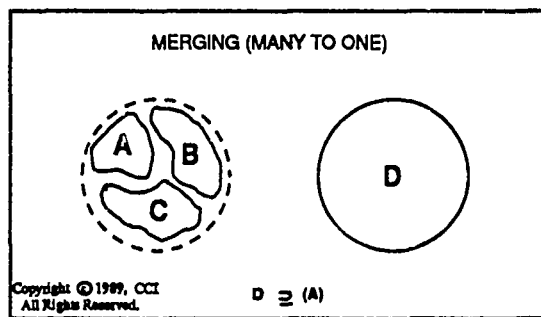


FIGURE 6. Cloud behavior 2: super-cloud

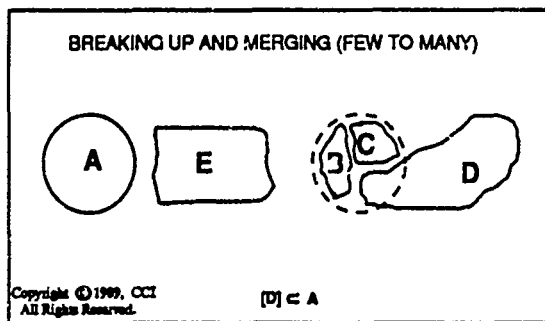


FIGURE 7. Cloud behavior 3: hyper-cloud

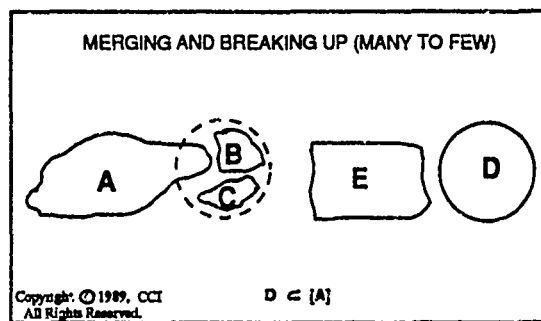


FIGURE 8. Cloud behavior 4: meta-cloud

#### 4.4 KNOWLEDGE RECONCILIATION

By the time the reconciliation process is ready to begin, a considerable amount of information or knowledge is readily available. For example, the locations of the orientation-vectors for all the leading-edges of the overlapping cloud-regions are known. The tracked-clouds and their locations are known. The matched-clouds and their locations are known. The behavior of all the target-clouds is known. This knowledge is now reconciled to determine the direction that the orientation-vectors are pointed.

Each orientation-vector is extended in both directions until it crosses the major medial axis (i.e., a major WEMA arc) of a matched-cloud and its corresponding tracked-cloud. The direction of the orientation-vector is from the tracked-cloud toward the matched-cloud. The process is repeated for all orientation-vectors. Thus, the output from this last processing step is the Cloud-Tracked Forward-Displacement Vector File (CT-FD-VF) which consists of all the cloud displacement vectors for the leading edges of all tracked-clouds for all five gray levels.

## 5. CONCLUSION

It is important to note that the goal of CIRRUS I is to extract systematic wind flow information from the movement (i.e., the displacement) of clouds as viewed from satellite imagery. Obviously, as little unsystematic error as possible is desired. However, if the CT-FD-VF is directly compared to a synoptic stream flow map, one could reasonably expect correlation, systematic bias, and non-systematic error. Although we once considered determining the "accuracy" of the CT-FD-VF by comparing it to a synoptic stream flow map, we finally realized that it was actually an irrelevant comparison given the intended purpose of CIRRUS I.

CIRRUS I is supposed to provide yet another source of candidate predictor variables that would be processed by the GOPAD forecast model development system. Consequently, CIRRUS I has been biased, relative to a synoptic wind flow map, because it produces displacement vectors only for the leading edges of cloud regions. While it may be very desirable for forecasting, this bias may appear to be unsystematic error if these CIRRUS vectors were compared to a synoptic steam flow map. Therefore, an accuracy measurement for CIRRUS I was not performed. It is speculated that a neural-net-based weather forecasting model like GOPAD will remove, to a great extent, the systematic bias, and mitigate the unsystematic error to some degree, even if CIRRUS I and the vorticity modeling program produce wind flow vectors that appear to have error relative to a stream flow map.

The ultimate test of the usefulness of CIRRUS I for mesoscale forecasting is the quality of systematic information contained in its candidate predictor variables that can contribute to the forecast relative to the information available from other sources. Therefore, the best way to correctly determine the value of the CIRRUS I and the vorticity modeling program is to produce a multi-year historical synoptic wind flow data base and measure the statistical contribution of CIRRUS I as a source of predictor variables relative to the candidate predictor variables from other sources (e.g., rawinsonde, mesonet, NGM, barotropic, etc.). The GOPAD model development system is an ideal tool for such a task (Young and Lampru, 1989).

## ACKNOWLEDGMENT

The authors gratefully acknowledge the outstanding assistance provided by Kathie Speas and Susan Winkler. This paper could not have been completed without their editing, graphics, and publication support.

## REFERENCES

- Parke, Peter S., 1986: Satellite Imagery Interpretation for Forecasters, Vol 1, General Interpretation Synoptic Analysis. Meteorological Monographs, The National Weather Association, 4400 Stamp Road, Temple Hill, MD, 1-A-18.
- Young, K. and P. Lampru, 1989: Goal Oriented Pattern Detection (GOPAD) for Mesoscale Weather Forecasting. In Proceedings from the Tenth Annual EQSAEL-TV/I Conference, November 29-30 and December 1, 1989, to be published.

**APPENDIX E**

**CIRRUS-I PROCESSING STEPS AND PERFORMANCE**

## CIRRUS-I PERFORMANCE

### 1.0 INTRODUCTION

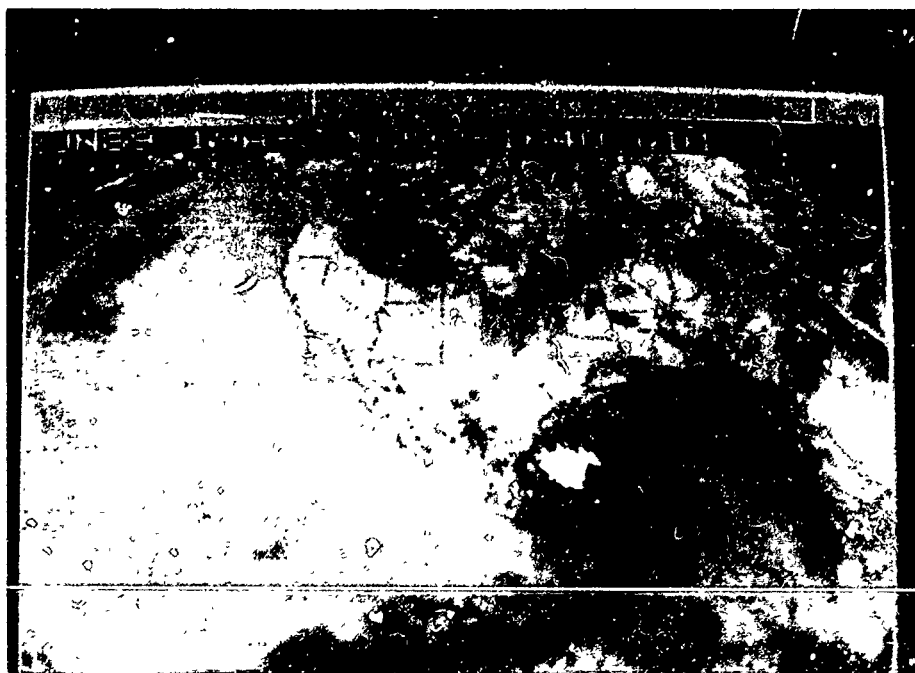
The performance of CIRRUS-I is shown in the following series of photographs.<sup>1</sup> These photographs illustrate the results obtained from the following image processing procedures:

- (a) digital image pre-processing
- (b) digital image to symbolic image transformation
- (c) symbolic cloud-object behavioral classification
- (d) symbolic cloud-object structural matching
- (e) calculation of leading edge orientation and magnitude displacements

However, before reading this Appendix, it may be helpful to refer to Appendix D first for a complete description on how CIRRUS-I operates.

### 2.0 DIGITAL IMAGE PRE-PROCESSING

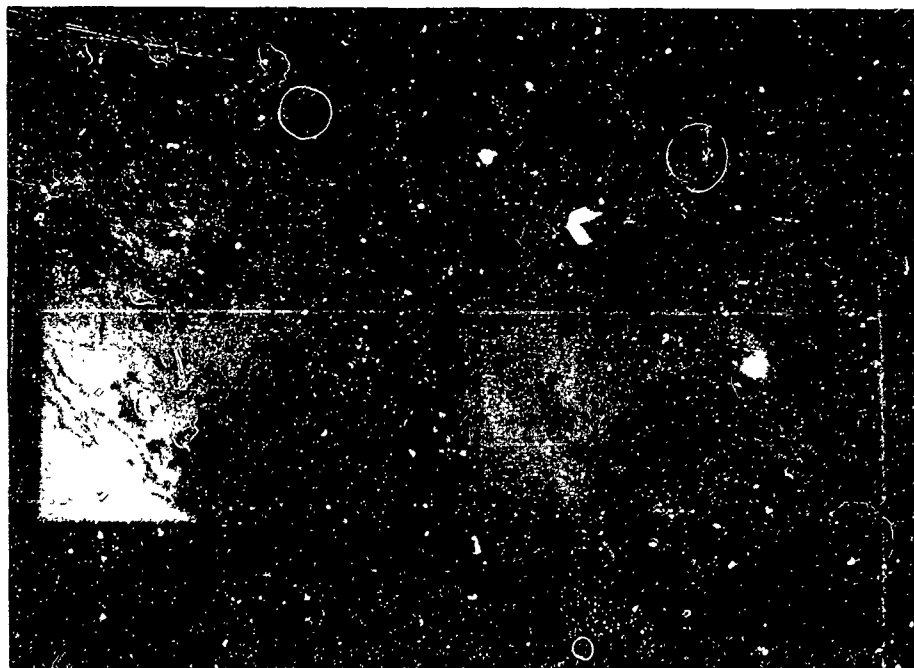
#### 2.1 RAW GOES-IR IMAGE



<sup>1</sup>These photographs were taken with a Minolta X 700, manual focus camera with F8, 1/8 second exposure on Kodak Gold 400/32 film.

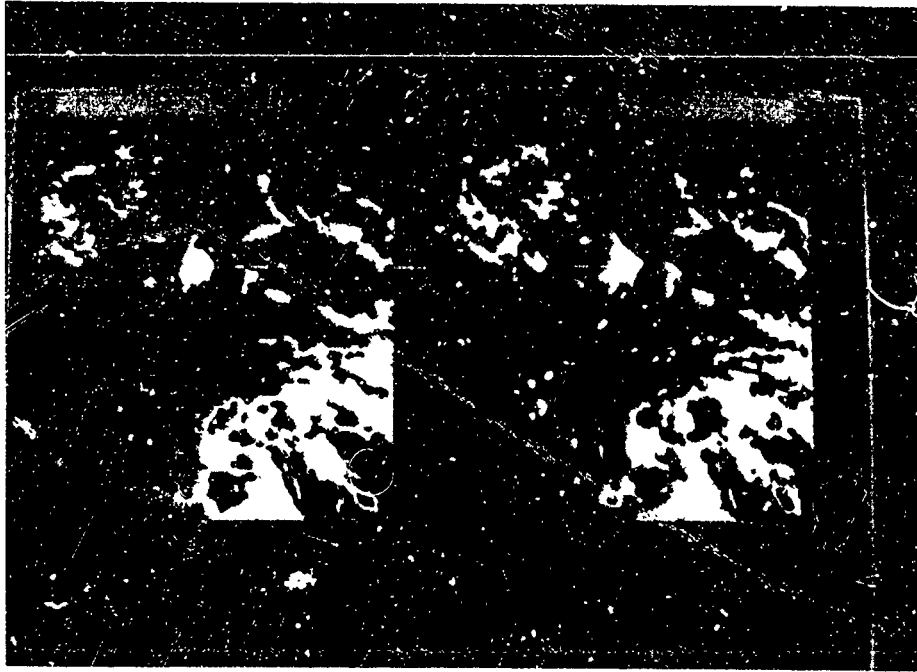
This photograph shows a raw, ZA-unenhanced, IR, 640x400, GOES Central image that was captured on June 22, 1989 at 20:01 hours GMT. This image is referred to as T+0. The dark yellow color represents warm clouds and/or thin clouds in which the warm temperature from the earth's surface have bleed-through. The yellow-green and greenish-blue colors represent intermediate temperatures, while the darker blue represents the coldest clouds.

## 2.2 CUTTING AND FILTERING



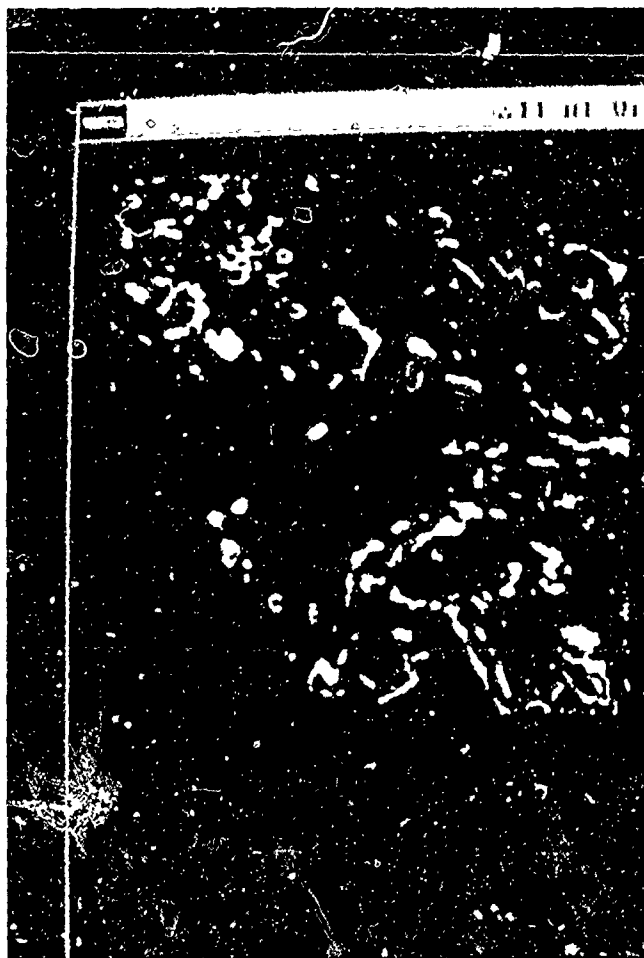
The raw GOES IR image is cut with the following offsets:  $x=256$  and  $y=32$ . This cutting produced a sub-image, shown on the left, that is 256x256 pixels in size. After cutting, a 5x5 median filter is applied to produce the image shown on the right in which the IR regions are more homogeneous.

### 2.3 LEVEL SLICING



The T+0 image and the T+1 are Level 1 slices taken after the median filter is applied. The temperature range for this level is +16° to +28°C. Notice the changes in shape and the movement of the cloud regions from one slice to the next.

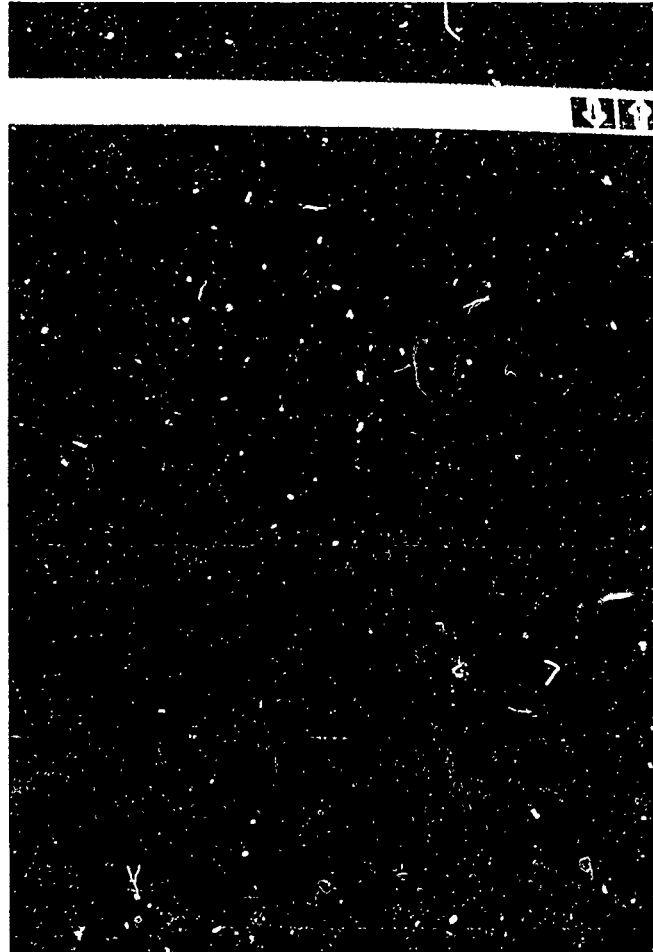
## 2.4 DIFFERENCING LEVEL PAIRS



The sequential slices are now differenced to identify the leading edges of clouds (+1), the trailing edges of clouds (-1), and the overlapping regions (0). This photograph shows the leading edges.

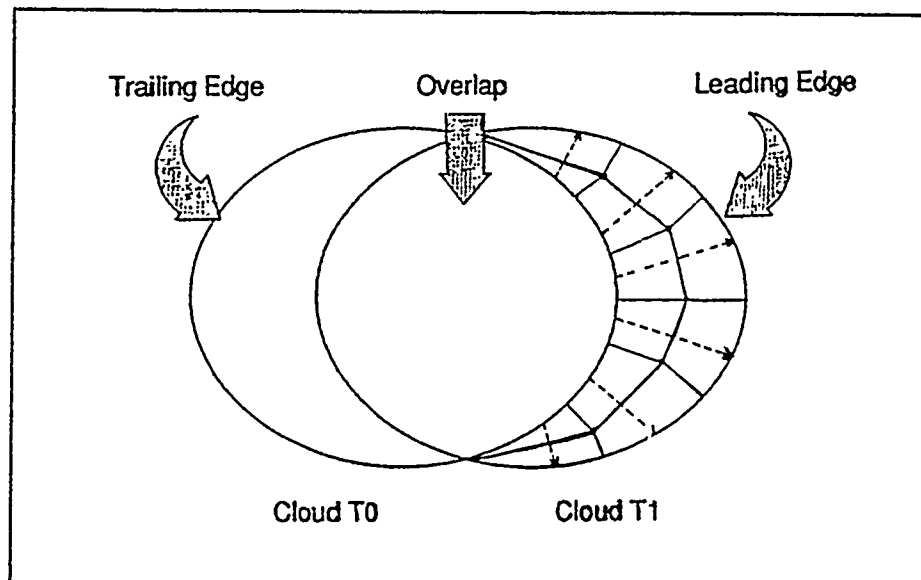
### 3.0 DIGITAL TO SYMBOLIC IMAGE TRANSFORMATION

#### 3.1 TRANSFORMATION OF LEADING EDGES



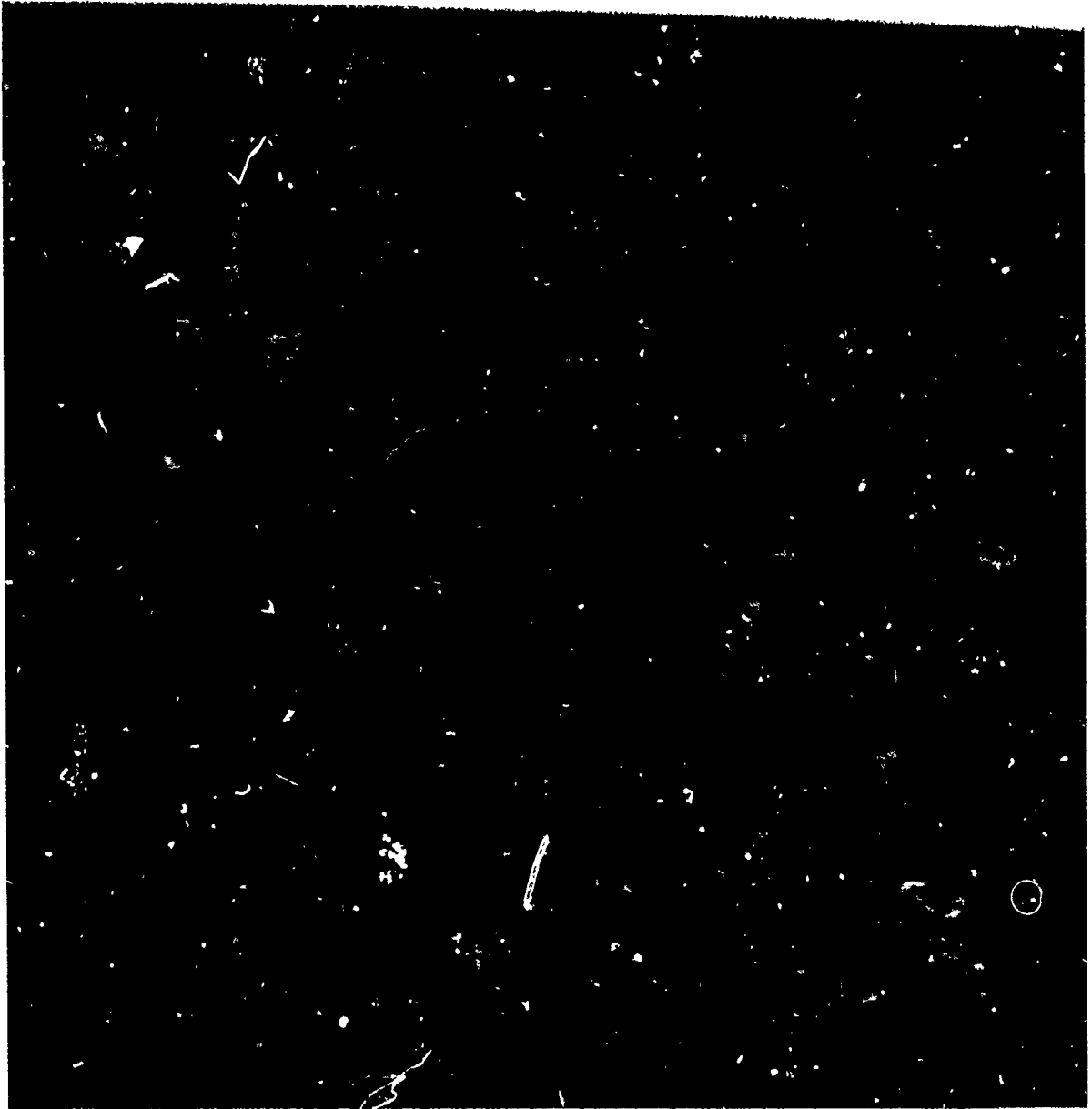
When differencing is completed, the differenced image and all binary slices are transformed into a symbolic or WEMA representation. This photograph displays the medial axis of the leading edges redrawn from the WEMA. The width encodation is not displayed.

### 3.2 CALCULATION OF LEADING EDGE ORIENTATION AND MAGNITUDE DISPLACEMENT



This diagram shows how the WEMA for the leading edge of a cloud are used to calculate orientation and magnitude displacement data. The orientation is calculated from the perpendicular bisection of the WEMA. The magnitude is calculated from the width data explicit in this symbolic representation. During intelligent reconciliation, the direction of movement is derived by using behavioral and structural information to determine the track of a target cloud to all its candidate clouds.

3.3 CALCULATION OF CLOUD DISPLACEMENT DATA



This photograph shows the leading edge displacement data drawn to scale.

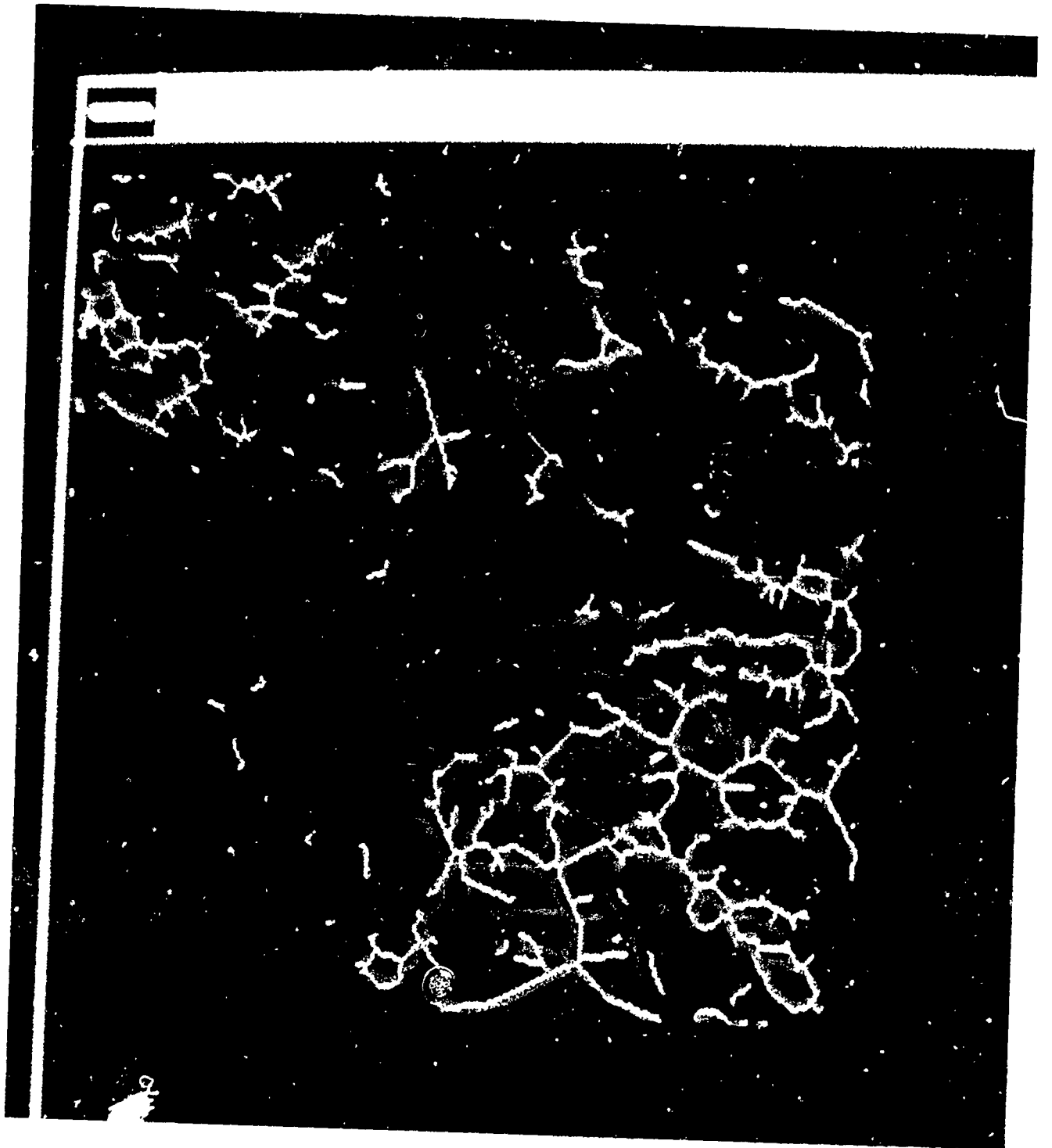
#### 4.0 IMAGE SET 1

The overall goal CIRRUS-I is (a) to classify the behavior of cloud-objects, (b) to structurally match target-cloud arcs to candidate-cloud arcs, (c) to intelligently use all the accumulated behavioral and structural knowledge to produce the Cloud-Tracked Forward-Displacement Vector File (CT-FD-VF). **Behavioral classification** determines how a target-cloud might be evolving so that this information can be used to decide which candidates will be structurally matched. **Structural matching** determines which arcs in the target's WEMA correspond to arcs in a candidate's WEMA. This information is important for two reasons. First, structural matching helps the behavioral classification process to correctly discriminate between relevant and irrelevant clouds. Second, structural information is used, along with behavioral information, during an intelligent reconciliation process to determine the direction in which each target cloud is displacing.

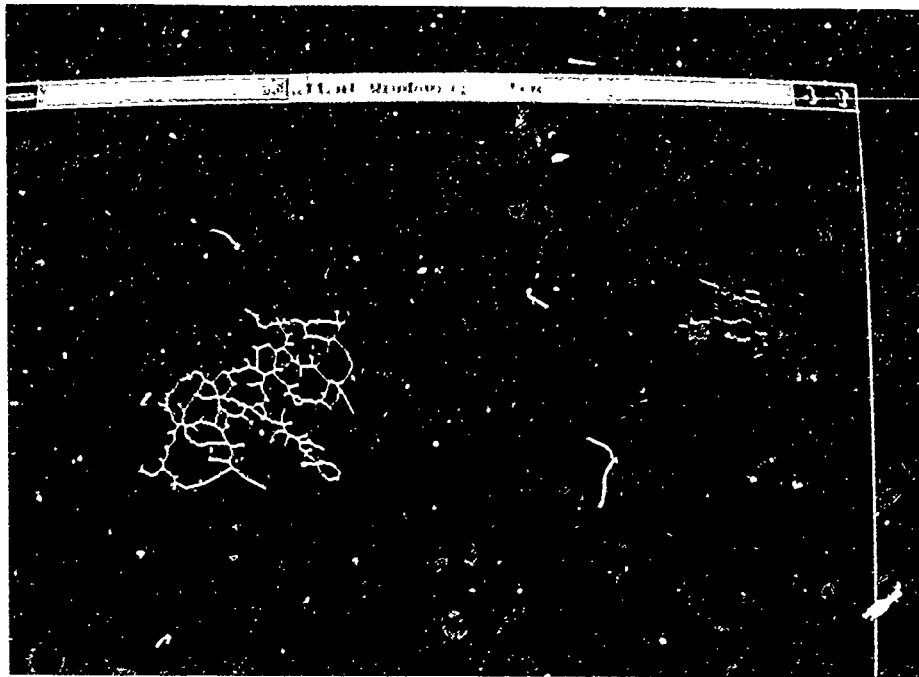
In the series of photographs that follow, pairs of symbolic images are shown which were taken at one-hour intervals. In each photograph, the left image contains the medial axis of the target clouds, while the right image contains the medial axis of the candidate clouds.

#### 4.1 OVERLAY OF TARGET AND CANDIDATE CLOUDS

In the following photograph, the medial axes from the T+0 slice and the T+1 slice at Level 1 are overlaid so spatial and shape information can be observed. The target clouds are shown in blue; the candidate clouds are shown in green; and the overlapping axes are shown in aqua.



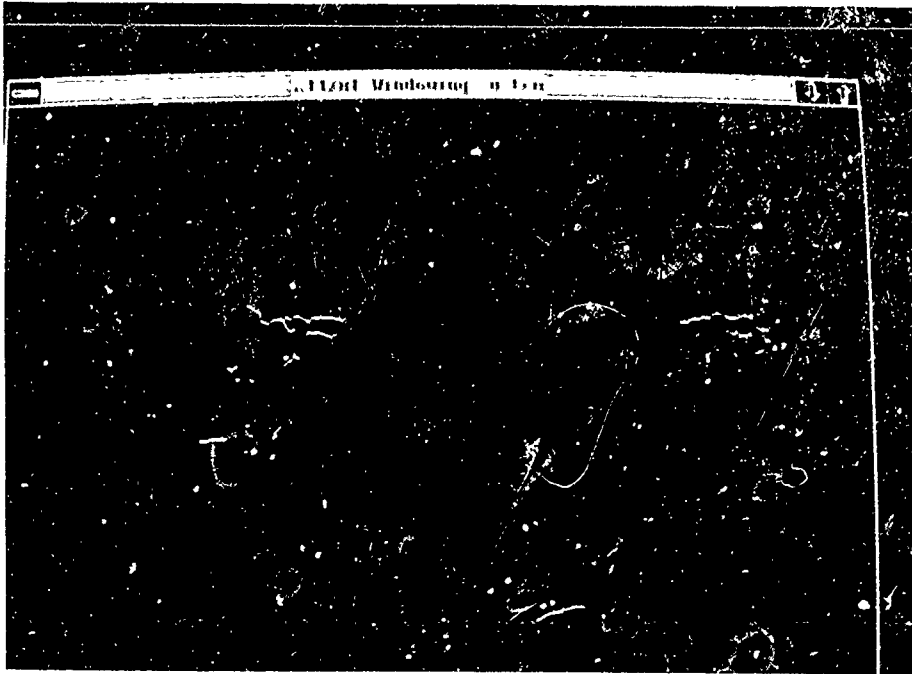
## 4.2 BEHAVIORAL CLASSIFICATION (SUB-CLOUD AND HYPER-CLOUD)



On the left, a massive target cloud, shown in white, is selected to begin the tracking process. Note that cloud-objects are defined as a single, unbroken linkage of arcs.

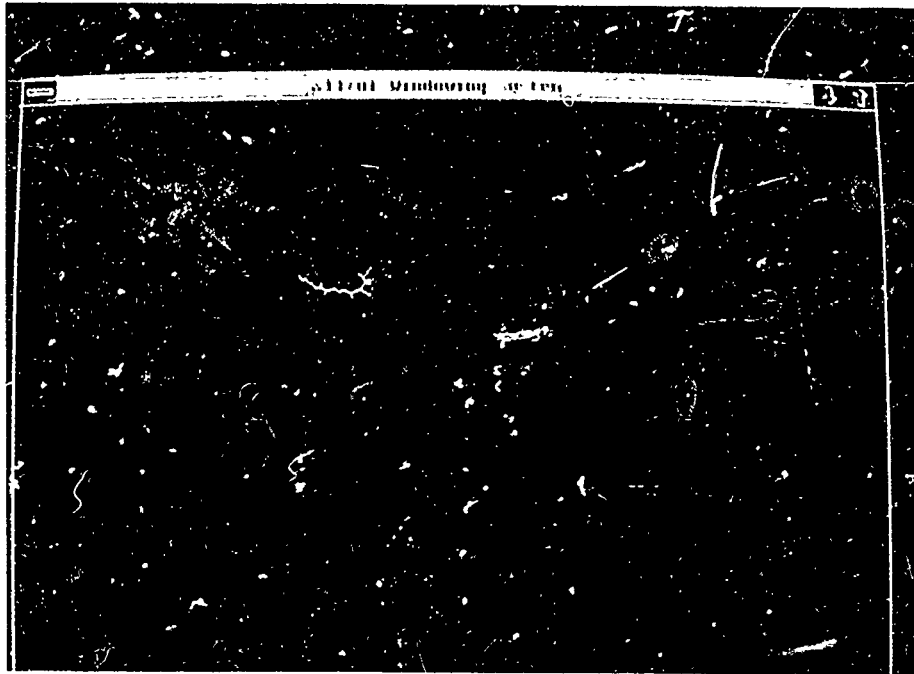
On the right, the T+1 is shown with the color-coded results obtained after CIRRUS-I has completed behavioral classification. The **blue** arcs are non-candidate clouds. The two **red** structures are candidate clouds that broke off from the target cloud. They are classified as sub-clouds (i.e., dissolving and breaking up). The **magenta** cloud structure apparently has broken off from the target cloud and combined with another cloud that was north of the target cloud. It is classified as a hyper-cloud (i.e., breaking up and merging). Although it is difficult to see, there are scattered **brown** cloud structures which are located close to the magenta cloud and that were considered to be candidates. After classification was completed, these clouds were determined to be irrelevant.

#### 4.3 STRUCTURAL MATCHING (SUB-CLOUDS AND HYPER-CLOUDS)



When behavioral classification is completed, a WEMA structural match between the target cloud and the behaviorally classified candidates is performed. The target cloud's arcs that structurally match the arcs in the candidate clouds are shown in **red** and **pink** in both images. The intermixed **white** fragments in the target cloud now depict the arcs where no structural match is found. Notice the long, horizontal, white arc in the lower portion of the target cloud. This arc cannot be matched by a similar arc in any candidate cloud because that portion of the target cloud apparently dissolved.

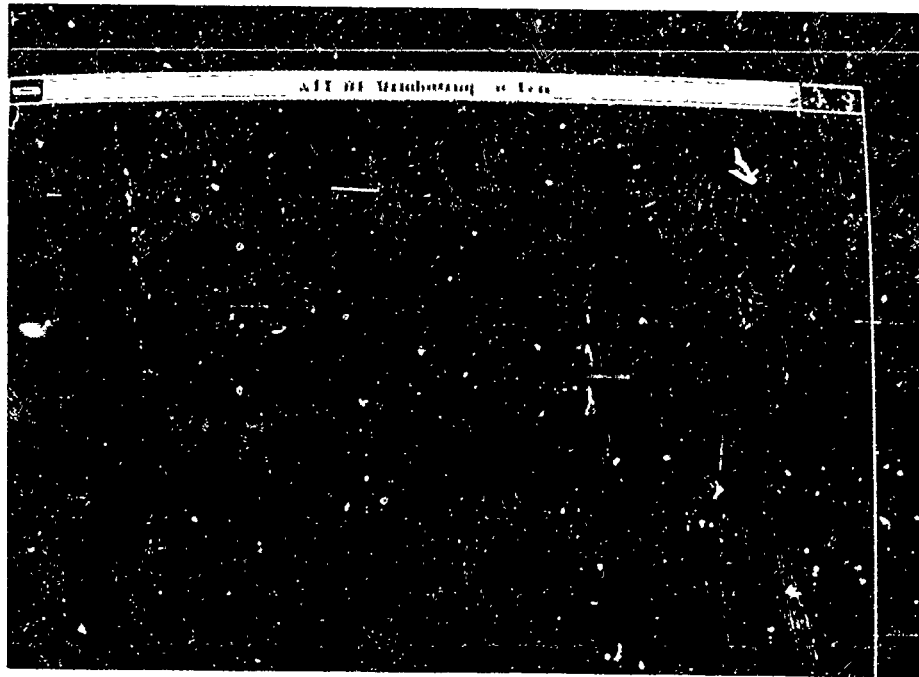
#### 4.4 BEHAVIORAL CLASSIFICATION (SUB-CLOUD AND META-CLOUD)



The white target cloud is behaviorally matched to three candidate clouds shown on the right in green, red, and brown.

The **green** candidate cloud is classified as a meta-cloud (i.e., merging and breaking up) because it has combined with a cloud to the south which is breaking off another, larger structure. The **red** candidate cloud is classified as a sub-cloud (i.e., breaking up) because it broke off the northern part of the target cloud. The **brown** candidate cloud which is very difficult to see is irrelevant because it is too far away from the target cloud to have broken off.

#### 4.5 STRUCTURAL MATCHING (SUB-CLOUD AND META-CLOUD)



The target cloud is now colored **green** to indicate the arcs that are structurally matched to the **green** arcs in the candidate cloud. Likewise, the **red** arcs in the target cloud are structurally matched to the **red** arcs that broke off to the north.

#### 4.6 BEHAVIORAL CLASSIFICATION (SUPER-CLOUD)



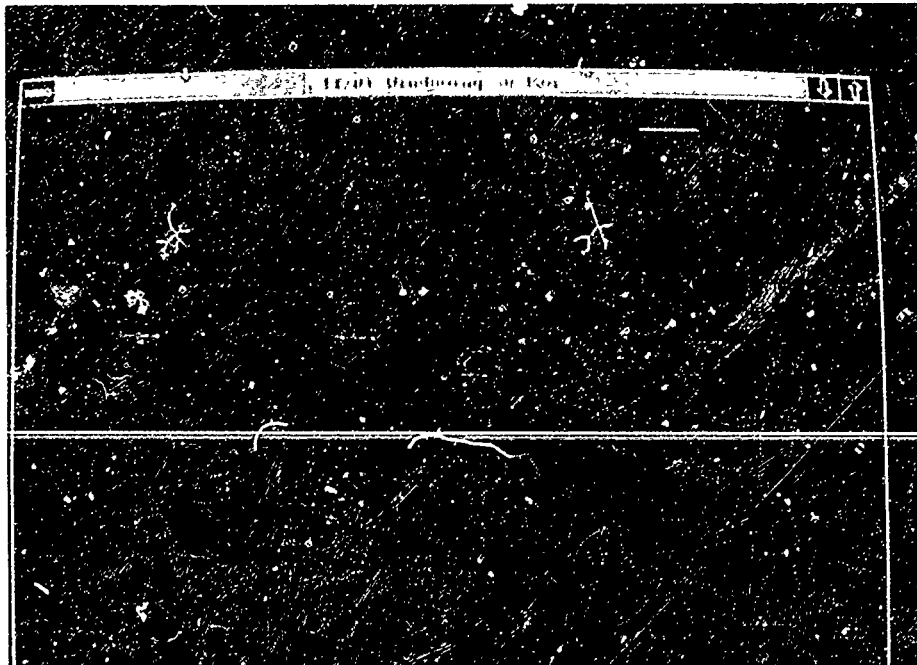
The small, **white** target cloud on the left is behaviorally matched to two candidate clouds shown in yellow and brown on the right. The large, **yellow** candidate is classified as a super-cloud (i.e., merging and/or growing) because it combines with several cloud regions that were north of the target cloud. A small, **brown** candidate cloud, which is very difficult to see, was determined to have no relevant behavior.

#### 4.7 STRUCTURAL MATCHING (SUPER-CLOUD)



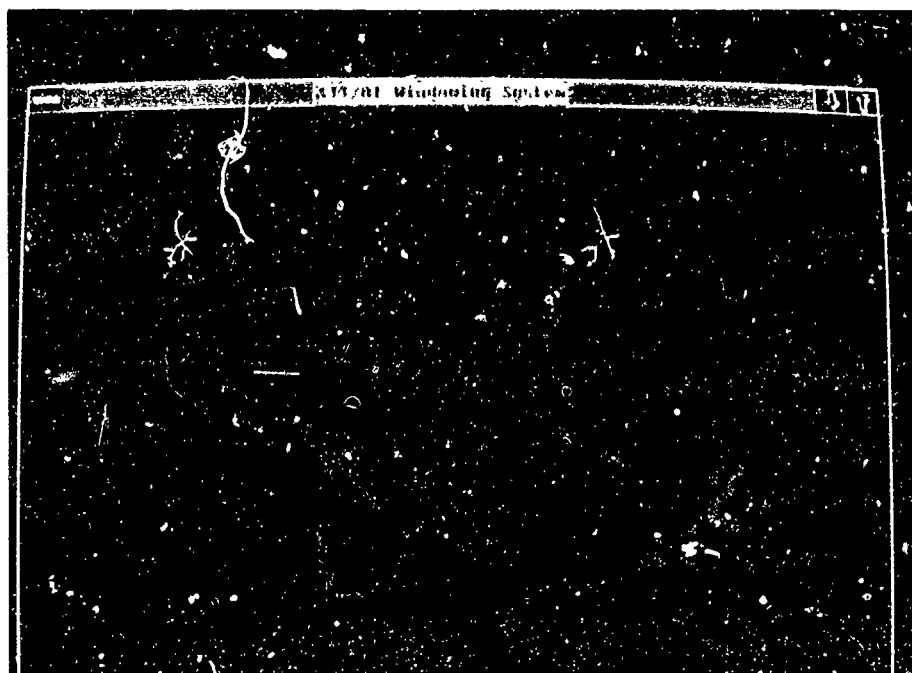
The target cloud is now structurally matched to that portion of the super-cloud to which it correctly corresponds.

#### 4.8 BEHAVIORAL CLASSIFICATION (SUPER-CLOUD)



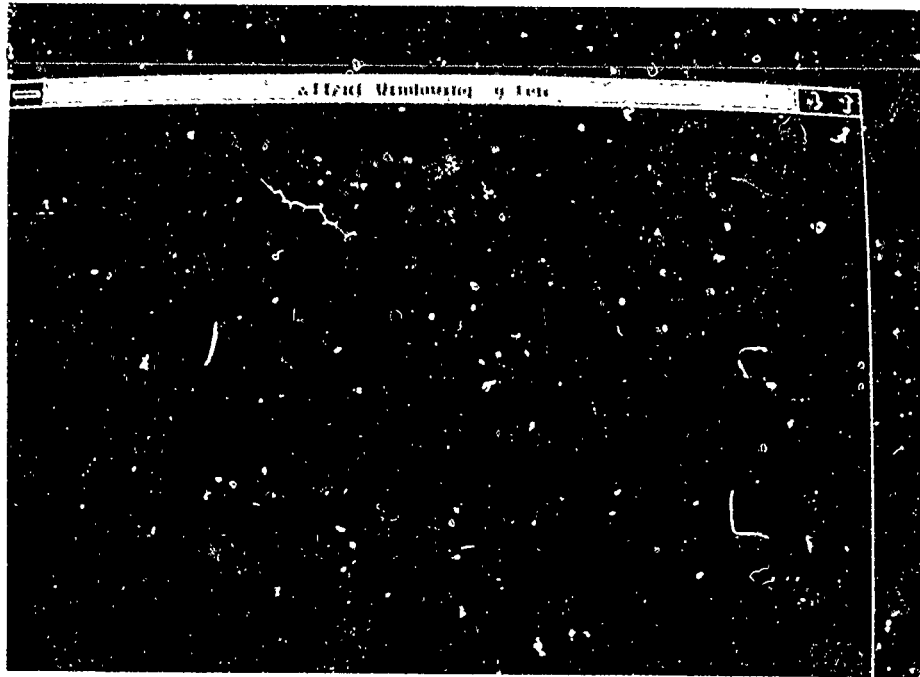
The **white** target cloud is behaviorally matched to two candidate clouds shown in yellow and brown. The **yellow** cloud is classified as a super-cloud (i.e., merging and/or growing) because it has a larger area than the target cloud suggesting that the target cloud has grown. A small, **brown** candidate cloud to the northwest of the yellow candidate cloud is determined to be irrelevant.

#### 4.9 STRUCTURAL MATCHING (SUPER-CLOUD)



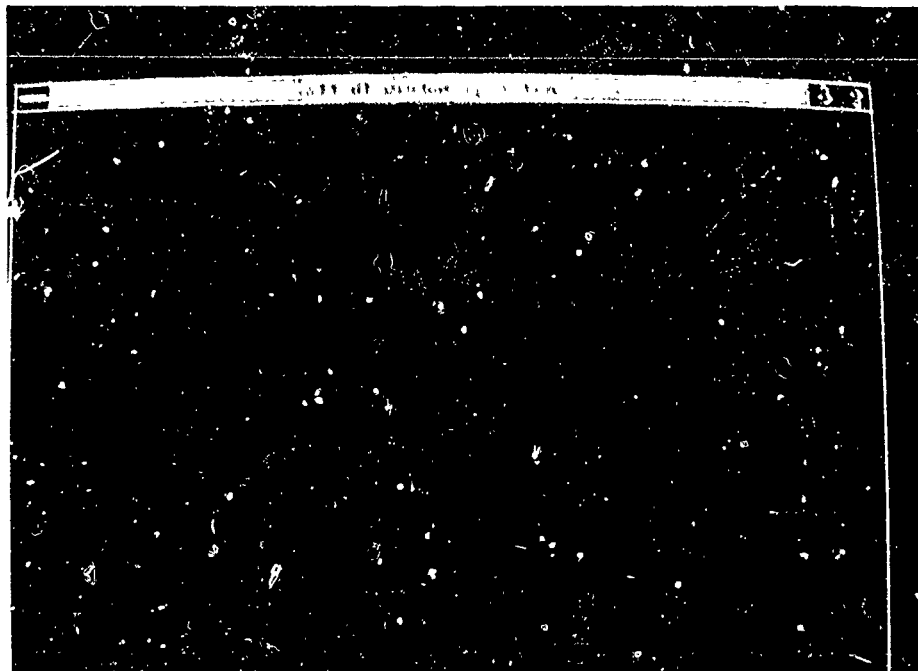
The yellow target cloud arcs are structurally matched to the yellow candidate cloud arcs. Notice that the **white** arc in the upper middle portion of the target cloud is not matched, while the arc at the tip is matched. The white arc is considered to be unmatched because its structure is too different from the candidate cloud. However, the tip of the arc was matched because it is similar.

#### 4.10 BEHAVIORAL CLASSIFICATION (SUB-CLOUD AND HYPER-CLOUD)



The **white** target cloud is behaviorally matched to eight candidate clouds shown in red, magenta, and brown. The **red** clouds are classified as sub-clouds because they broke up into smaller clouds. The **magenta** cloud is correctly classified as a hyper-cloud, yet incorrectly selected as a relevant candidate. Evidently, CIRRUS-I considered the magenta cloud to be a candidate which might have broken off from the target cloud and merged with other clouds. However, the magenta cloud is actually formed by the combination of the **blue** clouds to the north of the target cloud. As will be seen in the next photograph, this temporary mismatch is corrected during the structural matching process.

#### 4.11 STRUCTURAL MATCHING (SUB-CLOUD AND HYPER-CLOUD)

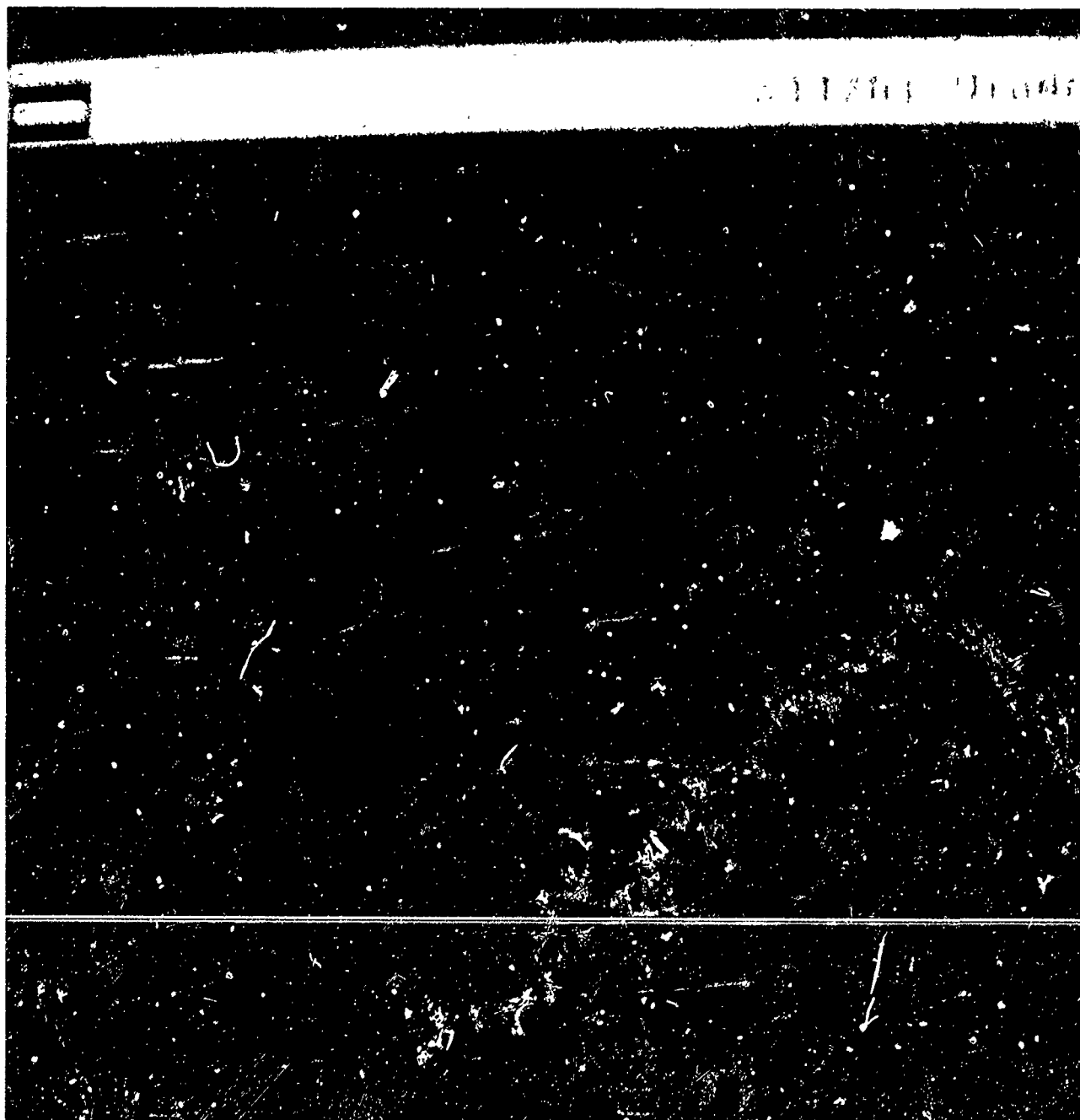


The **red** arcs in both images show the arcs that structurally match. Notice that the **magenta** hyper-cloud is determined to be irrelevant (unmatched) to the target cloud and is now correctly colored **blue**. The **white** arc on the tip of the target cloud indicates it is not structurally matched to the **red** candidate cloud because [we assume] its displacement exceeds the maximum allowed.

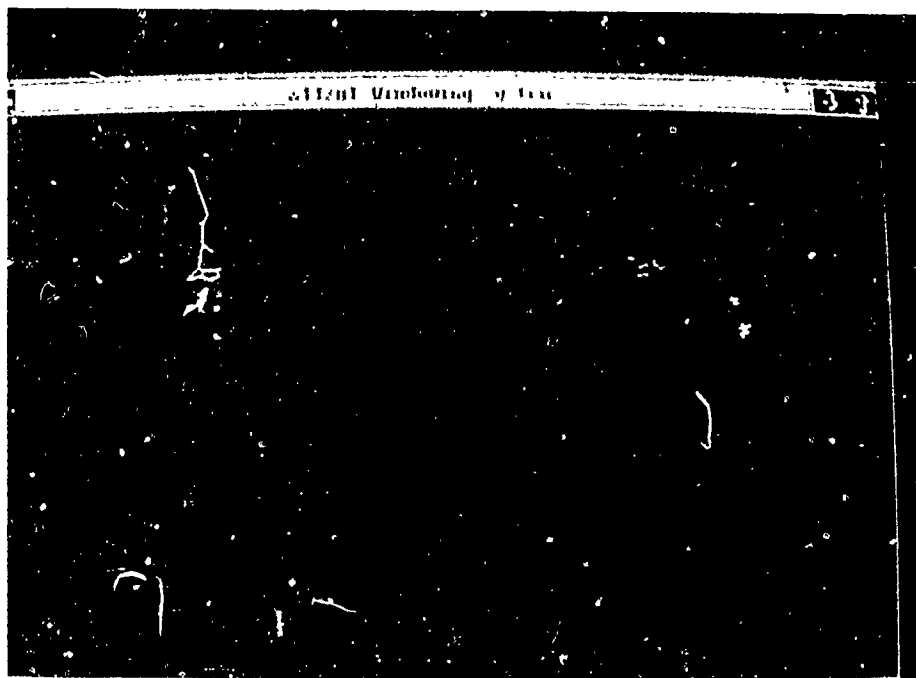
## 5.0 IMAGE SET 2

The remaining GOES IR images were taken on January 23, 1989, at 11:00 and 12:00 hours GMT. The first photo shows the results obtained by behavior classification while the second shows structural matching. This series of photographs provides additional tracking scenarios to demonstrate the robustness of CIRRUS-I.

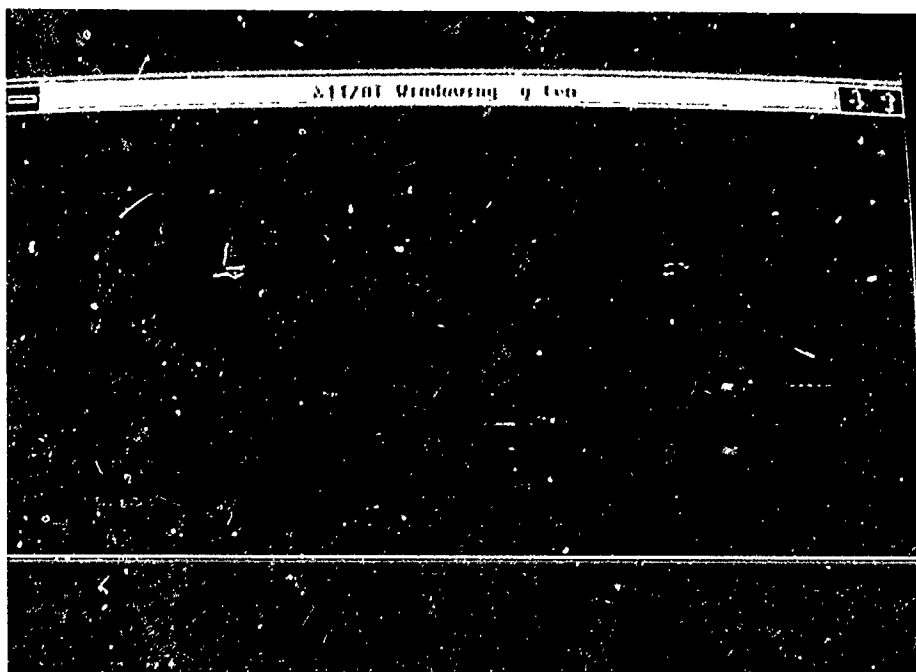
### 5.1 OVERLAY OF TARGET AND CANDIDATE CLOUDS



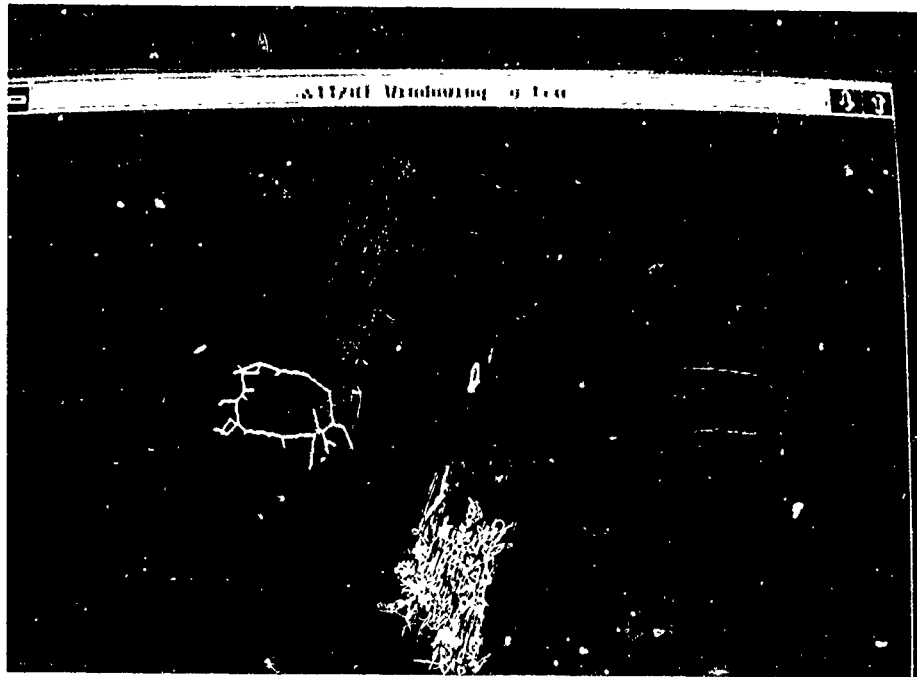
5.2 BEHAVIORAL CLASSIFICATION (SUB-CLOUD AND HYPER-CLOUD)



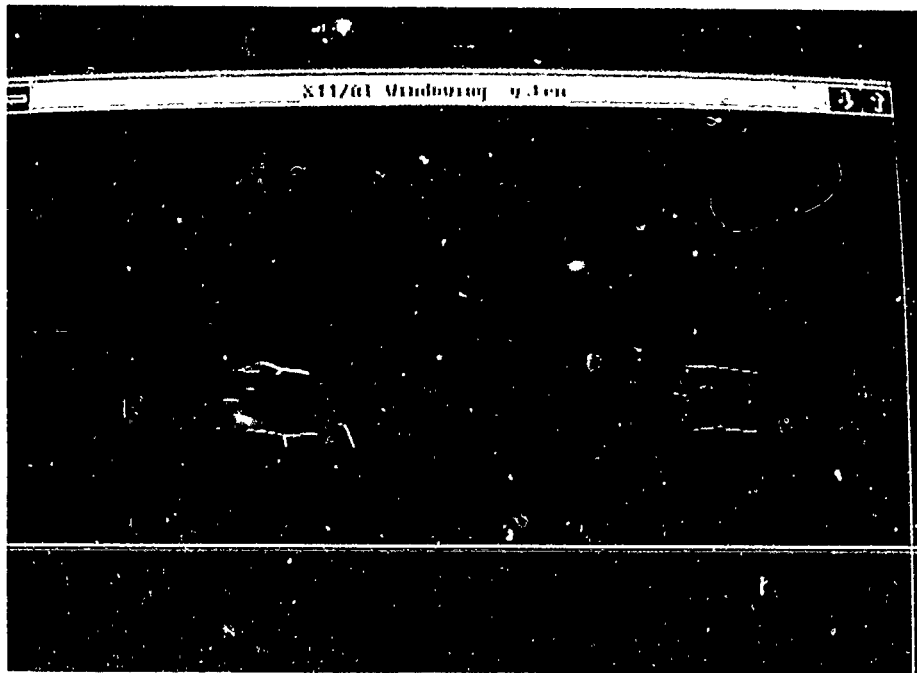
5.3 STRUCTURAL MATCHING (SUB-CLOUD AND HYPER-CLOUD)



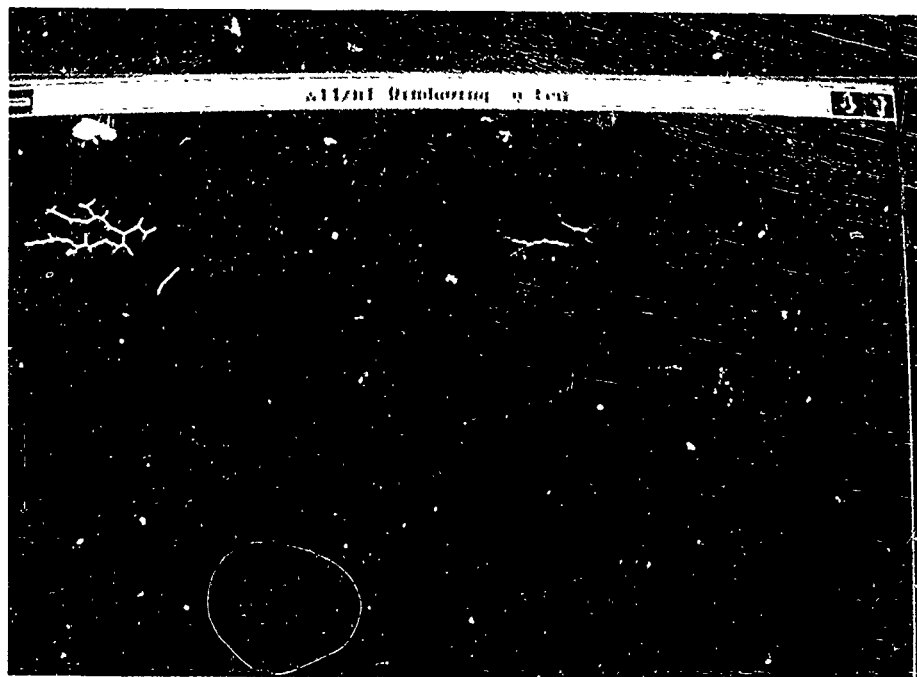
5.4 BEHAVIORAL CLASSIFICATION (META-CLOUD)



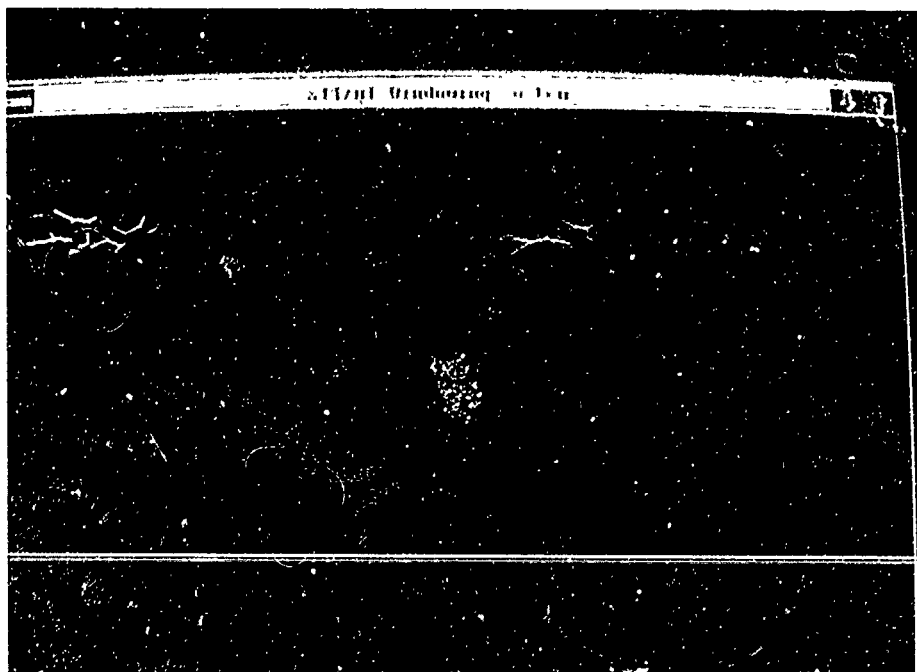
5.5 STRUCTURAL MATCHING (META-CLOUD)



5.6 BEHAVIORAL CLASSIFICATION (SUB-CLOUD AND HYPER-CLOUD)



5.7 STRUCTURAL MATCHING (SUB-CLOUD AND HYPER-CLOUD)



5.8 LEADING EDGE ORIENTATION/MAGNITUDE DISPLACEMENT DATA

